



ISO 17025 LABORATORY
TESTING CERT # 2937.01

*Midwest Pooled Fund Research Program
Fiscal Years 2016-2017 (Year 27)
Research Project Number TPF-5(193) Supplement #104
NDOT Sponsoring Agency Code RFPF-17-CONC-2*

DEVELOPMENT AND TESTING OF AN OPTIMIZED MASH TL-4 CONCRETE BRIDGE RAIL



Submitted by

Scott K. Rosenbaugh, M.S.C.E.
Research Engineer

Ronald K. Faller, Ph.D., P.E.
MwRSF Director, Research Professor

Jeremiah Dixon, B.S.C.E.
Former Graduate Research Assistant

Andrew Loken, B.S.C.E.
Graduate Research Assistant

Jennifer D. Rasmussen, Ph.D., P.E.
Former Research Associate Professor

Jaryd Flores
Research Assistant

MIDWEST ROADSIDE SAFETY FACILITY

Nebraska Transportation Center
University of Nebraska-Lincoln

Main Office

Prem S. Paul Research Center at Whittier School
Room 130, 2200 Vine Street
Lincoln, Nebraska 68583-0853
(402) 472-0965

Outdoor Test Site

4630 N.W. 36th Street
Lincoln, Nebraska 68524

Submitted to

MIDWEST POOLED FUND PROGRAM

Nebraska Department of Transportation
1500 Nebraska Highway 2
Lincoln, Nebraska 68502

MwRSF Research Report No. TRP-03-415-21
March 26, 2021

TECHNICAL REPORT DOCUMENTATION PAGE

1. Report No. TRP-03-415-21	2. Government Accession No.	3. Recipient's Catalog No.	
4. Title and Subtitle Development and Testing of an Optimized MASH TL-4 Bridge Rail		5. Report Date March 26, 2021	
		6. Performing Organization Code	
7. Author(s) Rosenbaugh, S.K., Faller, R.K., Dixon, J., Loken, A., Rasmussen, J.D., and Flores, J.		8. Performing Organization Report No. TRP-03-415-21	
9. Performing Organization Name and Address Midwest Roadside Safety Facility (MwRSF) Nebraska Transportation Center University of Nebraska-Lincoln Main Office: Prem S. Paul Research Center at Whittier School Room 130, 2200 Vine Street Lincoln, Nebraska 68583-0853		10. Work Unit No.	
		11. Contract TPF-5(193) Supplement #104	
12. Sponsoring Agency Name and Address Midwest Pooled Fund Program Nebraska Department of Transportation 1500 Nebraska Highway 2 Lincoln, Nebraska 68502		13. Type of Report and Period Covered Final Report: 2016 – 2021	
		14. Sponsoring Agency Code RPPF-17-CONC-2	
15. Supplementary Notes Prepared in cooperation with U.S. Department of Transportation, Federal Highway Administration.			
16. Abstract A new concrete bridge rail was developed and optimized using recently updated <i>Manual for Assessing Safety Hardware</i> (MASH) Test-Level 4 (TL-4) design loads. The rail was optimized to maximize vehicle stability, minimize installation costs, and mitigate the potential for deck damage by minimizing loads transferred to the deck. Additionally, the bridge rail was designed with a 39-in. installation height so that it would remain crashworthy after future roadway overlays up to 3 in. thick. The barrier had a front face with a 3-degree slope (i.e., batter) away from vertical to promote vehicle stability during impacts while also providing some slope to allow for slipforming real-world installations. Yield-line theory was utilized to design both interior and end regions of the barrier. Further, minimum deck strengths were determined and a deck overhang design procedure was provided for users desiring to modify their existing deck details. Finally, MASH test designation no. 4-12 was conducted on the new bridge rail to evaluate its safety performance as well as the potential for damage to the barrier and bridge deck. In test no. 4CBR-1, the 22,198-lb single-unit truck impacted the concrete bridge rail at a speed of 57.6 mph and an angle of 16 degrees. The single-unit truck was successfully contained and redirected, and all safety performance criteria were within acceptable limits as defined in MASH. Therefore, test no. 4CBR-1 was determined to be acceptable according to MASH test designation no. 4-12. Conclusions and recommendations for implementation were provided.			
17. Key Words Highway Safety, Crash Test, Compliance Test, AASHTO, MASH 2016, Test Level 4, TL-4, Bridge Rail, Concrete Parapet, Bridge Deck, Deck Overhang, Cost-Optimization		18. Distribution Statement No restrictions. This document is available through the National Technical Information Service. 5285 Port Royal Road Springfield, VA 22161	
19. Security Classification (of this report) Unclassified	20. Security Classification (of this page) Unclassified	21. No. of Pages 125	22. Price

DISCLAIMER STATEMENT

This material is based upon work supported by the Federal Highway Administration, U.S. Department of Transportation and the Midwest Pooled Fund Program under TPF-5(193) Supplement #104. The contents of this report reflect the views and opinions of the authors who are responsible for the facts and the accuracy of the data presented herein. The contents do not necessarily reflect the official views or policies of the University of Nebraska-Lincoln, state highway departments participating in the Midwest Pooled Fund Program, nor the Federal Highway Administration, U.S. Department of Transportation. This report does not constitute a standard, specification, or regulation. Trade or manufacturers' names, which may appear in this report, are cited only because they are considered essential to the objectives of the report. The United States (U.S.) government and the State of Nebraska do not endorse products or manufacturers.

UNCERTAINTY OF MEASUREMENT STATEMENT

The Midwest Roadside Safety Facility (MwRSF) has determined the uncertainty of measurements for several parameters involved in standard full-scale crash testing and non-standard testing of roadside safety features. Information regarding the uncertainty of measurements for critical parameters is available upon request by the sponsor and the Federal Highway Administration.

INDEPENDENT APPROVING AUTHORITY

The Independent Approving Authority for the data contained herein was Mojdeh Asadollahi Pajouh, Research Assistant Professor.

ACKNOWLEDGEMENTS

The authors wish to acknowledge several sources that made a contribution to this project: (1) the Midwest Pooled Fund Program funded by the California Department of Transportation, Florida Department of Transportation, Georgia Department of Transportation, Hawaii Department of Transportation, Illinois Department of Transportation, Indiana Department of Transportation, Iowa Department of Transportation, Kansas Department of Transportation, Kentucky Department of Transportation, Minnesota Department of Transportation, Missouri Department of Transportation, Nebraska Department of Transportation, New Jersey Department of Transportation, North Carolina Department of Transportation, Ohio Department of Transportation, South Carolina Department of Transportation, South Dakota Department of Transportation, Utah Department of Transportation, Virginia Department of Transportation, Wisconsin Department of Transportation, and Wyoming Department of Transportation for sponsoring this project; and (2) MwRSF personnel for constructing the barrier and conducting the crash test.

Acknowledgement is also given to the following individuals who contributed to the completion of this research project.

Midwest Roadside Safety Facility

J.D. Reid, Ph.D., Professor
J.C. Holloway, M.S.C.E., Research Engineer & Assistant Director –Physical Testing Division
K.A. Lechtenberg, M.S.M.E., Research Engineer
R.W. Bielenberg, M.S.M.E., Research Engineer
C.S. Stolle, Ph.D., Research Assistant Professor
J.S. Steelman, Ph.D., P.E., Associate Professor
M. Asadollahi Pajouh, Ph.D., P.E., Research Assistant Professor
A.T. Russell, B.S.B.A., Testing and Maintenance Technician II
E.W. Krier, B.S., Construction and Testing Technician II
S.M. Tighe, Construction and Testing Technician I
D.S. Charroin, Construction and Testing Technician I
R.M. Novak, Construction and Testing Technician I
T.C. Donahoo, Construction and Testing Technician I
J.T. Jones, Construction and Testing Technician I
J.E. Kohtz, B.S.M.E., Former CAD Technician
E.L. Urbank, B.A., Research Communication Specialist
Z.Z. Jabr, Engineering Technician
Undergraduate and Graduate Research Assistants

California Department of Transportation

Bob Meline, Chief, Roadside Safety Research Branch
David Whitesel, P.E., Transportation Engineer
John Jewell, P.E., Senior Transportation Engineer,
Specialist

Florida Department of Transportation

Derwood C. Sheppard, Jr., P.E., Design Standards
Publication Manager, Roadway Design Engineer

Georgia Department of Transportation

Christopher Rudd, P.E., State Design Policy Engineer
Frank Flanders IV, P.E., Assistant State Design Policy
Engineer

Hawaii Department of Transportation

James Fu, P.E., State Bridge Engineer
Dean Takiguchi, P.E., Engineer, Bridge Design Section
Kimberly Okamura, Engineer, Bridge Design Section

Illinois Department of Transportation

Filiberto Sotelo, Safety Evaluation Engineer
Martha Brown, P.E., Safety Evaluation Unit Chief

Indiana Department of Transportation

Katherine Smutzer, P.E., Standards Engineer
Elizabeth Phillips, P.E., Highway Design Director

Iowa Department of Transportation

Chris Poole, P.E., Roadside Safety Engineer
Brian Smith, P.E., Methods Engineer
Daniel Harness, P.E., Transportation Engineer Specialist
Stuart Nielsen, P.E., Transportation Engineer
Administrator, Design
Elijah Gansen, P.E., Geometrics Engineer

Kansas Department of Transportation

Ron Seitz, P.E., Director of Design
Scott King, P.E., Road Design Bureau Chief
Thomas Rhoads, P.E., Road Design Leader, Bureau of
Road Design
Brian Kierath Jr., Engineering Associate III, Bureau of
Road Design

Kentucky Department of Transportation

Jason J. Siwula, P.E., Assistant State Highway Engineer
Kevin Martin, P.E., Transportation Engineer Specialist
Gary Newton, Engineering Tech III, Design Standards

Minnesota Department of Transportation

Michael Elle, P.E., Design Standards Engineer
Michelle Moser, P.E., Assistant Design Standards Engineer

Missouri Department of Transportation

Sarah Kleinschmit, P.E., Policy and Innovations Engineer

Nebraska Department of Transportation

Phil TenHulzen, P.E., Design Standards Engineer
Jim Knott, P.E., Construction Engineer
Mike Owen, P.E., State Roadway Design Engineer
Mick Syslo, P.E., Materials and Research Engineer &
Division Head
Mark Fischer, P.E., PMP, Research Program Manager
Lieska Halsey, Research Project Manager
Angela Andersen, Research Coordinator
David T. Hansen, Internal Research Coordinator
Jodi Gibson, Former Research Coordinator

New Jersey Department of Transportation

Hung Tang, Senior Engineer, Transportation
Joseph Warren, Assistant Engineer, Transportation

North Carolina Department of Transportation

Neil Mastin, P.E., Manager, Transportation Program
Management – Research and Development
D. D. “Bucky” Galloway, P.E., CPM, Field Operations
Engineer
Brian Mayhew, P.E., State Traffic Safety Engineer
Joel Howerton, P.E., Plans and Standards Engineer

Ohio Department of Transportation

Don Fisher, P.E., Roadway Standards Engineer

South Carolina Department of Transportation

J. Adam Hixon, P.E., Design Standards Associate
Mark H. Anthony, P.E., Letting Preparation Engineer
Henry Cross, P.E., Design Standards Engineer
Jason Hall, P.E., Engineer

South Dakota Department of Transportation

David Huft, P.E., Research Engineer
Bernie Clocksin, P.E., Standards Engineer

Utah Department of Transportation

Shawn Debenham, Traffic and Safety Specialist
Glenn Blackwelder, Operations Engineer

Virginia Department of Transportation

Charles Patterson, P.E., Standards/Special Design Section
Manager
Andrew Zickler, P.E., Complex Bridge Design and ABC
Support Program Manager

Wisconsin Department of Transportation

Erik Emerson, P.E., Standards Development Engineer
Rodney Taylor, P.E., Roadway Design Standards Unit
Supervisor

Wyoming Department of Transportation

William Wilson, P.E., Architectural and Highway
Standards Engineer

Federal Highway Administration

David Mraz, Division Bridge Engineer, Nebraska Division
Office

SI* (MODERN METRIC) CONVERSION FACTORS				
APPROXIMATE CONVERSIONS TO SI UNITS				
Symbol	When You Know	Multiply By	To Find	Symbol
LENGTH				
in.	inches	25.4	millimeters	mm
ft	feet	0.305	meters	m
yd	yards	0.914	meters	m
mi	miles	1.61	kilometers	km
AREA				
in ²	square inches	645.2	square millimeters	mm ²
ft ²	square feet	0.093	square meters	m ²
yd ²	square yard	0.836	square meters	m ²
ac	acres	0.405	hectares	ha
mi ²	square miles	2.59	square kilometers	km ²
VOLUME				
fl oz	fluid ounces	29.57	milliliters	mL
gal	gallons	3.785	liters	L
ft ³	cubic feet	0.028	cubic meters	m ³
yd ³	cubic yards	0.765	cubic meters	m ³
NOTE: volumes greater than 1,000 L shall be shown in m ³				
MASS				
oz	ounces	28.35	grams	g
lb	pounds	0.454	kilograms	kg
T	short ton (2,000 lb)	0.907	megagrams (or "metric ton")	Mg (or "t")
TEMPERATURE (exact degrees)				
°F	Fahrenheit	$\frac{5(F-32)}{9}$ or $(F-32)/1.8$	Celsius	°C
ILLUMINATION				
fc	foot-candles	10.76	lux	lx
fl	foot-Lamberts	3.426	candela per square meter	cd/m ²
FORCE & PRESSURE or STRESS				
lbf	poundforce	4.45	newtons	N
lbf/in ²	poundforce per square inch	6.89	kilopascals	kPa
APPROXIMATE CONVERSIONS FROM SI UNITS				
Symbol	When You Know	Multiply By	To Find	Symbol
LENGTH				
mm	millimeters	0.039	inches	in.
m	meters	3.28	feet	ft
m	meters	1.09	yards	yd
km	kilometers	0.621	miles	mi
AREA				
mm ²	square millimeters	0.0016	square inches	in ²
m ²	square meters	10.764	square feet	ft ²
m ²	square meters	1.195	square yard	yd ²
ha	hectares	2.47	acres	ac
km ²	square kilometers	0.386	square miles	mi ²
VOLUME				
mL	milliliter	0.034	fluid ounces	fl oz
L	liters	0.264	gallons	gal
m ³	cubic meters	35.314	cubic feet	ft ³
m ³	cubic meters	1.307	cubic yards	yd ³
MASS				
g	grams	0.035	ounces	oz
kg	kilograms	2.202	pounds	lb
Mg (or "t")	megagrams (or "metric ton")	1.103	short ton (2,000 lb)	T
TEMPERATURE (exact degrees)				
°C	Celsius	1.8C+32	Fahrenheit	°F
ILLUMINATION				
lx	lux	0.0929	foot-candles	fc
cd/m ²	candela per square meter	0.2919	foot-Lamberts	fl
FORCE & PRESSURE or STRESS				
N	newtons	0.225	poundforce	lbf
kPa	kilopascals	0.145	poundforce per square inch	lbf/in ²

*SI is the symbol for the International System of Units. Appropriate rounding should be made to comply with Section 4 of ASTM E380.

TABLE OF CONTENTS

DISCLAIMER STATEMENT ii

UNCERTAINTY OF MEASUREMENT STATEMENT ii

INDEPENDENT APPROVING AUTHORITY..... ii

ACKNOWLEDGEMENTS iii

LIST OF FIGURES viii

LIST OF TABLES xi

1 INTRODUCTION 1

 1.1 Background 1

 1.2 Objective 1

 1.3 Scope..... 2

2 LITERATURE REVIEW 3

 2.1 Bridge Rail Height 3

 2.2 Bridge Rail Design Loads 5

 2.3 Traffic Face Geometry 7

 2.4 Barrier Strength..... 8

 2.4.1 Effective Load Height and Flexure Strength 8

 2.4.2 Punching Shear 8

 2.5 Deck Design..... 10

 2.5.1 Deck Design Cases 11

 2.5.2 Critical Deck Sections..... 11

 2.5.3 Deck Loading and Distribution..... 12

 2.6 Head Slap Mitigation 14

3 BARRIER ANALYSIS AND DESIGN 16

 3.1 Barrier Geometry 16

 3.2 Design Load 17

 3.3 Barrier Reinforcement Optimization 17

 3.4 Bridge Rail End Region Design..... 19

4 DECK ANALYSIS AND DESIGN..... 20

 4.1 Deck Design Methodology 20

 4.2 Deck Design Results 23

5 TEST REQUIREMENTS AND EVALUATION CRITERIA 25

 5.1 Test Requirements 25

 5.2 Evaluation Criteria 26

6 DESIGN DETAILS 28

7 TEST CONDITIONS..... 46

- 7.1 Test Facility 46
- 7.2 Vehicle Tow and Guidance System 46
- 7.3 Test Vehicle 46
- 7.4 Simulated Occupant 52
- 7.5 Data Acquisition Systems 52
 - 7.5.1 Accelerometers 52
 - 7.5.2 Rate Transducers 52
 - 7.5.3 Retroreflective Optic Speed Trap 52
 - 7.5.4 Digital Photography 53

- 8 FULL-SCALE CRASH TEST NO. 4CBR-1 55
 - 8.1 Weather Conditions 55
 - 8.2 Test Description 55
 - 8.3 Barrier Damage 63
 - 8.4 Vehicle Damage 68
 - 8.5 Occupant Risk 74
 - 8.6 Impact Loads 75
 - 8.7 Discussion 76

- 9 SUMMARY, CONCLUSIONS, AND RECOMMENDATIONS 78

- 10 MASH EVALUATION 81

- 11 REFERENCES 83

- 12 APPENDICES 87
 - Appendix A. Material Specifications 88
 - Appendix B. Vehicle Center of Gravity Determination 100
 - Appendix C. Vehicle Deformation Records 102
 - Appendix D. Accelerometer and Rate Transducer Data Plots, Test No. 4CBR-1 108

LIST OF FIGURES

Figure 1. SUT Rollover in MwRSF TL-4 Test with 32-in. Tall Barrier [4].....	3
Figure 2. SUT Rollover in TTI TL-4 Test with 32-in. Tall Barrier [5]	4
Figure 3. SUT Critical Scenario in Simulated TL-4 Test with 36-in. Tall Barrier [9]	4
Figure 4. SUT Stability in TL-4 Test with 36-in. Tall Barrier [9].....	5
Figure 5. 1100C Small Car Roll during MASH Impacts into Various Barrier Shapes	7
Figure 6. Punching Shear Failures of Concrete Barriers [29].....	9
Figure 7. Punching Shear Failure Patterns for (a) Interior Sections and (b) End Sections.....	10
Figure 8. AASHTO LRFD BDS Bridge Deck Overhang Design Cases	11
Figure 9. Deck Overhang Design Sections	12
Figure 10. Transmission of Impact Loads into Deck Overhang, Interior Section.....	13
Figure 11. Transmission of Impact Loads into Deck Overhang, End Section	14
Figure 12. Measurement of Head Ejection Envelope [7]	15
Figure 13. Head Ejection Envelope for Barrier Design [7]	15
Figure 14. Barrier Geometries	16
Figure 15. Cross Sections of Concrete Bridge Rail Design.....	19
Figure 16. Photo [27] and Diagram Showing Locations for Critical Deck Design Sections	21
Figure 17. Distribution of Impact Demands to Deck Design Sections 1 and 2, Interior Section.....	22
Figure 18. Distribution of Impact Demands to Deck Design Sections 1 and 2, End Section.....	22
Figure 19. TL-4 Bridge Rail Test Installation, Test No. 4CBR-1	30
Figure 20. Isometric View, Test No. 4CBR-1	31
Figure 21. System Cross Sections, Test No. 4CBR-1.....	32
Figure 22. TL-4 Bridge Rail Design Details, Test No. 4CBR-1.....	33
Figure 23. Rail, Deck, and Grade Beam Assemblies, Test No. 4CBR-1.....	34
Figure 24. Bridge Deck and Rail Sections, Test No. 4CBR-1.....	35
Figure 25. Bridge Deck Assembly, Test No. 4CBR-1.....	36
Figure 26. Bridge Deck Assembly, Test No. 4CBR-1.....	37
Figure 27. Bridge Deck Details, Test No. 4CBR-1	38
Figure 28. Modified Bridge Rail for Downstream Half of System, Test No. 4CBR-1	39
Figure 29. Design Details for Downstream Half of System, Test No. 4CBR-1	40
Figure 30. Concrete Grade Beam Assembly, Test No. 4CBR-1	41
Figure 31. System Rebar, Test No. 4CBR-1.....	42
Figure 32. System Rebar, Test No. 4CBR-1.....	43
Figure 33. Bill of Materials, Test No. 4CBR-1.....	44
Figure 34. Test Installation Photographs, Test No. 4CBR-1	45
Figure 35. Test Vehicle, Test No. 4CBR-1.....	47
Figure 36. Test Vehicle Ballast, Test No. 4CBR-1.....	48
Figure 37. Test Vehicle’s Interior Floorboards and Undercarriage, Test No. 4CBR-1	49
Figure 38. Vehicle Dimensions, Test No. 4CBR-1	50
Figure 39. Target Geometry, Test No. 4CBR-1.....	51
Figure 40. Camera Locations, Speeds, and Lens Settings, Test No. 4CBR-1	54
Figure 41. Impact Location, Test No. 4CBR-1.....	57
Figure 42. Sequential Photographs, Test No. 4CBR-1	58
Figure 43. Additional Sequential Photographs, Test No. 4CBR-1	59
Figure 44. Additional Sequential Photographs, Test No. 4CBR-1	60

Figure 45. Documentary Photographs, Test No. 4CBR-1	61
Figure 46. Vehicle Final Position and Trajectory Marks, Test No. 4CBR-1.....	62
Figure 47. Overall System Damage, Test No. 4CBR-1	64
Figure 48. System Damage, Downstream Gouge Details, Test No. 4CBR-1	65
Figure 49. System Damage, Backside of Bridge Rail, Test No. 4CBR-1	66
Figure 50. Deck Damage, Test No. 4CBR-1	67
Figure 51. Permanent Set, Dynamic Deflection, and Working Width, Test No. 4CBR-1	68
Figure 52. Vehicle Damage after Primary Impact	69
Figure 53. Left- and Right-Side Vehicle Damage, Test No. 4CBR-1	70
Figure 54. Rear Vehicle Damage, Test No. 4CBR-1.....	71
Figure 55. Post-Test Undercarriage Photos, Test No. 4CBR-1	72
Figure 56. Post-Test Floor Pan Photos, Test No. 4CBR-1	73
Figure 57. Perpendicular and Tangential Impact Forces, Test No. 4CBR-1	75
Figure 58. Summary of Test Results, Test No. 4CBR-1	77
Figure A-1. Bridge Deck Concrete Material Specification, Test No. 4CBR-1 (Item No. a1).....	90
Figure A-2. Bridge Deck, Concrete Strength Tests, Test No. 4CBR-1 (Item No. a1)	91
Figure A-3. Bridge Rail Concrete Material Specification, Test No. 4CBR-1 (Item No. a2)	92
Figure A-4. Bridge Rail Concrete Material Specification, Test No. 4CBR-1 (Item No. a2)	93
Figure A-5. Grade Beam Concrete Material Specification, Test No. 4CBR-1 (Item No. a3).....	94
Figure A-6. Grade Beam, Concrete Strength Tests, Test No. 4CBR-1 (Item No. a3).....	95
Figure A-7. Overlay Material Specification, Test No. 4CBR-1 (Item No. a4).....	96
Figure A-8. #4 Rebar Material Specification, Test No. 4CBR-1 (Item Nos. b1, b2, b3, b7, and b11)	97
Figure A-9. #5 Rebar Material Specification, Test No. 4CBR-1 (Item Nos. b4, b6, b9, and b12)	97
Figure A-10. #4 Rebar Material Specification, Test No. 4CBR-1 (Item No. b5).....	98
Figure A-11. #5 Rebar Material Specification, Test No. 4CBR-1 (Item Nos. b8 and b10)	98
Figure A-12. #4 Rebar Material Certification, Test No. 4CBR-1 (Item No. b13).....	99
Figure B-1. Vehicle Mass Distribution, Test No. 4CBR-1	101
Figure C-1. Floor Pan Deformation Data – Set 1, Test No. 4CBR-1	103
Figure C-2. Floor Pan Deformation Data – Set 2, Test No. 4CBR-1	104
Figure C-3. Occupant Compartment Deformation Data – Set 1, Test No. 4CBR-1.....	105
Figure C-4. Occupant Compartment Deformation Data – Set 2, Test No. 4CBR-1.....	106
Figure C-5. Maximum Occupant Compartment Deformation, Test No. 4CBR-1.....	107
Figure D-1. 10-ms Average Longitudinal Acceleration (SLICE-1, cab), Test No. 4CBR-1	109
Figure D-2. Longitudinal Change in Velocity (SLICE-1, cab), Test No. 4CBR-1	110
Figure D-3. Longitudinal Occupant Displacement (SLICE-1, cab), Test No. 4CBR-1	111
Figure D-4. 10-ms Average Lateral Acceleration (SLICE-1, cab), Test No. 4CBR-1.....	112
Figure D-5. Lateral Change in Velocity (SLICE-1, cab), Test No. 4CBR-1.....	113
Figure D-6. Lateral Occupant Displacement (SLICE-1, cab), Test No. 4CBR-1	114
Figure D-7. Vehicle Angular Displacements (SLICE-1, cab), Test No. 4CBR-1	115
Figure D-8. Acceleration Severity Index (SLICE-1, cab), Test No. 4CBR-1	116
Figure D-9. 10-ms Average Longitudinal Acceleration (SLICE-2, c.g.), Test No. 4CBR-1	117
Figure D-10. Longitudinal Change in Velocity (SLICE-2, c.g.), Test No. 4CBR-1	118
Figure D-11. Longitudinal Occupant Displacement (SLICE-2, c.g.), Test No. 4CBR-1	119
Figure D-12. 10-ms Average Lateral Acceleration (SLICE-2, c.g.), Test No. 4CBR-1.....	120
Figure D-13. Lateral Change in Velocity (SLICE-2, c.g.), Test No. 4CBR-1	121

Figure D-14. Lateral Occupant Displacement (SLICE-2, c.g.), Test No. 4CBR-1122
Figure D-15. Vehicle Angular Displacements (SLICE-2, c.g.), Test No. 4CBR-1123
Figure D-16. Acceleration Severity Index (SLICE-2, c.g.), Test No. 4CBR-1124

LIST OF TABLES

Table 1. Design Loads for Traffic Railings, AASHTO LRFD BDS	5
Table 2. TL-4 Impact Force Variation with Barrier Height [19]	6
Table 3. NCHRP Report 22-20(2) TL-4 Design Parameters [19]	7
Table 4. Recommended MASH TL-4 Design Impact Loads for Traffic Barriers [19]	17
Table 5. Top Design Options Based on Optimization Analysis	18
Table 6. Design Cases for Bridge Deck Overhangs	20
Table 7. Results of Critical Deck Overhang Design Loads	23
Table 8. MASH 2016 [3] TL-4 Crash Test Conditions for Concrete Barriers	25
Table 9. MASH 2016 Evaluation Criteria for Longitudinal Barriers	27
Table 10. Weather Conditions, Test No. 4CBR-1	55
Table 11. Sequential Description of Impact Events, Test No. 4CBR-1	56
Table 12. Maximum Occupant Compartment Intrusion by Location, Test No. 4CBR-1	74
Table 13. Summary of OIV, ORA, THIV, PHD, and ASI Values, Test No. 4CBR-1	74
Table 14. Summary of Safety Performance Evaluation	80
Table A-1. Bill of Materials, Test No. 4CBR-1	89

1 INTRODUCTION

1.1 Background

The majority of existing standards for concrete bridge rails were designed and evaluated according to the safety performance criteria published in the National Cooperative Highway Research Program (NCHRP) Report 350 [1]. Testing according to Test Level 4 (TL-4) impact conditions of NCHRP Report 350 demonstrated that 32-in. tall barriers had sufficient height to contain and redirect a 17,600-lb single-unit truck (SUT) (designated 8000S). However, with the adoption of the American Association of State Highway and Transportation Officials (AASHTO) *Manual for Assessing Safety Hardware* (MASH) in 2009 [2] and its second edition in 2016 [3], the TL-4 SUT vehicle became 4,400 lb heavier, and the impact speed was increased from 50 mph to 56 mph. The increased mass and impact speed have resulted in the MASH 22,000-lb SUT (designated 10000S) rolling over the top of multiple 32-in. tall rigid barriers [4-5]. Thus, the minimum height of MASH TL-4 barriers was increased to 36 in. to satisfy the current crash testing standard.

Additionally, roadway overlays reduce the effective height of the barrier relative to the new roadway surface and increase the likelihood of an impacting vehicle overriding the barrier. Retrofitting existing barriers to account for this loss of height can be costly, so many state departments of transportation (DOTs) are beginning to install barriers taller than their nominal heights to account for future roadway overlays.

With the increase in vehicle mass and impact speed, the MASH criteria also resulted in increased impact loading for TL-4 bridge rails. These increased loads may potentially result in premature failure of existing bridge rails that were designed for lower impact loads. Additionally, these higher impact loads may be transferred to the bridge deck and cause greater damage. New bridges should be designed with railings and decks that can resist MASH impact loads while minimizing the potential for damage.

Many of the existing concrete bridge rail standards utilize New Jersey shape or F-shape configurations, commonly referred to as safety shapes. However, research has shown that taller slope break points for safety shape barriers can increase vehicle climb, instability, and rollover rates, especially for passenger vehicles. One study found that 5.7 percent of safety shape barrier crashes result in rollover, and that safety shape barriers have roughly twice the rollover rate of vertical barriers [6], which becomes critical as rollover crashes are more likely to be severe or fatal than non-rollover crashes. Full-scale crash testing on safety shape barrier systems has also shown significant vehicle climb and roll during impact events with passenger vehicles. Alternatively, full-scale crash tests into vertical-faced barriers have demonstrated little to no propensity for passenger vehicles to climb the barrier or roll over [7]. Therefore, an optimized, MASH-compliant, TL-4 concrete bridge rail was desired to satisfy design loads, improve vehicle stability, and accommodate future roadway overlays up to 3 in. thick.

1.2 Objective

The objective of this research effort was to develop a MASH-compliant, TL-4 concrete bridge rail. The bridge rail had to remain crashworthy after roadway overlays up to 3 in. thick. The bridge rail design was to be optimized to satisfy MASH TL-4 design loads, improve vehicle

stability, minimize installation costs, and minimize the potential for deck damage. Details were desired for both interior and end regions of the barrier. Further, minimum deck strengths were determined, and a deck overhang design procedure was provided for users desiring to modify their existing deck details. Finally, full-scale crash testing was conducted to evaluate the MASH safety performance of the bridge rail, damage to barrier and deck, and the working width for the new barrier.

1.3 Scope

The research objective was achieved through the completion of several tasks. First, a review of existing literature and state DOT plans was conducted. Next, the barrier design was optimized to satisfy MASH TL-4 impact conditions, maximize vehicle stability, and minimize installation costs. Additionally, a deck overhang design methodology was established and used to design a bridge deck to support the new railing. One full-scale crash test was conducted on the TL-4 bridge rail according to MASH 2016 [3] test designation no. 4-12. The test was conducted in compliance with the Midwest Roadside Safety Facility's (MwRSF) list of accredited testing services granted by the A2LA laboratory accreditation body (A2LA Cert. No. 2937.01). The test results were analyzed, evaluated, and documented. Conclusions and recommendations were then made pertaining to the safety performance of the TL-4 bridge rail.

2 LITERATURE REVIEW

Transitioning from the prior NCHRP Report 350 [1] testing standards to the current MASH 2016 [3] testing standards involved significant changes to vehicle characteristics and impact conditions. Specific to TL-4, the weight of the SUT vehicle increased 25 percent, and the impact speed increased from 50 mph to 56 mph, thus increasing the impact severity of this test by 56 percent. This increased impact severity imposed more severe demands on MASH TL-4 bridge rails. Thus, a literature review was conducted to form a base of information from which the optimized bridge rail could be designed. Key areas of interest included (1) the required bridge rail height to contain the 10000S test vehicle, (2) updated MASH TL-4 design loads, (3) optimal bridge rail shape, (4) overhang deck design, and (5) head slap mitigation.

2.1 Bridge Rail Height

In 2006, MwRSF conducted a full-scale crash test according to the proposed impact conditions MASH test designation no. 4-12 on a 32-in. tall New Jersey safety shape barrier [4]. Note, MASH had not yet been finalized and published at the time of the crash test. While the 32-in. test article was proven adequate for TL-4 conditions under NCHRP Report 350, it failed to redirect the impacting vehicle, and the SUT rolled over the barrier, as shown in Figure 1.



Figure 1. SUT Rollover in MwRSF TL-4 Test with 32-in. Tall Barrier [4]

In a similar study, Texas A&M Transportation Institute (TTI) conducted a MASH test designation no. 4-12 crash test on another 32-in. tall New Jersey safety shape bridge rail [5]. In this 2010 test, the SUT rolled 101 degrees, traversed past the end of the test installation, and ultimately came to rest upright. Researchers determined that the vehicle would have rolled over the barrier had the test installation length been longer. The roll angle experienced near the end of the barrier installation is shown in Figure 2. Both of these studies illustrated that 32-in. tall barriers were no longer sufficient to contain the TL-4 SUT according to MASH impact conditions.



Figure 2. SUT Rollover in TTI TL-4 Test with 32-in. Tall Barrier [5]

Multiple studies were performed to establish a new minimum height for MASH TL-4 barriers. In 2011, researchers at TTI conducted a parametric simulation study using a nonlinear finite element analysis software called LS-DYNA [8] to investigate the effect of barrier height on vehicle stability [9]. Rigid, single-slope barriers of varying height were impacted in a series of simulated tests consistent with MASH test designation no. 4-12. Beginning with a barrier height of 42 in., the height was incrementally reduced until a critical vehicle roll angle was observed at a barrier height of 36 in., as shown in Figure 3. As a result, a minimum height requirement of 36 in. was proposed for further evaluation in that study.

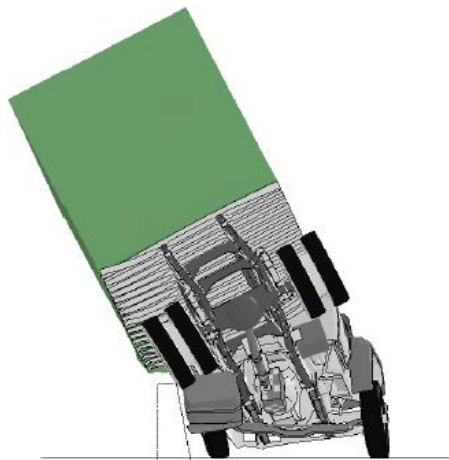


Figure 3. SUT Critical Scenario in Simulated TL-4 Test with 36-in. Tall Barrier [9]

Subsequently, a full-scale crash test conforming to MASH test designation no. 4-12 was performed on a 36-in. tall single-slope concrete barrier. The results of the test were consistent with the simulation study, and the SUT was contained and redirected while maintaining its stability, as shown in Figure 4. To date, the minimum rigid barrier height (including all concrete barrier shapes and steel bridge rails) to satisfy MASH TL-4 criteria has been 36 in.



Figure 4. SUT Stability in TL-4 Test with 36-in. Tall Barrier [9]

2.2 Bridge Rail Design Loads

A multitude of methods for estimating traffic impact loads have been described in roadside safety literature. An early, widespread method was Olson’s 1970 method documented in NCHRP Report No. 86, which relied on simplified vehicle and impact geometry [10]. In 1978, Hirsch proposed a modification to this method, converting Olson’s average force estimate to a peak estimate with further idealization of the impact scenario [11]. Alternatively, in 1993, Fallor proposed a rudimentary impulse-momentum based method [12]. Although these methods have been used in prior roadside safety designs and evaluations, more robust methods have been developed since their formulation.

While the above methods relied on mechanics and idealizations of the impact scenario, alternative methods involving actual load measurement have also been utilized. Instrumented wall tests, in which impacted barriers were equipped with load cells and accelerometers to directly measure impact loads, were performed by Noel et al. in 1981 [13] and by Beason et al. in 1989 [14]. The instrumented wall tests were robust, accounting for complicated impact behavior that was not considered in a theoretical analysis. In fact, the current lateral design loads presented in the *AASHTO LRFD Bridge Design Specifications*, 8th Edition (AASHTO LRFD BDS) [15] were derived from the results of the instrumented wall tests performed by Beason et al. [14]. The AASHTO LRFD BDS design loads are shown in Table 1.

Table 1. Design Loads for Traffic Railings, AASHTO LRFD BDS

Design Forces and Designations	Railing Test Levels					
	TL-1	TL-2	TL-3	TL-4	TL-5	TL-6
Impact Force, F_t (kips)	13.5	27.0	54.0	54.0	124.0	175.0
Friction Force, F_L (kips)	4.5	9.0	18.0	18.0	41.0	58.0
Vertical Force, F_v (kips)	4.5	4.5	4.5	18.0	80.0	80.0
Length of Force, L_t and L_L (ft)	4.0	4.0	4.0	3.5	8.0	8.0
Length of Vertical Force, L_v (ft)	18.0	18.0	18.0	18.0	40.0	40.0
Effective Load Height, H_e (in.)	18.0	20.0	24.0	32.0	42.0	56.0
Minimum Height of Rail, H (in.)	27.0	27.0	27.0	32.0	42.0	90.0

Another method to measure actual crash test impact loads utilized the on-board vehicle accelerometers and the inertia of the vehicle. Typically, in full-scale crash tests, the test vehicle is equipped with accelerometers to measure lateral, longitudinal, and vertical accelerations. Using the acceleration data from these instruments, impact force estimates can be derived from Newton’s second law of motion, force equals mass times acceleration. A procedure for estimating impact forces using vehicle deceleration data was outlined by Eller et al. [16]. The lateral and longitudinal coordinate system was transformed to coincide with that of the barrier using yaw measurements, and lateral impact forces were calculated accordingly using vehicle deceleration measurements. Utilizing this load analysis method on test data from the RESTORE barrier [17] and a steel tube bridge rail [18], the TL-4 impact loads have been estimated to be between 95 kips and 110 kips.

Impact forces can also be estimated from computer simulations. The most recent estimation of TL-4 impact demands was produced by Bligh et al. in 2017 under NCHRP Project 22-20(2) [19] using LS-DYNA [8]. In this effort, simulations of SUT impacts with rigid barriers of varying heights were performed, and impact loads and load application locations were extracted. Impact forces were found to vary significantly with the barrier height, as shown in Table 2. Taller barrier heights resulted in more direct contact between the side of the cargo box and the barrier, which increases the magnitude and height of the lateral loads during impact.

Table 2. TL-4 Impact Force Variation with Barrier Height [19]

Design Parameter	Barrier Height (in.)			
	36	39	42	Tall
Impact Force, F_t (kips)	67.2	72.3	79.1	93.3
Friction Force, F_L (kips)	21.6	23.6	26.8	27.5
Vertical Force, F_v (kips)	37.8	32.7	22.0	N/A
Length of Forve, L_t and L_L (ft)	4	5	5	14
Effective Load Height, H_e (in.)	25.1	28.7	30.2	45.5

N/A – Not Applicable

Due to the variation of impact forces with respect to barrier height, Bligh et al. recommended the division of TL-4 into subcategories based on the height of the barrier. Proposed subcategory TL-4-1 corresponded to the minimum barrier height of 36 in. required for vehicle stability. Subcategory TL-4-2 corresponded to barriers taller than the minimum height. The final design parameters are collected in Table 3. It should be noted that the parameters proposed in this study were associated with simulated impacts with rigid barriers. In reality, any barrier deformations or displacements would result in decreasing the sustained impact force. Since concrete barriers only minimally deform, the design loads for rigid barriers were applicable.

Table 3. NCHRP Report 22-20(2) TL-4 Design Parameters [19]

Design Parameter	Railing Test Level	
	TL-4-1	TL-4-2
Bridge Rail Height, H (in.)	36	> 36
Lateral Force, F_t (kips)	70	80
Longitudinal Force, F_L (kips)	22	27
Vertical Force, F_v (kips)	38	33
Length of Lateral Force, L_L (ft)	4	5
Length of Vertical Force, L_v (ft)	18	18
Effective Load Height, H_e (in.)	25	30

2.3 Traffic Face Geometry

In a 2011 analysis of actual crash data, Albuquerque et al. investigated the relationship between rollover propensity (i.e., the propensity for a redirected vehicle to roll at least 90 degrees on the roadway) and the traffic face shape of the impacted barrier [20]. In this investigation, it was determined that safety shape rails are at 1.7 to 2.1 times more likely to cause vehicle rollovers as compared to vertical-faced barriers. Since vehicle rollovers are associated with increased risk of fatalities and serious injuries, these findings would support vertical-faced barriers being a safer barrier shape than safety shapes.

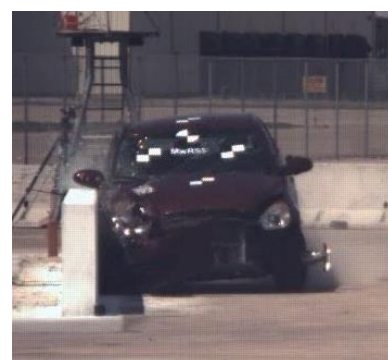
A 2007 study of over 100 previously conducted crash tests reached similar conclusions [21]. Safety shape barriers showed higher tire climb and vehicle roll during crash testing. Single slope barriers showed improved vehicle stability over safety shape barriers, but still had moderate amounts of climb and roll. Vertical face barriers minimized tire climb and vehicle roll with only slightly increased vehicle decelerations (well within MASH safety limits). Examples of vehicle roll and climb are shown in Figure 5.



New Jersey
Test No. 2214NJ-1 [22]



Single Slope
Test No. 140MASH3c16-04 [23]



Vertical
Test No. H34BR-1 [24]

Figure 5. 1100C Small Car Roll during MASH Impacts into Various Barrier Shapes

2.4 Barrier Strength

For decades, the strength of concrete bridge rails has been calculated using yield-line theory, which is based on the plastic bending failure of the barrier over a predetermined failure shape. Equations for calculating barrier capacity using yield-line theory are provided in Section 13 of AASHTO LRFD BDS [15]. Contemporary research has identified mechanisms contributing to the capacity of concrete barriers, which have not been considered in past design efforts. These mechanisms include punching shear failure and the relationship of effective load height on barrier capacity.

2.4.1 Effective Load Height and Flexure Strength

The current yield-line calculations published within AASHTO LRFD BDS assume that the load is applied at the top of the barrier. However, recent research conducted as part of NCHRP Project 22-20(2) has quantified effective impact heights and found them to be significantly lower than typical barrier heights [19]. Due to the overestimation of load application height in the current methodology, Silvestri-Dobrovoly et al. suggested many concrete barriers have been designed with an unintentional reserve capacity over the historical AASHTO design loads [25].

In the derivation of yield-line equations, the internal absorbed energy within the bending failure was set equal to the external work done (i.e., impact load multiplied by displacement within the barrier's deformed shape). The internal energy at failure is assumed to be constant, but the displacement of the barrier would vary along the height of the barrier. As such, the failure load increases as the effective impact load height decreases. Altering the current yield-line equations to account for the effective load height of an impact event results in the modified barrier strength, $R_{w\text{-eff}}$, being equal to the standard yield-line strength, R_w , multiplied by the ratio of the barrier height, H , over the effective load height, H_e [26]. This relationship is shown in Equation 1.

$$R_{w\text{-eff}} = R_w \left(\frac{H}{H_e} \right) \quad (1)$$

2.4.2 Punching Shear

Existing AASHTO LRFD BDS guidance does not discuss punching shear as a possible failure mechanism for concrete barriers. However, recent research has demonstrated that punching shear behavior can occur and may control the strength of concrete barriers [27-29]. Examples of punching shear failures in concrete barriers are shown in Figure 6.



Figure 6. Punching Shear Failures of Concrete Barriers [29]

According to ACI 318 [30], punching shear strength can be conservatively estimated with Equation 2 for strip loading:

$$V_c = 2\lambda\sqrt{f'_c}b_o d \quad (2)$$

where λ is the lightweight concrete factor, f'_c is the concrete compressive strength (psi), b_o is the critical perimeter, and d is the average depth of the barrier across the punching shear region. Consideration of the shear strength of the steel is permitted if the barrier is at least 6 in. thick and at least sixteen times as deep as the shear reinforcement bar diameter.

The critical perimeter for barrier punching shear can be defined by a box formed around the impact load applied over a length of L_t and at a height of H_e [26]. Shear failure surfaces extend outward from the loaded region at approximately 45-degree angles. Thus, mid-depth of the shear failure region extends a distance equal to half the depth, $d/2$, below the impact region and on both the upstream and downstream ends of the impact region. The assumed shear failure perimeters for both interior and end section conditions are demonstrated in Figure 7.

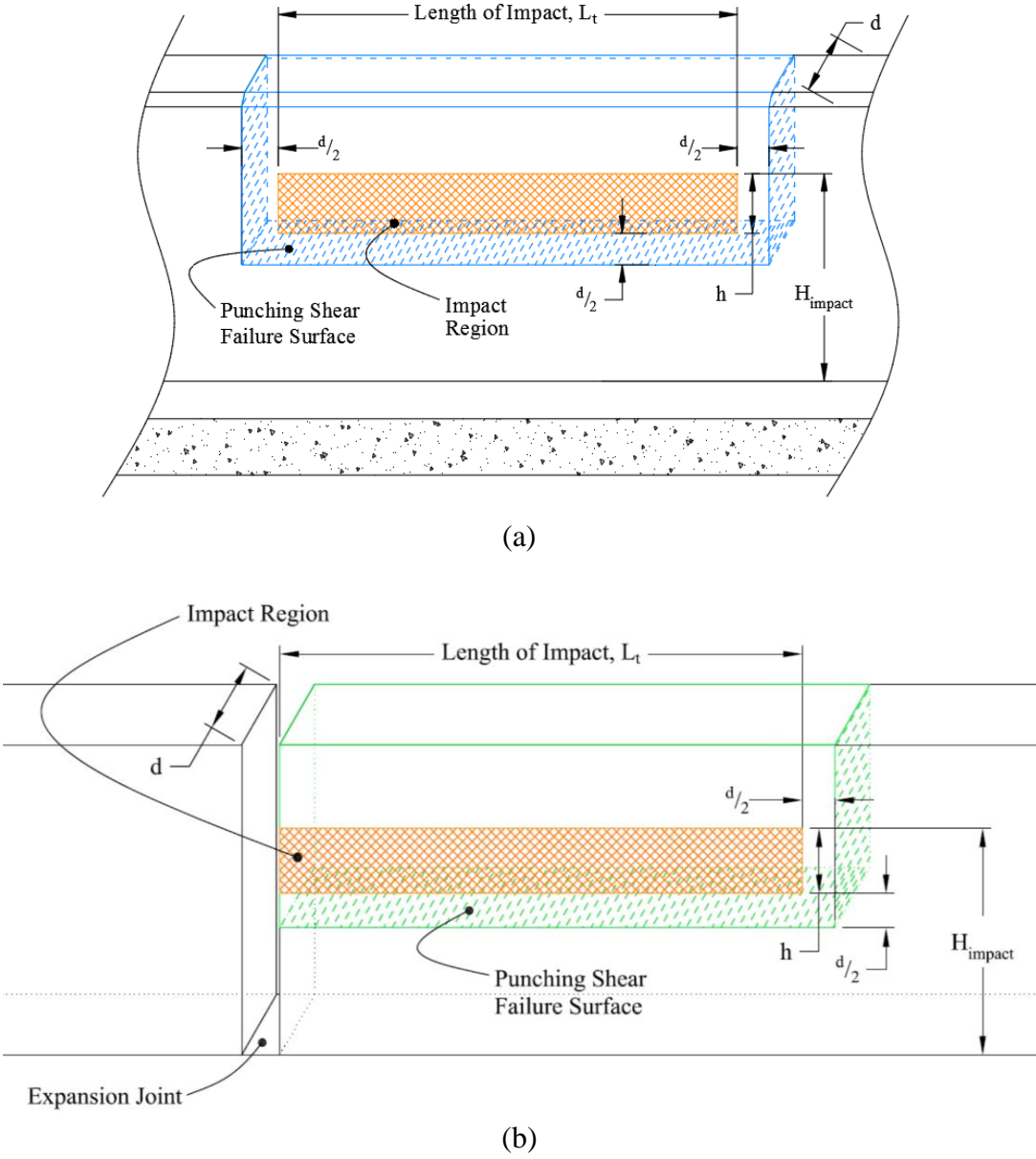


Figure 7. Punching Shear Failure Patterns for (a) Interior Sections and (b) End Sections

2.5 Deck Design

The integrity of any bridge rail system is dependent upon the deck structure to which it is secured. The design of the bridge deck is of equal importance to that of the bridge rail, as either can limit the strength of the overall system in the event of a vehicle impact. The bridge deck overhang, or the cantilevered portion of the bridge deck protruding from the outermost girder, is particularly sensitive to railing impacts.

2.5.1 Deck Design Cases

Bridge deck overhangs are subjected to a suite of loads varying in application, magnitude, direction of force, and likelihood of occurrence. As such, the design of bridge deck overhangs requires consideration of multiple load cases. AASHTO LRFD BDS [15] guidance specifies three design cases by which deck overhangs must be analyzed. Cases are considered independently, though dead loads produced by the barrier, deck slab, and wearing surface are considered in each case.

Design Case 1 includes the lateral impact forces, F_t , developed during vehicle impacts with the bridge rail, and is analyzed considering the Extreme Event Load Combination II limit state. Design Case 2 includes the vertical impact forces, F_v , resulting from vehicle impacts to the bridge rail, and is also analyzed with the Extreme Event Load Combination II limit state. Both the lateral and vertical impact loads are functions of the Test Level of the bridge railing, as discussed in Section 2.2. Finally, Design Case III addresses the vertical vehicle wheel loads occupying the overhang region at any point in time. As such, Design Case 3 is independent of bridge rail impact considerations, and is analyzed with the Load Combination Strength I limit state. All three Design Cases are shown in Figure 8.

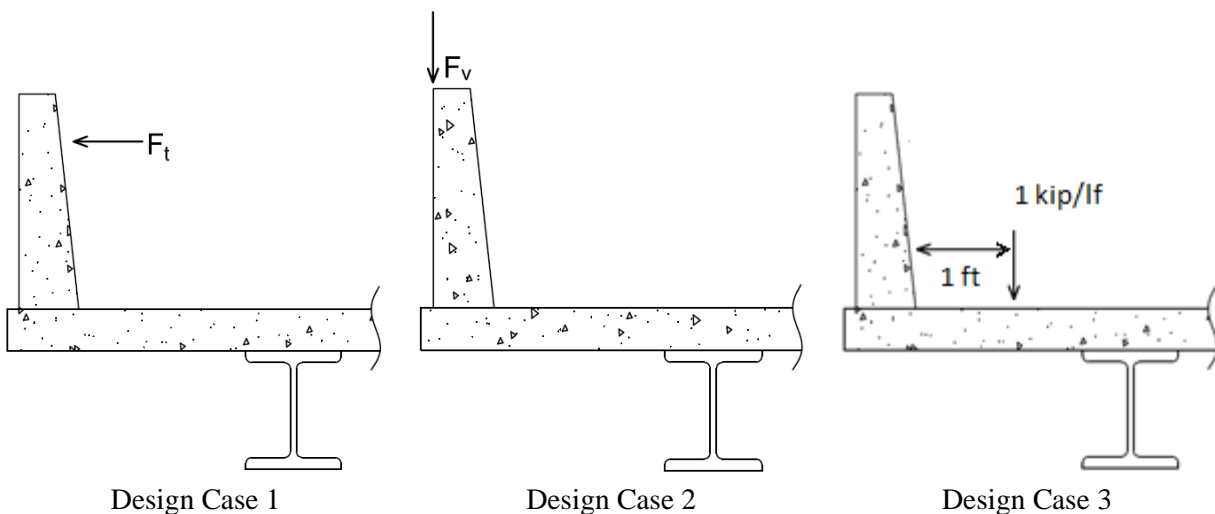


Figure 8. AASHTO LRFD BDS Bridge Deck Overhang Design Cases

2.5.2 Critical Deck Sections

AASHTO LRFD BDS does not specify the critical deck sections in which to analyze the provided design cases. However, other sources [27, 31-32] have identified two critical sections to be evaluated: (1) the deck section coincident with the face of the rail and (2) the deck section coincident with the critical girder section, where the critical girder section is determined in AASHTO LRFD BDS Article 4.6.2.1.6. For example, the critical section of an overhang on a concrete box is at the face of the box, and the critical section an overhang on a precast I-shaped concrete beam is at one-third of the flange width inset from the outer face of the flange. These recommendations are shown in Figure 9. Note, for Design Case 2, the deck section coincident with the rail face does not require analysis, as the vertical impact force acts at a very small moment arm.

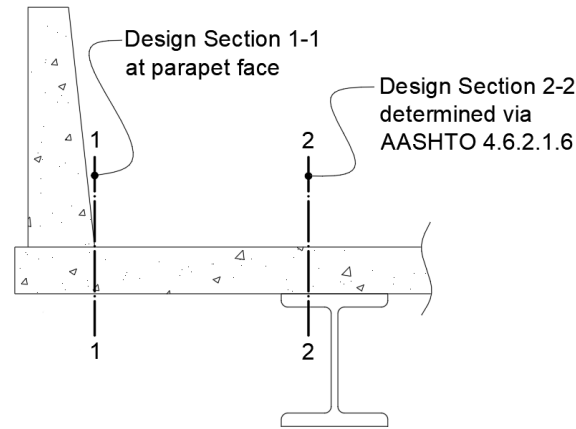


Figure 9. Deck Overhang Design Sections

2.5.3 Deck Loading and Distribution

For solid concrete bridge rails, AASHTO LRFD BDS suggests that for Design Case 1 the deck overhang may be designed to resist a unit-length flexural demand, M_s , acting coincident with a unit-length tensile force, T . The overhang design moment, M_s , may be greater than or equal to the overturn bending strength of the concrete barrier, M_c , at its base. The unit-length tensile force acting on the overhang section ($^k/ft$) is calculated as:

$$T = \frac{R_w}{L_c + 2H} \quad (3)$$

where R_w is the yield-line capacity of the barrier, L_c is the critical length of the barrier calculated during the Yield Line analysis, and H is the barrier height.

This methodology does not account for any longitudinal distribution of the impact loads along the deck and neglects to consider barriers designed with strengths far exceeding design loads. Thus, the AASHTO LRFD BDS methodology is highly conservative and can result in significantly oversized deck overhangs. In fact, both static testing and full-scale crash tests have been performed on deck overhangs with lower flexural strength than the barriers they support [33-34].

This conservatism is widely known and has led to alternative design methods growing in popularity within state DOTs and roadside safety agencies. One methodology simply reduces the design moment on the deck to only a portion of the barrier overturning moment, or αM_c , where $\alpha < 1.0$. Typical factors for α range from 0.7 to 0.9.

Other design methods utilize a lateral impact load to determine the moment demand on the deck and an enlarged length of deck over which the load is distributed. The lateral load can be defined as a factor of the design load, βF_t , where β can range from 1.0 to 1.5, or as the design capacity of the barrier, R_w , depending on the specific roadway agency and how conservatively they wish to design their decks [35]. The lateral load is applied at the effective load height, H_e , or at the full height of the barrier, H , if using an R_w calculated at the top of the barrier.

The moments and tensile loads created by the lateral loads described above are then distributed longitudinally along the deck overhang. At design section 1 at the face of the barrier, the design deck length is typically taken as the critical barrier length, L_c , as calculated within the yield-line analysis of the barrier, plus two times the barrier height, H , as shown in Equation 4. Essentially, the impact loads are assumed to spread outward at a 45-degree angle from the calculated failure shape as they travel downward through the barrier and into the deck [27, 31-32, 36], as shown in Figure 10.

$$L_{1-1} = L_c + 2H \quad (4)$$

AASHTO LRFD BDS suggested that deck loads in post-and-beam installations distribute at a 45-degree angle as they translate inward toward deck section 2 [15]. However, AASHTO does not provide guidance for solid concrete bridge rails. The Precast Concrete Institute Bridge Design Manual [36] and the National Highway Institute [31-32] suggest that deck loads distribute at a 30-degree angle, as demonstrated in Figure 10. Using a 30-degree angle, the deck design length at deck section 2 is calculated using Equation 5:

$$L_{2-2} = L_{1-1} + 2Y \tan 30^\circ \quad (5)$$

where Y is the distance from the face of the barrier to Design Section 2 over the external girder.

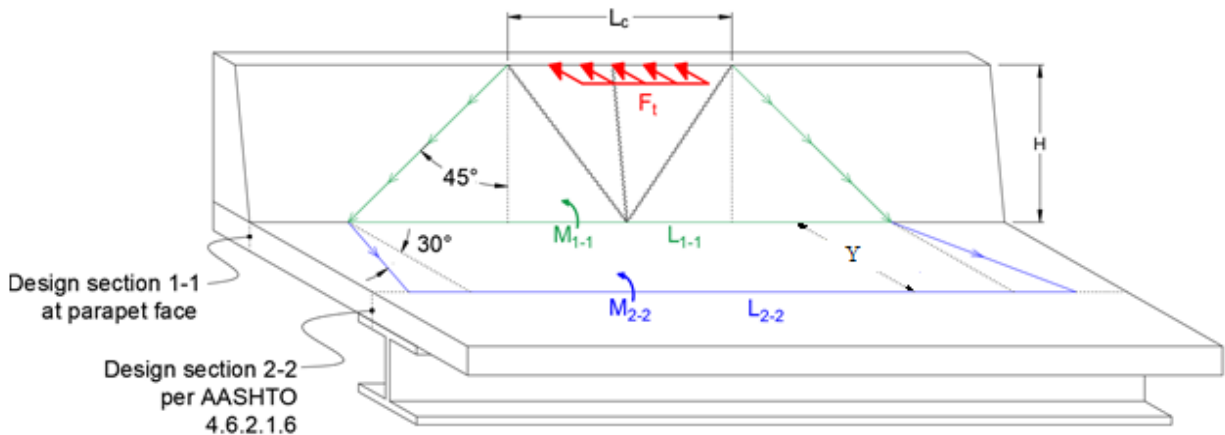


Figure 10. Transmission of Impact Loads into Deck Overhang, Interior Section

For impacts near discontinuities, such as expansion joints, impact loads would not distribute across the open joint. Thus, the load only distributes outward on the impact side, effectively shortening the deck design length, as shown in Figure 11.

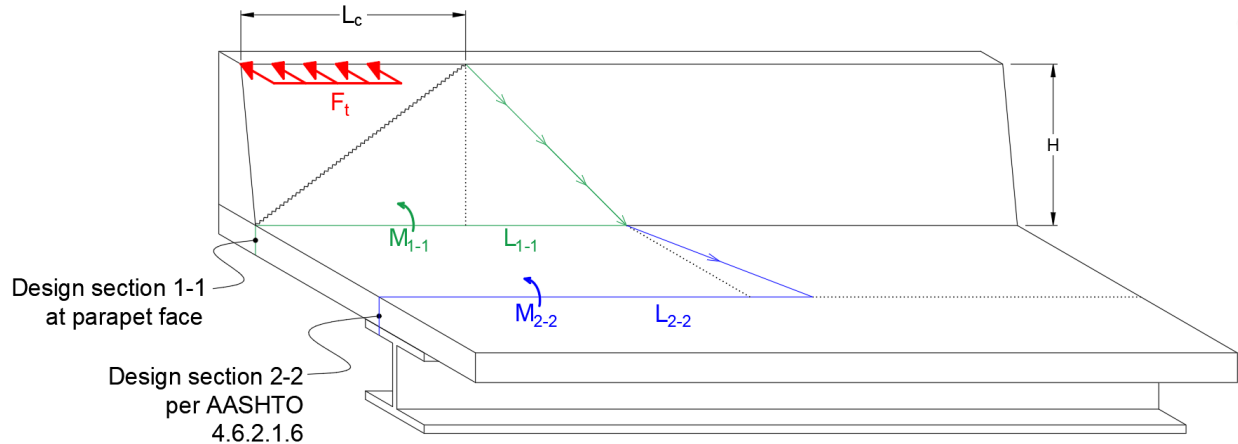


Figure 11. Transmission of Impact Loads into Deck Overhang, End Section

2.6 Head Slap Mitigation

Redirection of vehicles impacting safety shape barriers is typically characterized by vehicle roll away from the barrier. Alternatively, vertical and single-slope barriers do not allow significant climb and exert greater lateral forces onto impacting vehicles. As such, a significant risk of head-slap, or impact between the barrier and the vehicle occupant's head, arises for tall vertical and single-slope barriers. Head-slap is associated with high risks of serious injury or fatality.

In 2007, Rosenbaugh et al. analyzed digital video of full-scale crash tests to develop a head ejection envelope [7]. Lateral and vertical ejection of seatbelted dummies were measured from the lower edge of the window, as shown in Figure 12. By superimposing dummy head locations during multiple impacts, head ejection envelopes were developed for both small car and pickup truck impacts. The head ejection envelope was adjusted to account for vehicle roll toward the barrier and interpolated to account for midsize vehicles, such as SUVs and small pickup trucks. Barriers and attachments in violation of the head ejection envelope would be at risk for head slap during vehicle impacts. The final head ejection envelope is shown in Figure 13.



Figure 12. Measurement of Head Ejection Envelope [7]

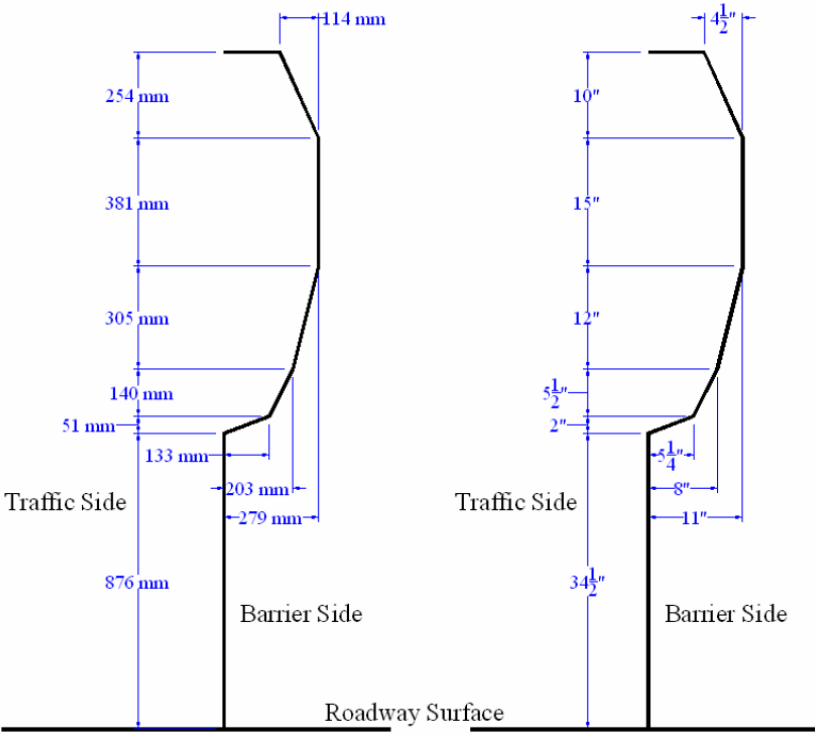


Figure 13. Head Ejection Envelope for Barrier Design [7]

3 BARRIER ANALYSIS AND DESIGN

3.1 Barrier Geometry

As discussed in Section 2.1, crash testing to MASH TL-4 impact criteria has demonstrated that the 10000S SUT will likely roll over the top of 32-in. tall rigid concrete barriers [4-5]. Conversely, 36-in. tall barriers have successfully contained and redirected the MASH TL-4 SUT [9, 18]. Thus, the height for the new TL-4 concrete bridge rail was required to be at least 36 in. A roadway overlay would reduce the effective height of the bridge rail, so the design height of the barrier needed to be increased by the thickness of any anticipated future overlays. This project assumed a maximum overlay thickness of 3 in.; thus, a 39-in. design height was selected for the new TL-4 bridge rail.

The barrier shape was designed to maximize vehicle stability during impacts while also being easy to construct. Studies have shown that vertical-faced barriers provide the best performance in terms of vehicle climb and stability during impact events as compared to safety shape, or even standard single-slope barriers [6-7], which typically have sloped front faces of either 9 degrees or 11 degrees away from vertical. However, tall vertical parapets are not easy to slipform and often result in concrete slumping near the base of the barrier. In a nationwide survey, most slipform contractors indicated they were confident in slipforming barriers with slopes (i.e., batters) as steep as 1H:24V. Taking these survey responses into consideration and desiring to have barrier dimensions be whole numbers, the top of the front face of the barrier was set back 2 in. from the base, which created a 1H:19.5V front slope.

Several state DOTs sponsoring this project desired to minimize the width of the bridge rail to maximize the traversable roadway width on narrow bridges. Accordingly, the back side of the barrier could be made vertical to reduce the width of the barrier. However, installations with a vertical back may require conventional formwork as opposed to slipforming. Barrier cross section options with a sloped back face and vertical back face with a top width, W , are shown in Figure 14.

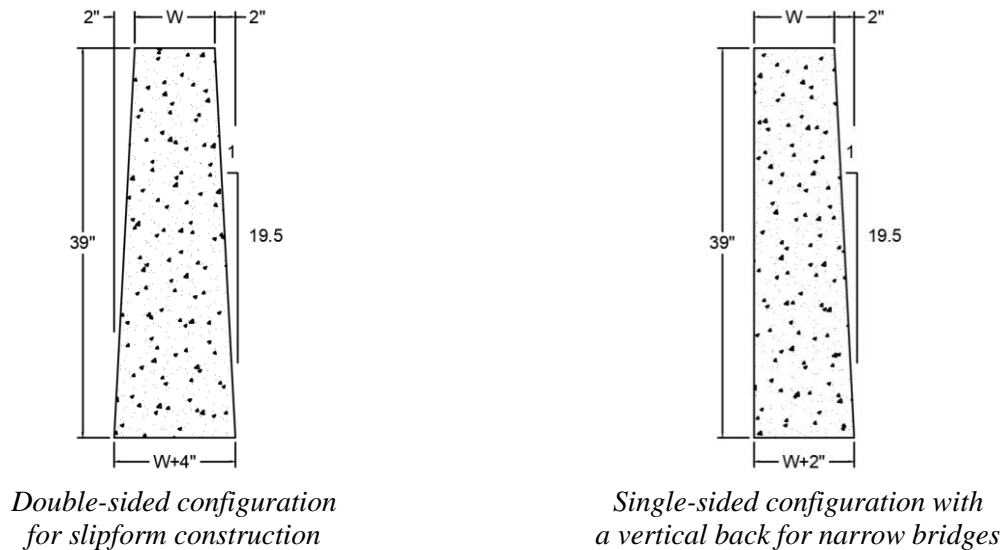


Figure 14. Barrier Geometries

3.2 Design Load

Section 13 of AASHTO LRFD BDS [15] provides design loads for traffic barriers based on test level. For a TL-4 barrier, the transverse impact load, F_t , is 54 kips. However, this design load was determined for the TL-4 impact conditions specified by NCHRP Report 350 [1], and Section 13 of AASHTO LRFD BDS has not been revised to include design loads for MASH barriers. Due to the increases in MASH SUT weight and speed as compared to NCHRP Report 350 conditions, MASH TL-4 design loads were expected to be higher than those listed in AASHTO LRFD BDS.

As discussed in Section 2.2, researchers at TTI recently conducted an LS-DYNA simulation study to evaluate barrier design loads under MASH impact conditions as part of NCHRP Project 22-20(2) [19]. MASH TL-4 impacts were simulated with rigid barriers ranging from 36-in. to 90-in. heights. As the barrier height increased, the amount of roll experienced by the TL-4 truck decreased, the magnitude of the impact force increased, and the effective height of the impact force increased. Subsequently, different TL-4 design loads were recommended for 36-in. tall barriers (designated TL-4-1) and barriers taller than 36 in. (designated TL-4-2), as shown in Table 4. Since the new TL-4 concrete bridge rail was designed with a 39-in. height, the design load was selected as 80 kips at an effective height of 30 in. above the roadway in accordance with the recommendations for TL-4-2.

Table 4. Recommended MASH TL-4 Design Impact Loads for Traffic Barriers [19]

Design Parameter	Railing Test Level	
	TL-4-1	TL-4-2
Bridge Rail Height, H (in.)	36	> 36
Lateral Force, F_t (kips)	70	80
Longitudinal Force, F_L (kips)	22	27
Vertical Force, F_v (kips)	38	33
Distribution of Lateral Force, L_L (ft)	4	5
Distribution of Vertical Force, L_v (ft)	18	18
Height of Resultant Load, H_e (in.)	25	30

3.3 Barrier Reinforcement Optimization

The optimal bridge rail configuration was defined as having the strength to satisfy MASH TL-4 design loads while minimizing installation costs. As such, strength and cost analyses were conducted on hundreds of possible bridge rail configurations to identify the optimum design. Each configuration varied in longitudinal bar size, number of longitudinal bars, stirrup bar size, stirrup spacing, and bridge rail width.

Both longitudinal and transverse steel bar size options included #4, #5, and #6 rebar. Longitudinal bar quantities included six, eight, and ten, with the bars split evenly between the front

and back faces of the bridge rail. A 2.5-in. clear cover was required for all reinforcement. Possible bridge rail widths, as measured at the top of the rail, varied from 8 in. to 12 in. at 1-in. intervals. Note, 8 in. was the minimum width required to fit a bent stirrup within the parapet and satisfy the clear cover requirement.

The strength of each bridge rail configuration was calculated using modified yield-line equations, which included a height scaling ration of (H/H_e) , as discussed in Section 2.4.1. The applied load height, H_e , and length, L_L , were taken from the values recommended by NCHRP Project 22-20(2) and shown previously in Table 4. Note, the actual load height used in the equations was 33 in. to account for a future 3-in. thick overlay in a worst-case scenario. Additionally, each design configuration was checked for punching shear failure along the top of the barrier, consistent with the discussion presented in Section 2.4.2. Both the flexural (yield-line) and punching shear capacities had to satisfy the 80-kip design load for a design configuration to be considered a viable option. All strength calculations were conducted on the single-sided, vertical-back, railing configuration since the reduced width would result in a reduced strength as compared to the corresponding double-sided configuration, shown previously in Figure 14.

Installation costs were estimated based on a cost per linear foot of barrier. Concrete barrier installers from across the United States were surveyed to obtain average installation costs for concrete and steel rebar. At the time of the survey, the average costs were found to be \$122.50 per yd^3 of concrete and \$1.30 per pound of steel rebar. These estimates included material costs, transportation, and bending and tying of the rebar. The cost of concrete labor and formwork was not included in these estimates as these costs were considered consistent among all of the design options since each design had the same basic shape.

Three configurations satisfied the strength criteria and had similar installation costs well below other configurations. These three design options are shown in Table 5. However, one design had a significantly reduced M_c value, or the overturning moment capacity along the base of the barrier that would be transferred into the deck. Limiting the impact loads into the deck was preferred, as it would reduce the potential for deck damage during an impact event. This barrier design configuration, which consisted of an 8-in. top width, eight #5 longitudinal bars, and a #4 stirrup spaced at 12 in. on-center, was therefore selected for the new TL-4 concrete bridge rail. The barrier capacity for interior sections of this design was calculated to be 84.4 kips.

Table 5. Top Design Options Based on Optimization Analysis

Option	Top Width (in.)	Base Width (in.)	Stirrups	Longitudinal Steel		ϕM_c (k-ft)/ft.	Capacity, R_w (kips)	Weight (lb/ft)	Cost (\$/ft)
				Bar Size	Quantity				
1	8	10	#4 @ 9"	4	8	11.3	85.3	379	\$29.06
2	8	10	#4 @12"	5	8	8.6	84.4	380	\$30.19
3	9	11	#5 @16"	4	8	11.0	82.5	420	\$29.29

3.4 Bridge Rail End Region Design

End regions of bridge rails are found adjacent to discontinuities like expansion/contraction joints and the ends of installations. Barrier end regions are more susceptible to failure, as impact loads cannot be transferred across the open joint. Thus, bridge rail end regions often require additional reinforcement, additional width, or another mechanism to transfer loads to adjacent barrier sections.

An end region configuration was designed with the same methodology described above for interior regions, except the yield-line analysis equations were switched to the end region calculations provided in Section 13 of AASHTO LRFD BDS [15]. Additionally, it was desired to maintain the same bridge rail width and longitudinal steel pattern for construction purposes. Thus, only the stirrup sizes and spacing were varied. The optimal barrier end region design configuration consisted of an 8-in. top width, eight #5 longitudinal bars, and a #4 stirrup spaced at 4 in. on-center, which provided a capacity of 90.9 kips. The calculated critical length of the end section was 6.1 ft. Cross sections for both the interior and end regions of the new TL-4 barrier are shown in Figure 15.

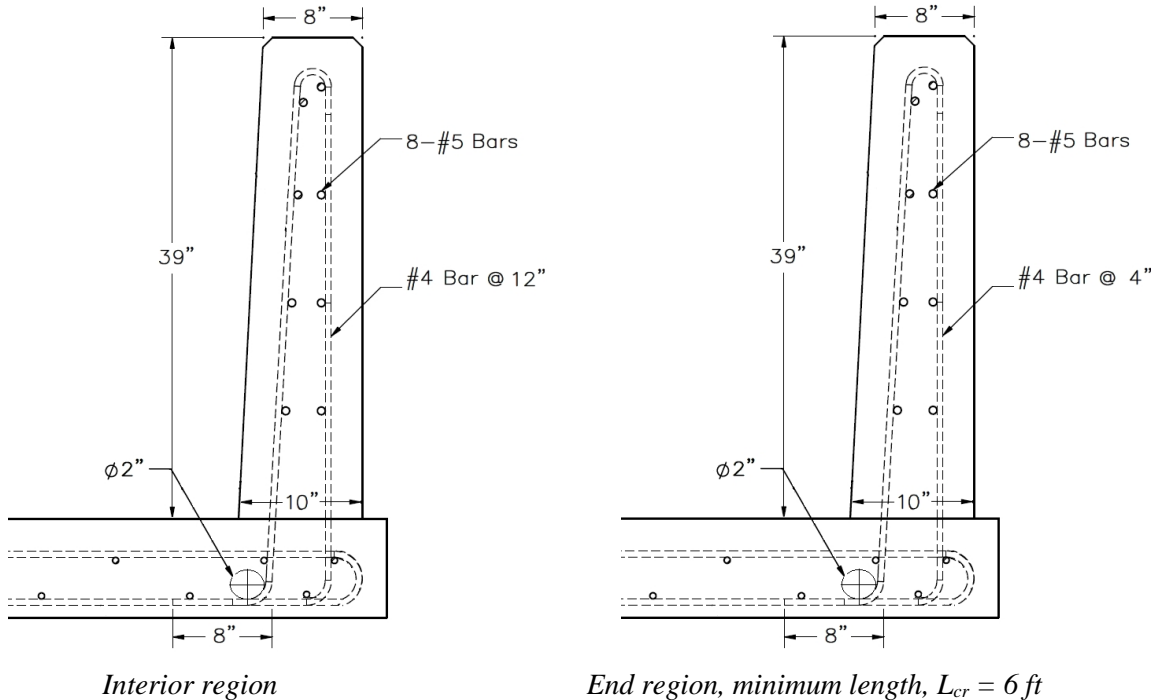


Figure 15. Cross Sections of Concrete Bridge Rail Design

4 DECK ANALYSIS AND DESIGN

4.1 Deck Design Methodology

Section 13 of AASHTO LRFD BDS [15] provides three design cases for the analysis of bridge deck overhangs in combination with bridge rails, as shown in Table 6. Design Cases 1 and 2 are the lateral and vertical design loads applied to the bridge rail, while Design Case 3 is a vehicle live load applied near the face of the barrier. As discussed previously, the design impact loads in AASHTO LRFD BDS have not yet been updated to reflect MASH 2016 impact conditions. Thus, the design loads recommended by NCHRP Project 22-20(2) [19] were used for Design Cases 1 and 2.

Table 6. Design Cases for Bridge Deck Overhangs

Design Case	Load Type	TL-4 Design Loads		Limit State
		AASHTO LRFD BDS [15]	NCHRP 22-20(2) [19]	
1	Horizontal impact load	54 kips at 32-in. height	80 kips at 30-in. height ¹	Extreme Event II
2	Vertical impact load	18 kips over 18 ft	33 kips over 18 ft	Extreme Event II
3	Live load	1 ^{kip} /ft at 1 ft from barrier	N/A	Strength I

¹ For barriers of heights greater than 36 in.

For concrete bridge railings, AASHTO LRFD BDS also states that for Design Case 1, the deck overhang may be designed with a flexural resistance equal to M_c , the barrier overturning moment, acting coincident with a tensile force, T , which is calculated from the yield-line capacity of the barrier. Thus, either the horizontal design load, as shown in Table 6, or the overturning capacity of the barrier, M_c , could be used for Design Case 1. The difference in magnitude between these design load methodologies depends on the bridge design.

In general, conservatively-designed bridge rails (those with capacities well above the horizontal design load) will have relatively high M_c values. Designing the deck based on these high M_c values will result in significantly oversized decks. Conversely, more optimal bridge rail designs (those with capacities at or near the horizontal design load) will likely have lower M_c values. The use of horizontal design load to configure the deck will result in an oversized deck that is significantly stronger than the loads that the barrier can physically transfer to it. In an effort to optimize the deck overhang for the new TL-4 concrete bridge rail, Design Case 1 design loads were calculated from both the 80-kip design load and the barrier M_c , and the lesser of the two approaches was selected as the demand on the deck. This methodology was applied at both the interior and end sections of the bridge deck using the load distribution patterns, barrier strength, and barrier critical length corresponding to interior and end conditions, respectively.

Section 13 of AASHTO LRFD BDS does not define the critical deck sections or the longitudinal length of the deck overhang in which the loads are distributed. With these aspects undefined, the design/analysis cannot be completed. Thus, guidance for these critical design

aspects was taken from a reference manual and design examples compiled by the Federal Highway Administration (FHWA) and the National Highway Institute [31-32]. Additionally, these critical sections are described by Frosch and Morel in an evaluation of existing deck overhangs [27].

Two critical deck sections were identified, as shown in Figure 16. Design Section 1 is located adjacent to the face of the bridge rail where barrier shear loads become tensile loads in the deck. Due to its close proximity to the edge of the deck, transverse deck bars may not have adequate development length, thereby limiting the effective strength of the rebar and reducing the strength of the deck. Design Section 2 is located over the external support girder and is often the location of maximum flexure in the deck overhang. The exact location of Design Section 2 is dependent upon the type of girder and is described in AASHTO LRFD BDS Section 4.6.2.1.6 [15]. For example, for a typical rolled steel girder, such as the girder shown in Figures 17 and 18, the critical section is considered to be one-fourth of the steel flange width away from the center of the girder [15, 31].

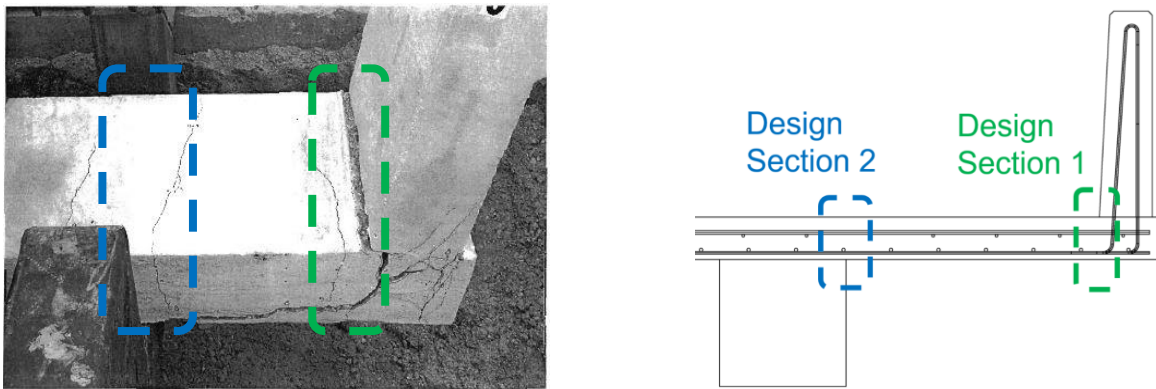


Figure 16. Photo [27] and Diagram Showing Locations for Critical Deck Design Sections

Research has shown that loads applied to a bridge rail are distributed along the length of the railing and into the deck. Thus, the loading to the deck is distributed over a much greater distance than the applied load [27]. Estimations for the effective load length at each deck section were formulated through recommendations shown in the previously referenced FHWA manuals [31-32]. The participating deck length for an interior section at Design Section 1, $L_{1,int}$, was estimated as shown in Equation 6:

$$L_{1,int} = L_{c,int} + 2H \quad (6)$$

where L_c is the critical length calculated during the yield-line analysis of the bridge rail and H is the height of the barrier. Note, L_1 matches the recommended distance over which to apply the tensile deck load, T , in Section 13 of AASHTO LRFD BDS. However, in this design process, L_1 was also used as the length over which the flexural loads were applied. Similarly, the participating deck length for an end condition at Design Section 1, $L_{1,end}$, was estimated using Equation 7:

$$L_{1,end} = L_{c,end} + H \quad (7)$$

Contemporary research suggests that impact demands penetrate inward through the deck, from Design Section 1 to Design Section 2, at a 30-degree angle, as shown in Figure 17 [27, 31-32, 36]. Thus, the load length for an interior section at Design Section 2, $L_{s2,int}$, was estimated using Equation 8:

$$L_{2,int} = L_{1,int} + 2Y \tan 30^\circ \quad (8)$$

where Y is the distance from Design Section 1 to Design Section 2. This behavior is demonstrated at an end condition in Figure 18. The load length for an exterior section at Design Section 2, $L_{s2,end}$, was estimated using Equation 9.

$$L_{2,end} = L_{1,end} + Y \tan 30^\circ \quad (9)$$

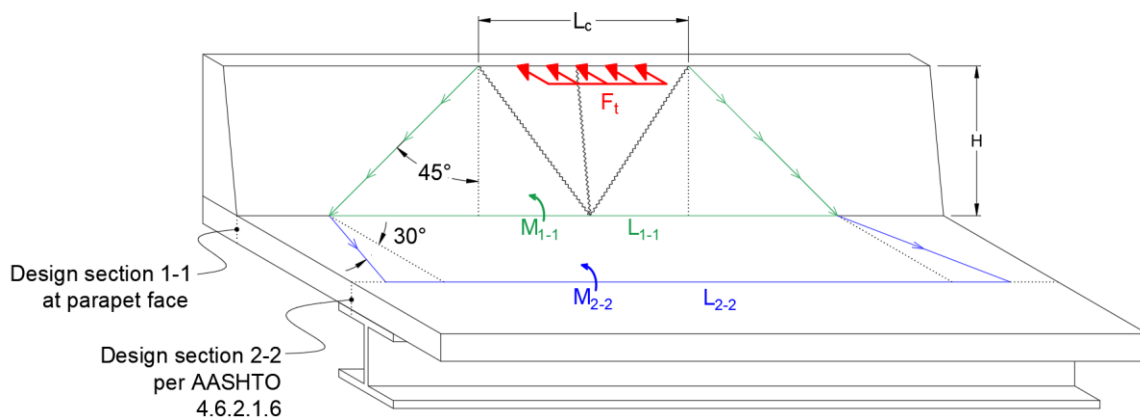


Figure 17. Distribution of Impact Demands to Deck Design Sections 1 and 2, Interior Section

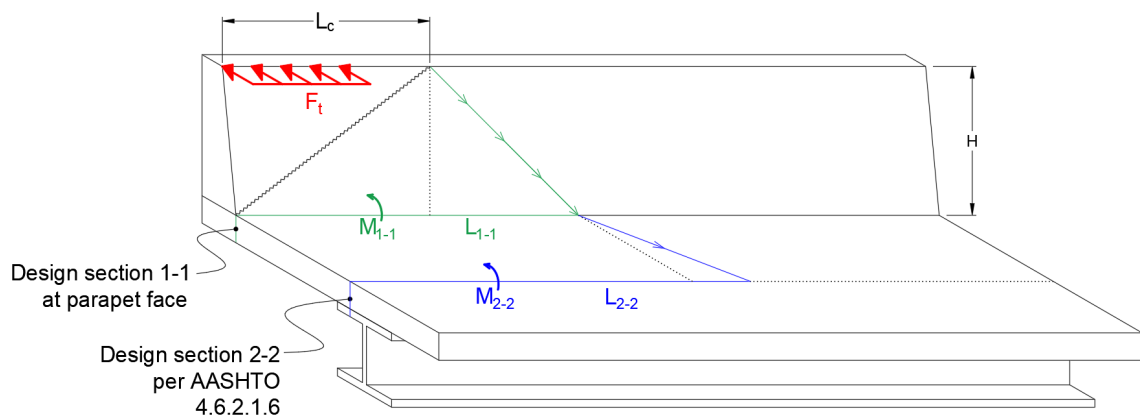


Figure 18. Distribution of Impact Demands to Deck Design Sections 1 and 2, End Section

It should be noted that impact forces will be distributed to the deck well outside the bounds of L_c . Since M_c is already in terms of moment per unit length, M_c was applied over the full length of each design section. This assumption is supported by the results of physical testing of long deck overhang sections performed by Frosch and Morel [27]. Conversely, the horizontal impact load, F_t , is a prescribed force that is divided by the length of the design section to obtain units of moment

per unit length. Finally, all other loads (i.e., dead loads) should be applied in terms of moment per unit length so that all factors can be summed together.

4.2 Deck Design Results

A survey of sponsoring state DOTs was conducted to determine the critical dimensions utilized in their existing deck standards. Multiple state DOTs desired deck overhang widths up to 5 ft long, and the most commonly-used deck thickness was 8 in. Additionally, the deck was assumed to have a 3-in. thick asphalt overlay, which increased the dead loads applied to the deck. The optimized TL-4 bridge rail design configuration selected previously had an interior yield-line capacity, R_w , of 84.4 kips, a cantilever bending capacity, M_c , of 8.6 ^{kip-ft}/ft, and critical length, L_c , equal to 13.0 ft. These capacities and dimensions were used with the design methodology described in the previous section to calculate deck overhang design loads for the new TL-4 bridge rail. The results of this analysis are summarized in Table 7 and shown in terms of M_1 and M_2 , which correspond to the design moments per unit length at Design Section 1 and Design Section 2, respectively.

Recall that the design loads for Design Case 1 were calculated from both the 80-kip lateral load and the barrier M_c , where only the lower of the two values would be used in the deck design process. Design loads calculated from M_c were lower at both design sections. Accordingly, deck demands calculated from the impact load were ignored, and M_c was used for the deck demand at both design sections for Design Case 1. Further, these design loads were identified as the critical load for both sections, as Design Case 1 controlled over Design Cases 2 and 3.

Table 7. Results of Critical Deck Overhang Design Loads

Design Case	Design Section 1		Design Section 2	
1 (M_c)	$M_1 = 8.86$ (k-ft)/ft	$T = 4.15$ k/ft	$M_2 = 13.73$ (k-ft)/ft	$T = 3.24$ k/ft
1* (80 kip)	$M_1 = 11.59$ (k-ft)/ft	$T = 4.11$ k/ft	$M_2 = 14.17$ (k-ft)/ft	$T = 3.17$ k/ft
2	$M_1 = 0.90$ (k-ft)/ft		$M_2 = 10.89$ (k-ft)/ft	
3	N/A		$M_2 = 11.72$ (k-ft)/ft	

* Loads from the 80-kip load were eliminated from consideration in Design Case 1.
N/A – Not Applicable

Design calculations for the strength of the deck at Design Section 1 considered the development length of the transverse steel bars and the design section's proximity to the deck edge. The barrier was offset 2 in. away from the outer vertical edge of the deck, and the deck utilized a 2-in. clear cover at the side of the deck. This meant the transverse steel bars had only 10 in. of development length between Design Section 1 and the outer edge of the deck. Since the development lengths for most bar sizes were greater than 10 in., the design capacity of transverse rebar in the deck was reduced by a ratio of the available development length (i.e., 10 in.) divided

by the required development length as estimated by ACI 318 [30]. Design Section 2 did not have the same development length issues.

The reinforcement configuration selected for the deck overhang incorporated one #5 bar and two #4 bars spaced at 4-in. intervals along the top mat of steel and a #4 bar spaced at 12-in. intervals in the bottom mat. This unusual reinforcement pattern was selected because its design strength nearly matched the applied loads estimated for the deck. Thus, the full-scale crash test incorporated a deck that was configured very near to the limits prescribed by the design methodology. If the testing was successful, other reinforcement configurations and decks designed using the same methodology would also be acceptable.

5 TEST REQUIREMENTS AND EVALUATION CRITERIA

5.1 Test Requirements

Longitudinal barriers, such as concrete bridge rails, must satisfy impact safety standards in order to be declared eligible for federal reimbursement by FHWA for use on the National Highway System. For new hardware, these safety standards consist of the guidelines and procedures published in MASH 2016 [3]. Note that there is no difference between MASH 2009 [2] and MASH 2016 for longitudinal barriers, such as the system tested in this project, except that additional occupant compartment deformation measurements, photographs, and documentation are required by MASH 2016. According to MASH 2016, TL-4 longitudinal barrier systems must be subjected to three full-scale vehicle crash tests, as summarized in Table 8.

Table 8. MASH 2016 [3] TL-4 Crash Test Conditions for Concrete Barriers

Test Article	Test Designation No.	Test Vehicle	Vehicle Weight, lb	Impact Conditions		Evaluation Criteria ¹
				Speed, mph	Angle, deg.	
Concrete Barrier	4-10	1100C	2,420	62	25	A,D,F,H,I
	4-11	2270P	5,000	62	25	A,D,F,H,I
	4-12	10000S	22,000	56	15	A,D,G

¹ Evaluation criteria explained in Table 9.

Following a review of previous crash testing into concrete barrier systems, only MASH test designation no. 4-12 was determined to be critical for evaluating the TL-4 concrete bridge rail. Due to the mass of the 10000S vehicle being more than four times that of the 2270P pickup truck, MASH test designation no. 4-12 has an impact severity 34 percent higher than MASH test designation no. 4-11 and 278 percent higher than MASH test designation no. 4-10. NCHRP Project 22-20(2) found that the increased impact severity translated to increased impact loads for the 10000S impacts as compared to the 2270P, as observed in the recommended impact loads for TL-3 and TL-4 MASH impacts [19]. Subsequently, the 10000S test would impart the highest impact loads to the barrier and be the critical test for evaluating the strength of both the bridge rail and bridge deck overhang.

Vehicle stability was not considered to be critical for the small car or pickup truck tests. Previous crash testing of the 2270P pickup into an 11-degree single-slope concrete bridge rail and vertical-faced concrete bridge rails resulted in successful MASH tests with minimal vehicle roll and pitch displacements [37-39]. Similarly, previous 1100C crash tests have been successfully conducted on both single slope and vertical face concrete bridge rails [23-24]. The 3-degree slope of the new concrete TL-4 bridge rail was between those of typical single slope barriers and vertical parapets. Thus, vehicle performance had been effectively bracketed by previous crash tests, and there were no concerns for vehicle instability or excessive occupant risk measures. Therefore, MASH test designation nos. 4-10 and 4-11 were not deemed critical and were not conducted as part of this study.

The bridge rail designed herein was to be crashworthy both before and after a 3-in. roadway overlay was applied to the bridge deck. Thus, the bridge rail had two different height configurations: a 39-in. tall configuration before an overlay and an effective 36-in. tall configuration after an overlay. At the time of this study, few MASH test designation no. 4-12 crash tests had been conducted, so there were some concerns with vehicle containment with the lower effective barrier height. Additionally, after an overlay, impact loads on the bridge rail would be applied higher on the barrier and result in higher moments transferred to the bridge deck. As such, the critical bridge rail configuration was determined to be the 36-in. effective barrier height after a 3-in. overlay was applied to the deck surface.

It should be noted that the test matrix detailed herein represents the researchers' best engineering judgement with respect to the MASH 2016 safety requirements and their internal evaluation of critical tests necessary to evaluate the crashworthiness of the barrier system. However, the recent switch to new vehicle types as part of the implementation of the MASH 2016 criteria and the lack of experience and knowledge regarding the performance of the new vehicle types with certain types of hardware could result in unanticipated barrier performance. Thus, any tests within the evaluation matrix deemed non-critical may eventually need to be evaluated based on additional knowledge gained over time or revisions to the MASH 2016 criteria.

5.2 Evaluation Criteria

Evaluation criteria for full-scale vehicle crash testing are based on three factors: (1) structural adequacy, (2) occupant risk, and (3) vehicle trajectory after collision. Criteria for structural adequacy are intended to evaluate the ability of the concrete bridge rail to contain and redirect impacting vehicles. In addition, controlled lateral deflection of the test article is acceptable. Occupant risk evaluates the degree of hazard to occupants in the impacting vehicle. Post-impact vehicle trajectory is a measure of the potential of the vehicle to result in a secondary collision with other vehicles and/or fixed objects, thereby increasing the risk of injury to the occupants of the impacting vehicle and/or other vehicles. These evaluation criteria are summarized in Table 9 and discussed in greater detail in MASH 2016 [3]. The full-scale vehicle crash test documented herein was conducted and reported in accordance with the procedures provided in MASH 2016.

In addition to the standard occupant risk measures, the Post-Impact Head Deceleration (PHD), the Theoretical Head Impact Velocity (THIV), and the Acceleration Severity Index (ASI) were determined and reported. Additional discussion on PHD, THIV and ASI is provided in MASH 2016.

Table 9. MASH 2016 Evaluation Criteria for Longitudinal Barriers

Structural Adequacy	A. Test article should contain and redirect the vehicle or bring the vehicle to a controlled stop; the vehicle should not penetrate, underride, or override the installation although controlled lateral deflection of the test article is acceptable.		
Occupant Risk	D. Detached elements, fragments or other debris from the test article should not penetrate or show potential for penetrating the occupant compartment, or present an undue hazard to other traffic, pedestrians, or personnel in a work zone. Deformations of, or intrusions into, the occupant compartment should not exceed limits set forth in Section 5.2.2 and Appendix E of MASH 2016.		
	F. The vehicle should remain upright during and after collision. The maximum roll and pitch angles are not to exceed 75 degrees.		
	G. It is preferable, although not essential, that the vehicle remain upright during and after collision.		
	H. Occupant Impact Velocity (OIV) (see Appendix A, Section A5.2.2 of MASH 2016 for calculation procedure) should satisfy the following limits:		
	Occupant Impact Velocity Limits		
	Component	Preferred	Maximum
Longitudinal and Lateral	30 ft/s	40 ft/s	
I. The Occupant Ridedown Acceleration (ORA) (see Appendix A, Section A5.2.2 of MASH 2016 for calculation procedure) should satisfy the following limits:			
Occupant Ridedown Acceleration Limits			
Component	Preferred	Maximum	
Longitudinal and Lateral	15.0 g's	20.49 g's	

6 DESIGN DETAILS

The test installation for the new TL-4 bridge rail was 150 ft long. The upstream half of the installation was attached to a simulated bridge deck, while the downstream half of the bridge rail was attached directly to the test site's concrete tarmac. The system was impacted on the upstream half of the installation in order to evaluate the bridge rail and deck under maximum loading conditions. The downstream half of the installation was only necessary to allow adequate time and distance for the single-unit truck box to lean on the barrier and return to an upright position before exiting the system, thus evaluating vehicle stability. The critical test configuration for the reinforced concrete bridge rail incorporated a 3-in. overlay on the bridge deck. Thus, the 39-in. tall bridge rail extended only 36 in. above the roadway surface. This configuration allowed for the greatest impact height and moment arm above the bridge deck. Design details for the TL-4 concrete bridge rail are shown in Figures 19 through 33, and photographs of the test installation are shown in Figure 34.

Under the upstream half of the system, a 24-in. by 24-in. reinforced concrete grade beam was constructed to simulate a bridge girder. An 8-in. thick, reinforced concrete, simulated bridge deck was cast on top of the grade beam, but it remained 3 in. below the surface of the surrounding tarmac. A 3-in. thick overlay, consisting of a weak concrete mix, was placed on the simulated bridge deck to create a uniform surface height with the surrounding tarmac. A polyethylene plastic was used between the overlay and the bridge deck so that the overlay could be removed after testing to inspect the bridge deck for damage. The simulated bridge deck was installed with a 5-ft lateral overhang from the outer face of the grade beam, and it was anchored to the tarmac to prevent lateral movement of the deck during the crash test. Lateral reinforcement in the deck consisted of two #4 bars and one #5 bar per foot of longitudinal distance. Each of these bars was spaced at 4 in. on-center and had a 180-degree hook at the edge of the deck, which tied the top and bottom steel mats together. Note that the #5 bar hooks had to be rotated from vertical in order to fit within the 8-in. thick deck. Longitudinal steel in the deck consisted of #4 bars at 12 in. on-center in both the top and bottom mats of steel.

The bridge rail was installed with a 39-in. height relative to the top of the bridge deck, which corresponded to a 36-in. effective height after the 3-in. overlay. The surface of the bridge deck was left rough at the rail location before the bridge rail was poured. The bridge rail was 8 in. wide at the top and 10 in. wide at the base. The back of the bridge rail was offset 2 in. away from the edge of deck. Eight #5 longitudinal bars were divided between the front and the back faces of the bridge rail, and #4 transverse U-bars were spaced at 12-in. intervals. The concrete clear cover in the bridge rail was 2½ in. Note, the test installation was constructed with interior region reinforcement only as a joint was not placed in the bridge rail or deck. Design calculations showed that the interior region of the bridge rail was structurally weaker than the end region. Thus, the full-scale test was conducted on the critically weak interior section.

On the downstream half of the test installation, the bridge rail was anchored directly to the existing tarmac. A narrow strip of the tarmac was ground down 3 in. so that the same bridge rail cross section could be continued downstream from the simulated deck. Vertical no. 4 dowel bars were epoxied into the tarmac and placed adjacent to the transverse steel in the barrier.

End regions were developed for the TL-4 bridge rail as discussed in Section 3.4 and shown previously in Figure 15. However, since the vehicle impact was occur in the middle of the test

installation and loading of the upstream and downstream ends of the test article would be minimal, end region reinforcement was not included in the test article. Note, for real-world installations, the 6-ft long end regions should be placed adjacent to any bridge rail ends, expansion/contraction gaps, or other discontinuities in the railing.

The bridge rail and deck were designed for a concrete compressive strength of 5,000 psi. The actual compressive strength for the deck and bridge rail were 6,170 psi and 5,090 psi, respectively. All steel rebar had a minimum yield strength of 60 ksi. Material specifications, mill certifications, and certificates of conformity for the system materials are shown in Appendix A.

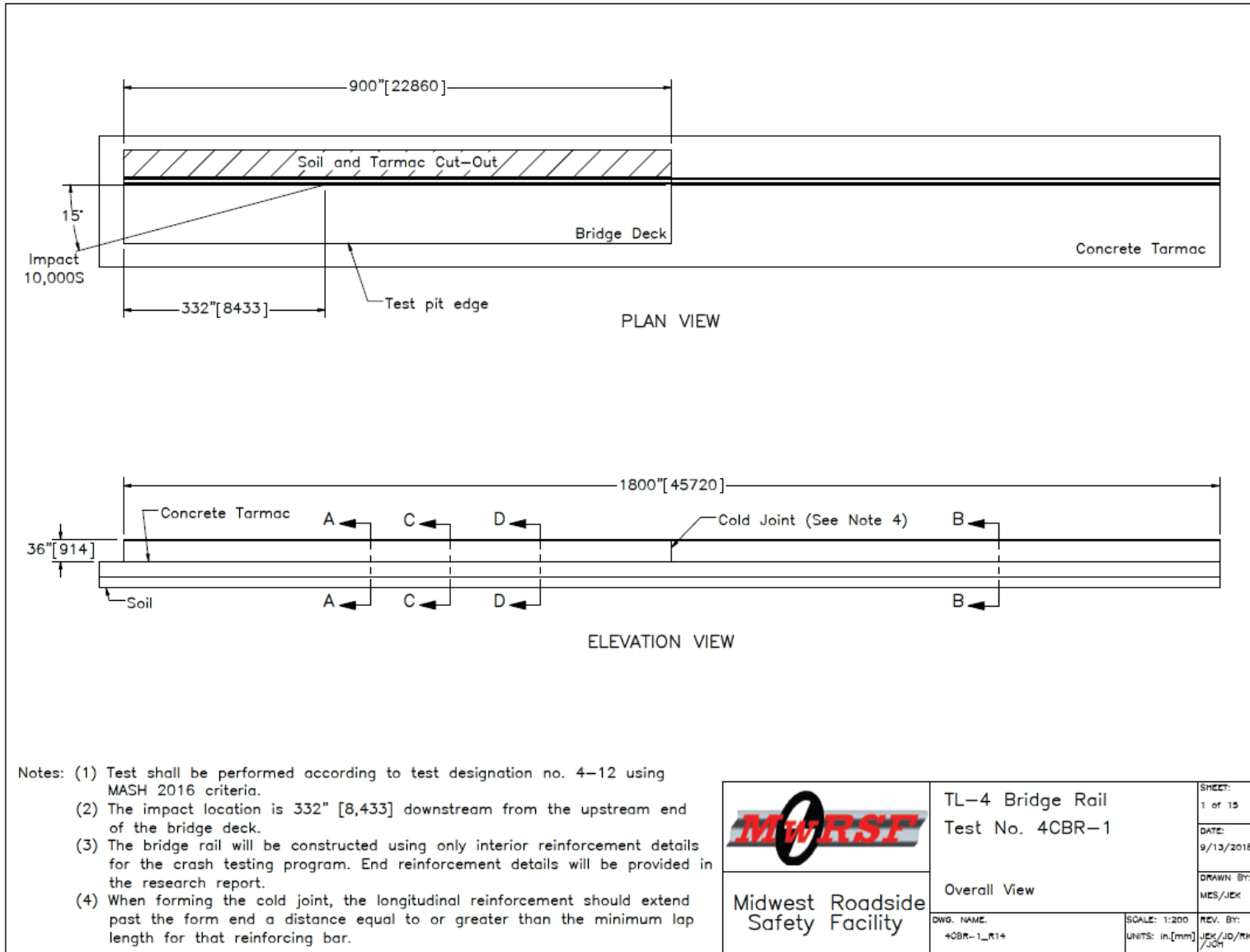


Figure 19. TL-4 Bridge Rail Test Installation, Test No. 4CBR-1

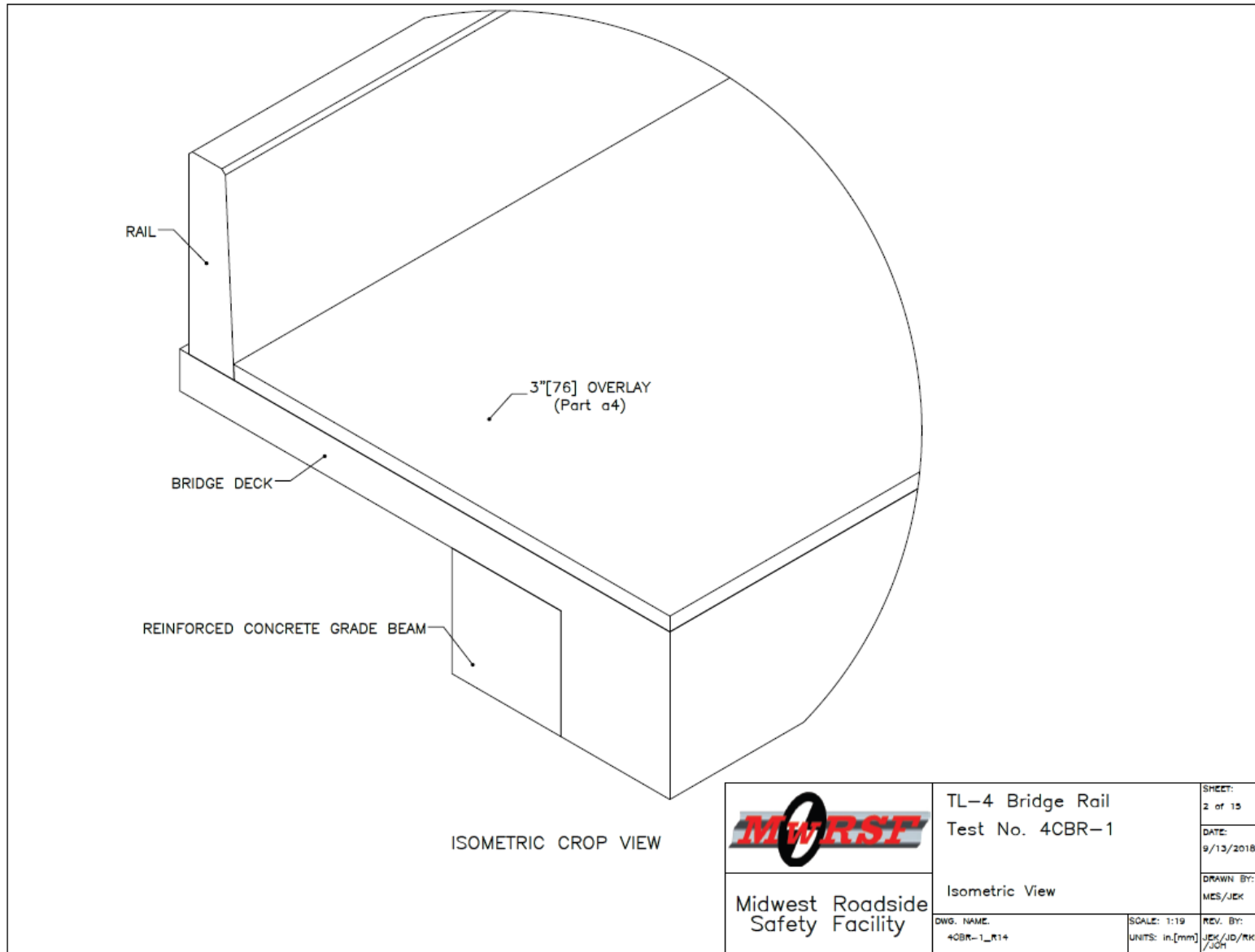


Figure 20. Isometric View, Test No. 4CBR-1

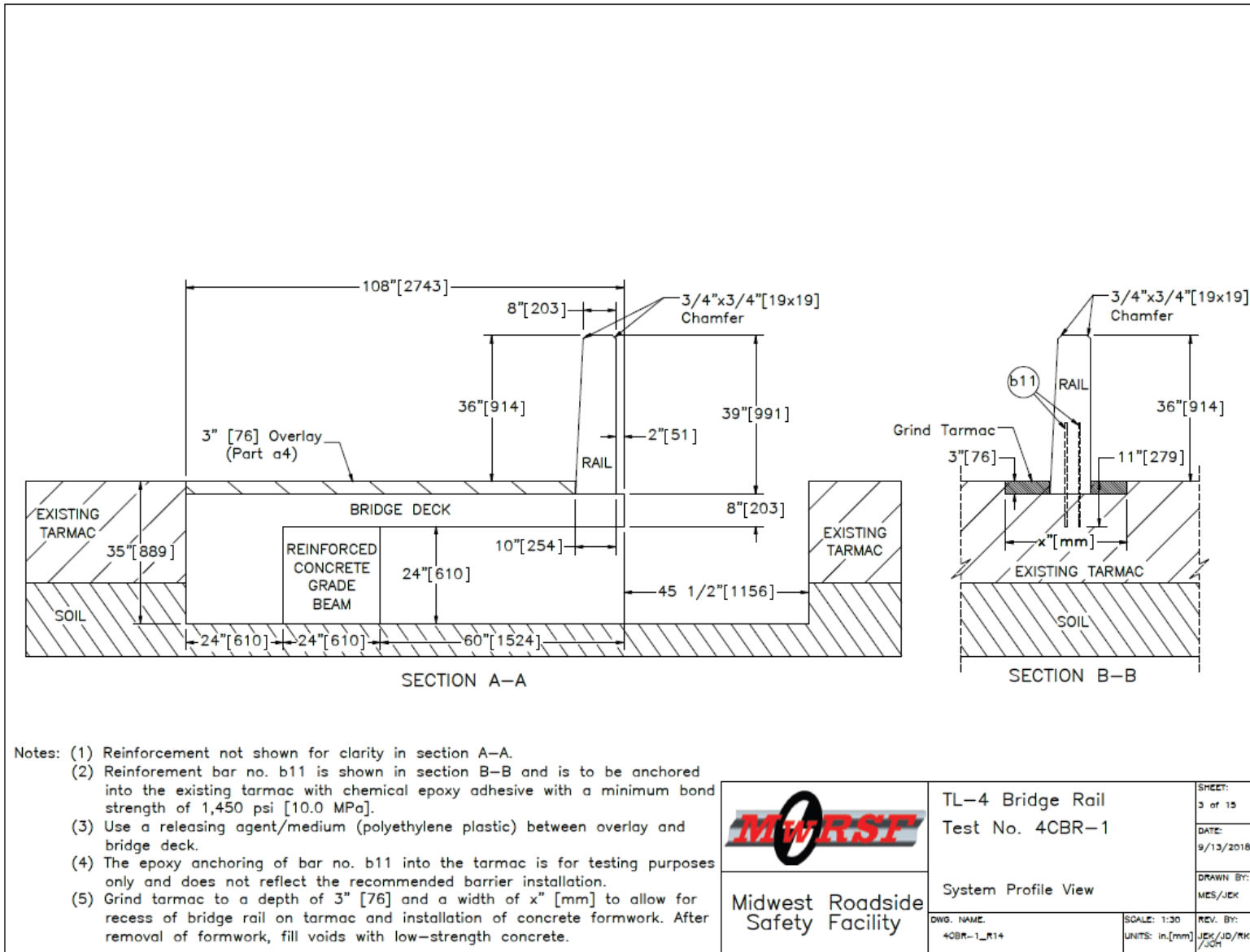


Figure 21. System Cross Sections, Test No. 4CBR-1

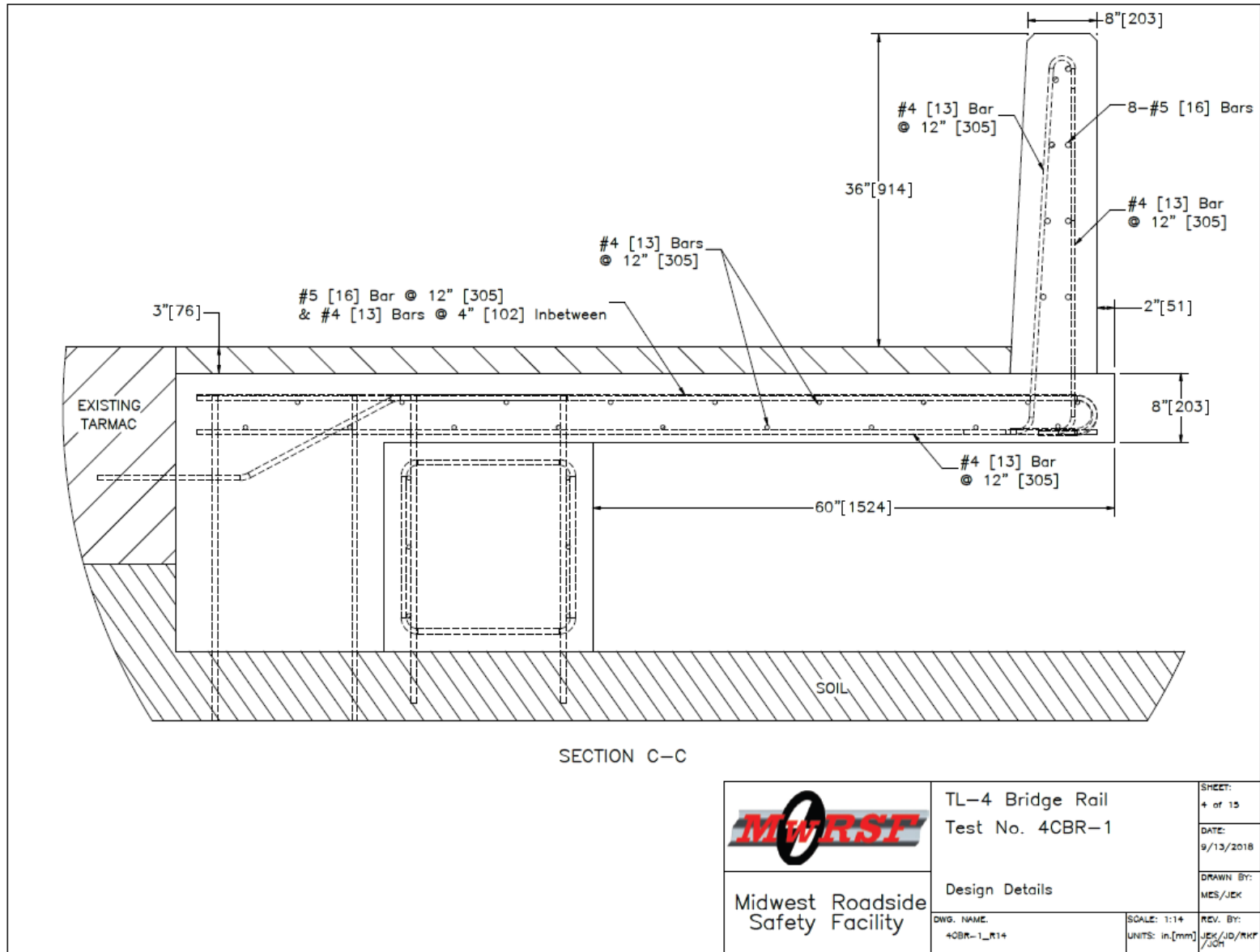


Figure 22. TL-4 Bridge Rail Design Details, Test No. 4CBR-1

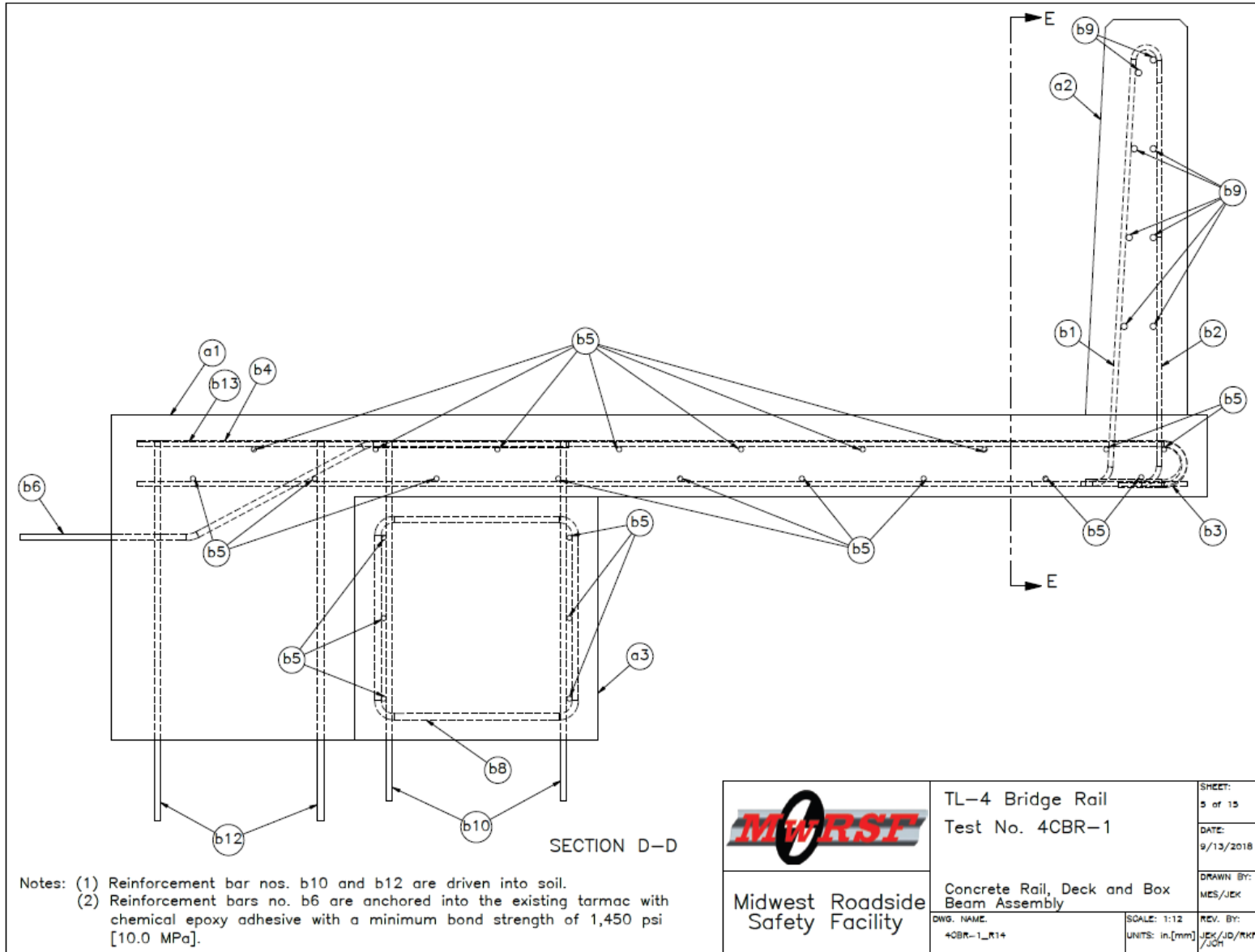


Figure 23. Rail, Deck, and Grade Beam Assemblies, Test No. 4CBR-1

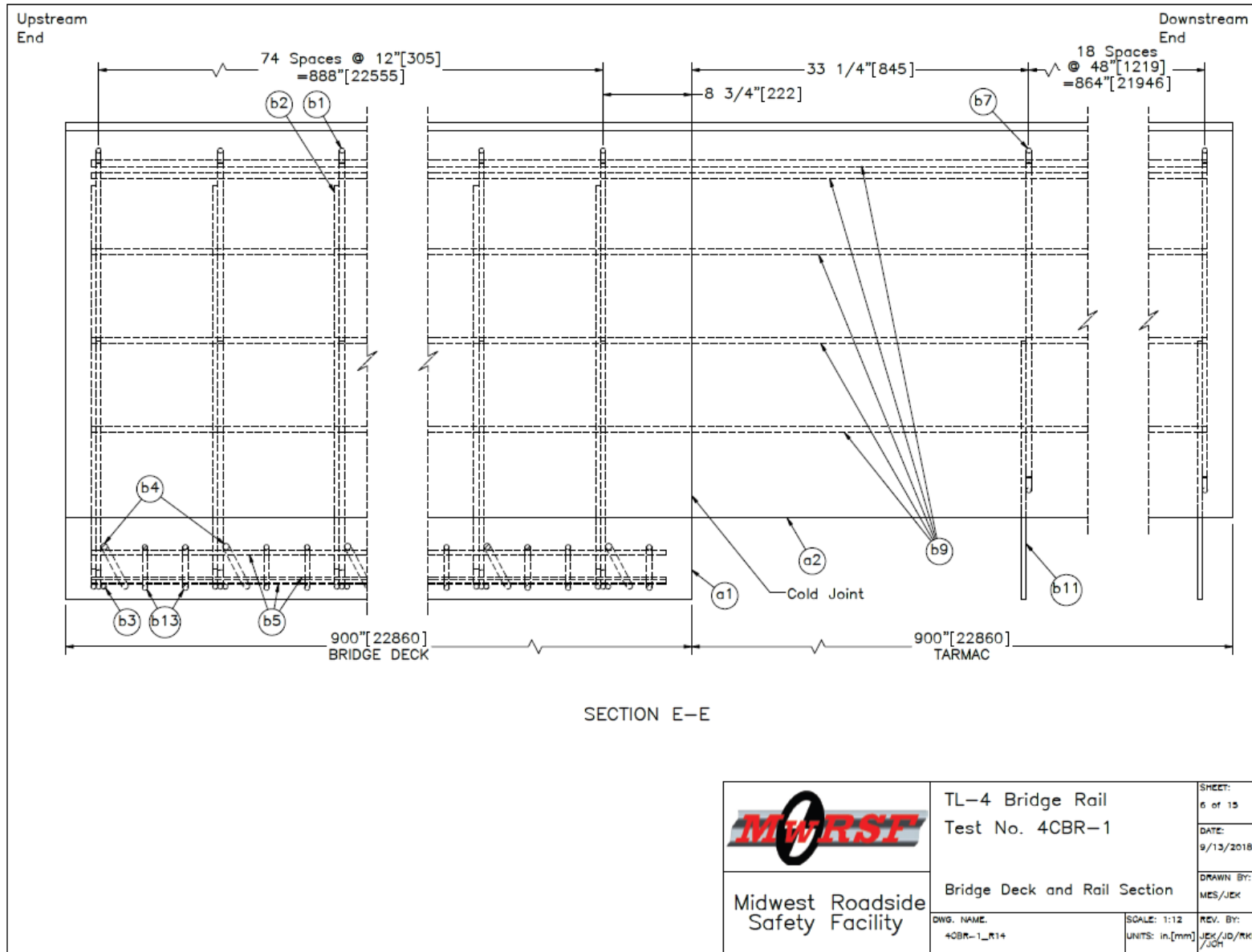


Figure 24. Bridge Deck and Rail Sections, Test No. 4CBR-1

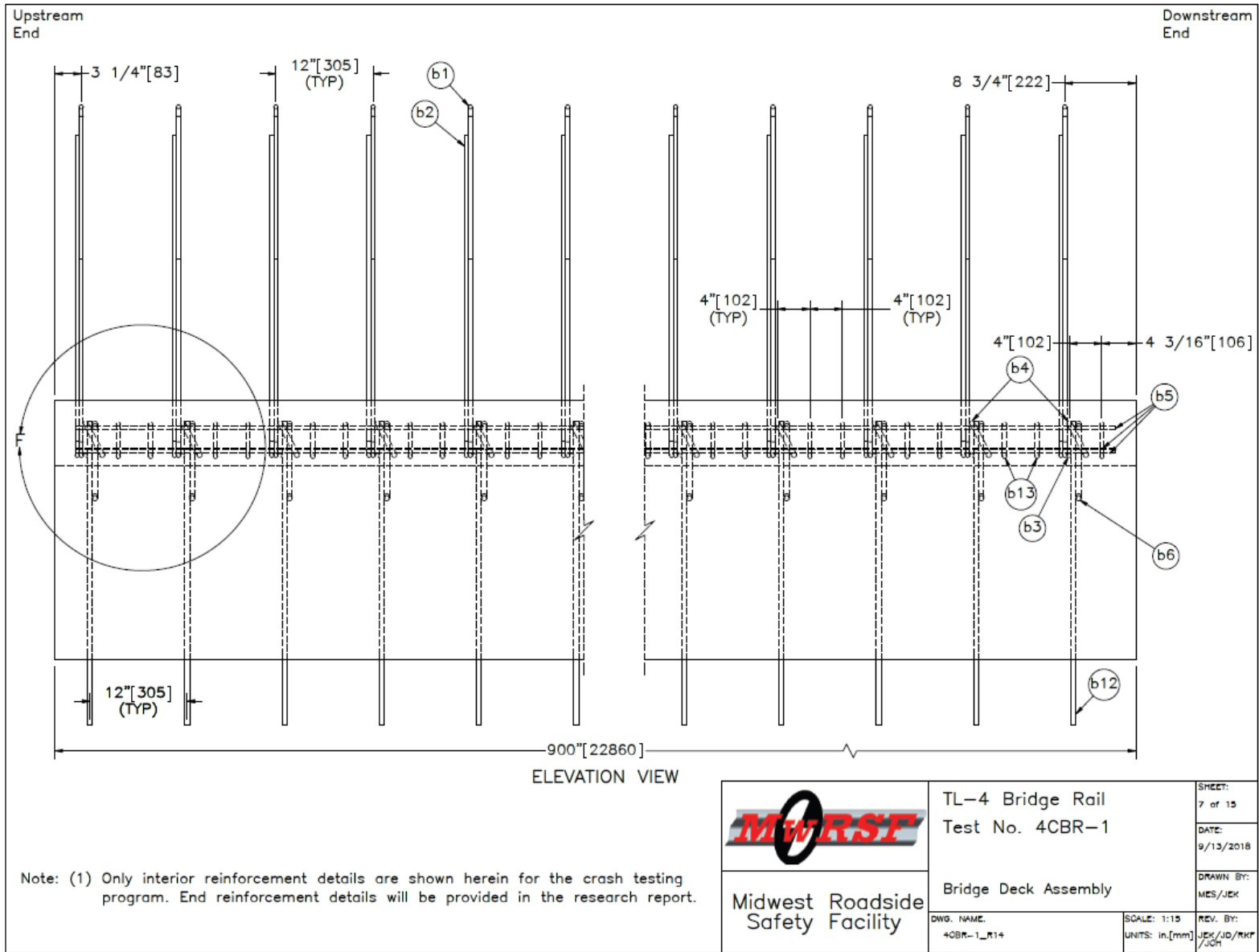


Figure 25. Bridge Deck Assembly, Test No. 4CBR-1

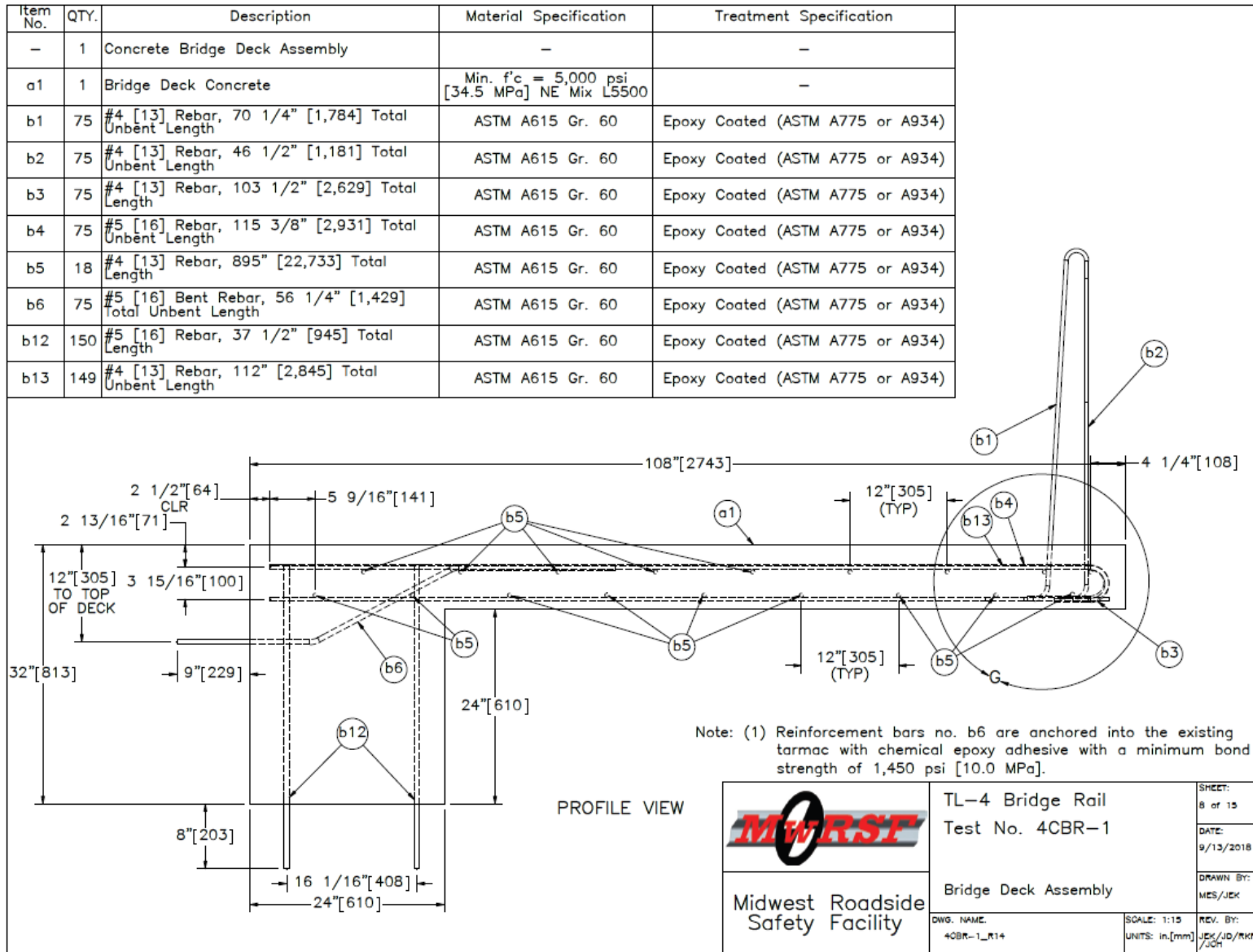


Figure 26. Bridge Deck Assembly, Test No. 4CBR-1

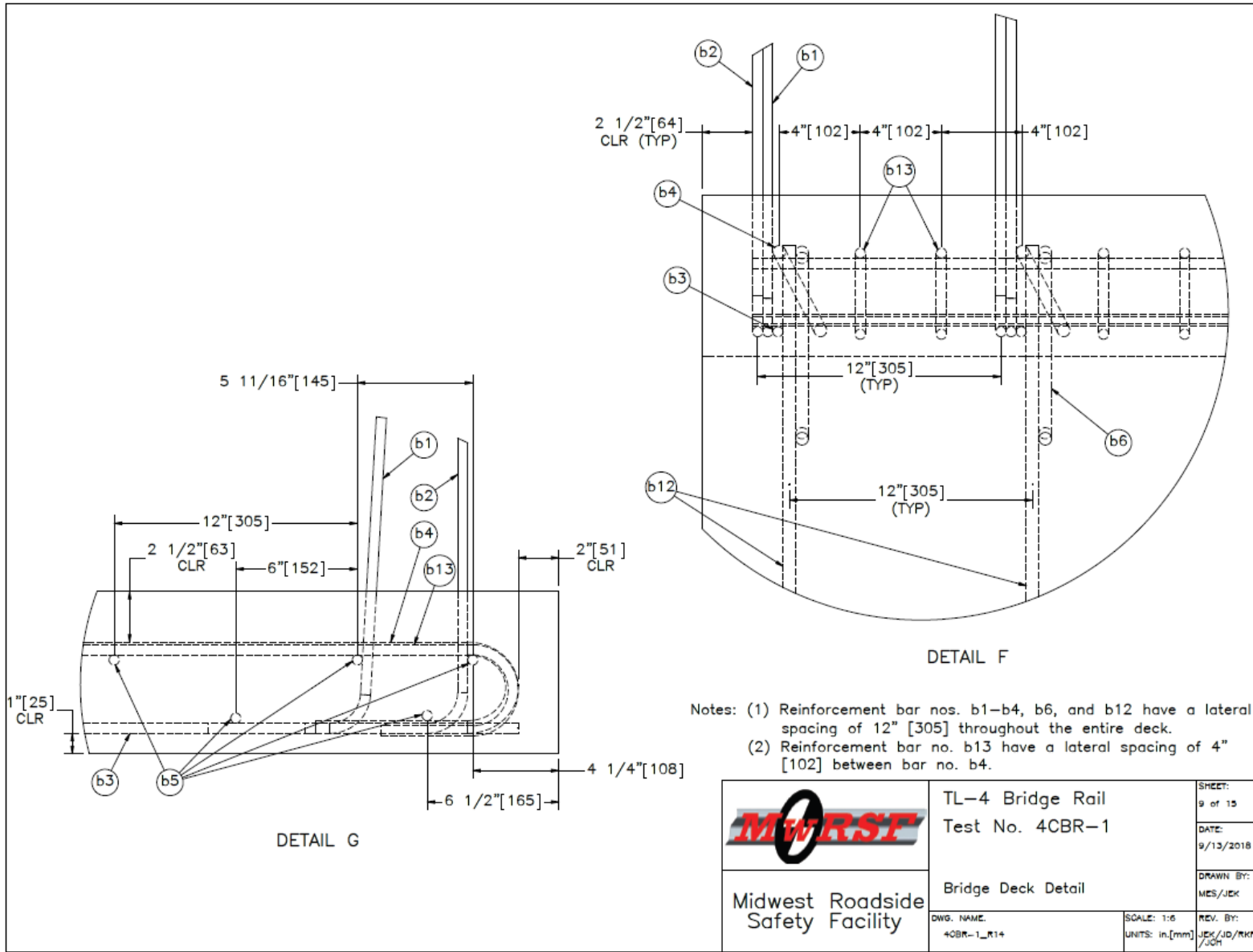


Figure 27. Bridge Deck Details, Test No. 4CBR-1

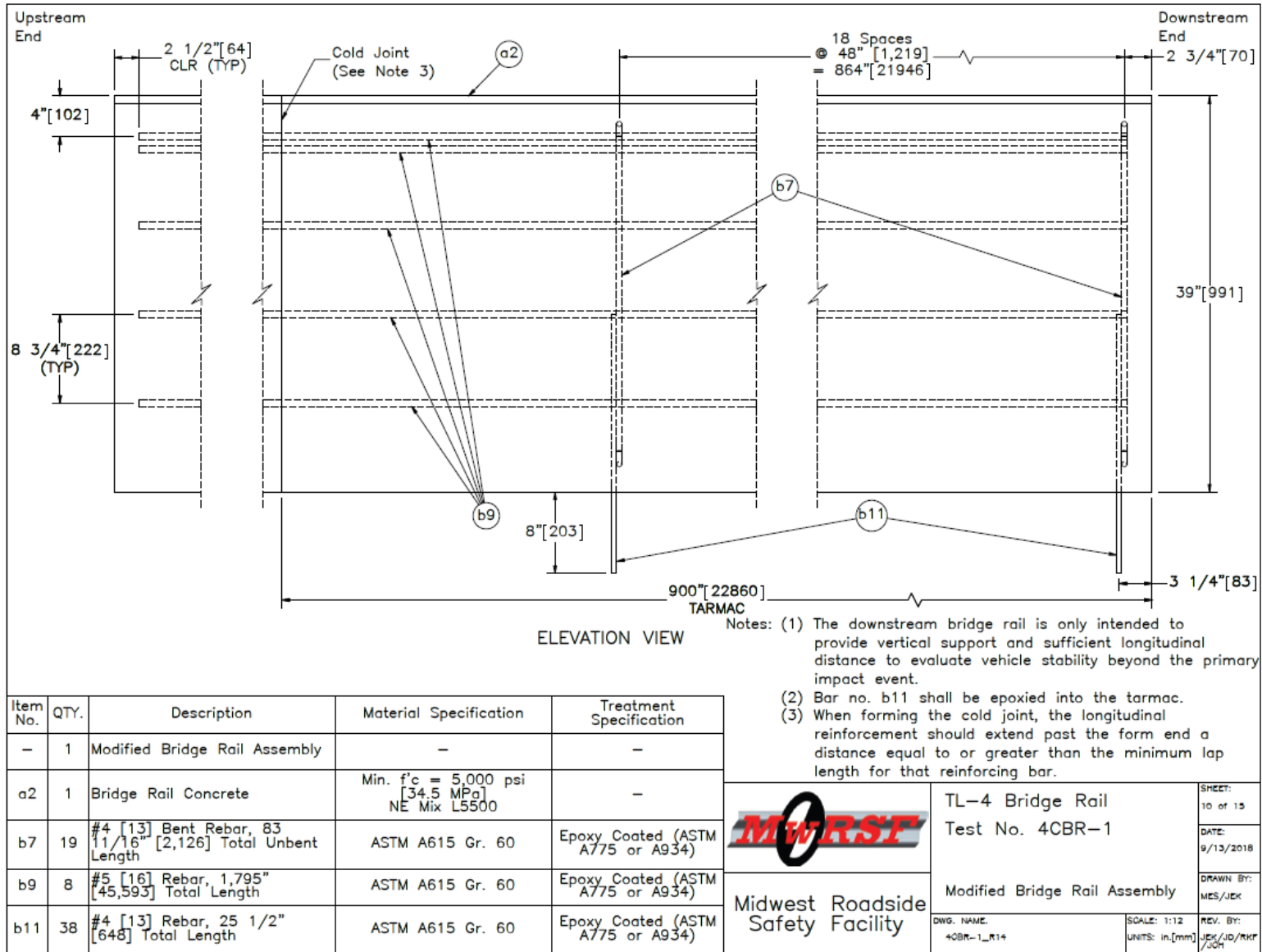


Figure 28. Modified Bridge Rail for Downstream Half of System, Test No. 4CBR-1

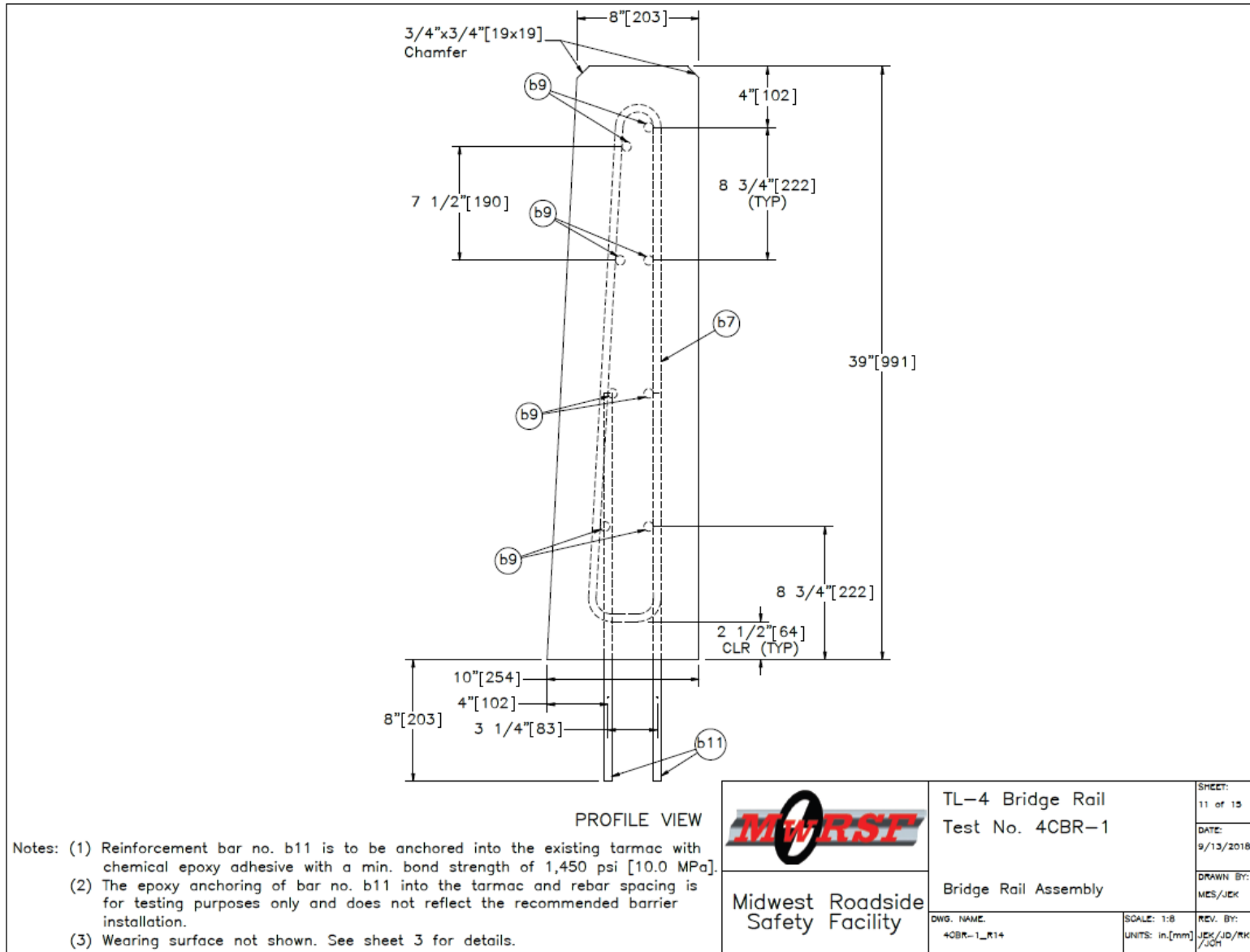


Figure 29. Design Details for Downstream Half of System, Test No. 4CBR-1

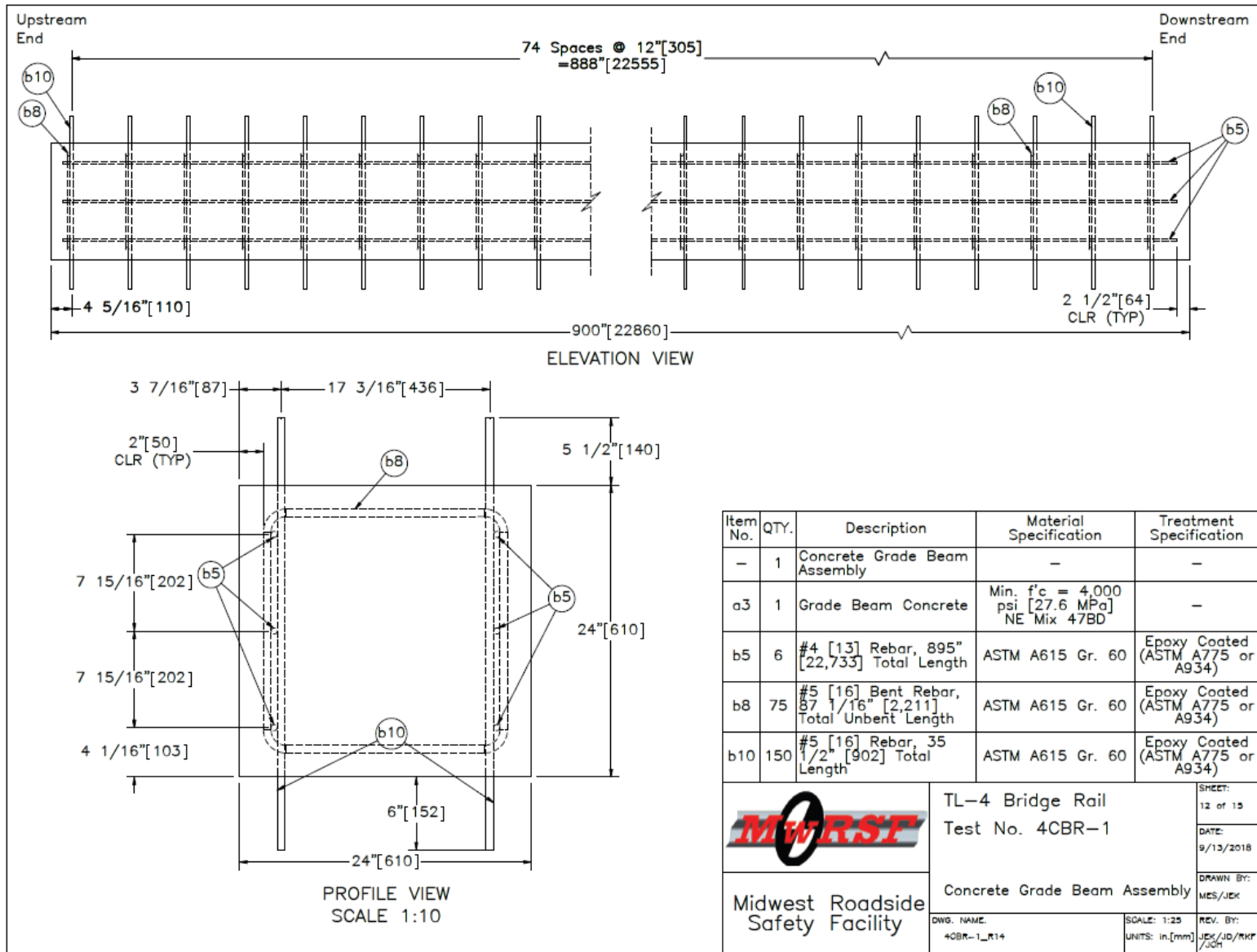


Figure 30. Concrete Grade Beam Assembly, Test No. 4CBR-1

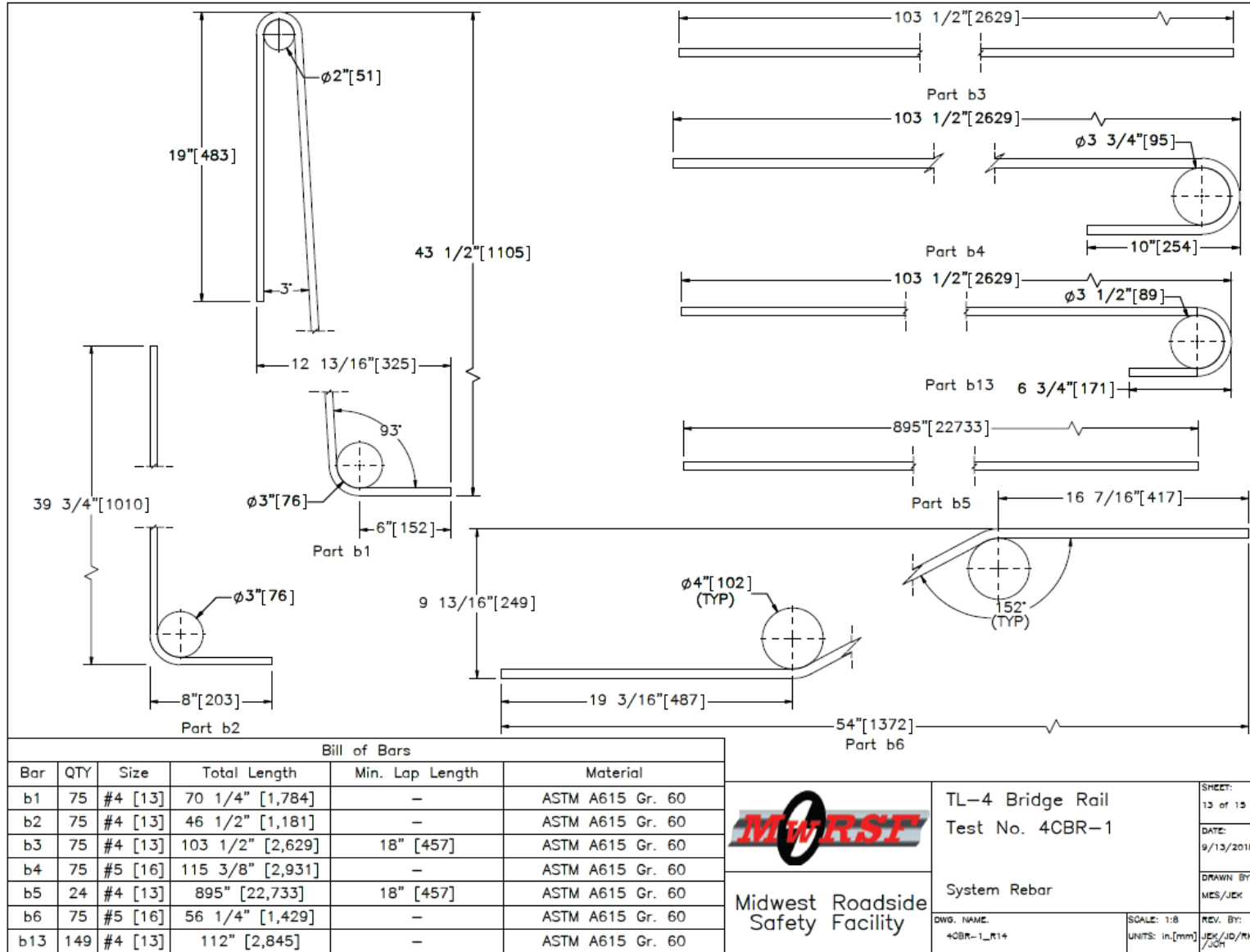


Figure 31. System Rebar, Test No. 4CBR-1

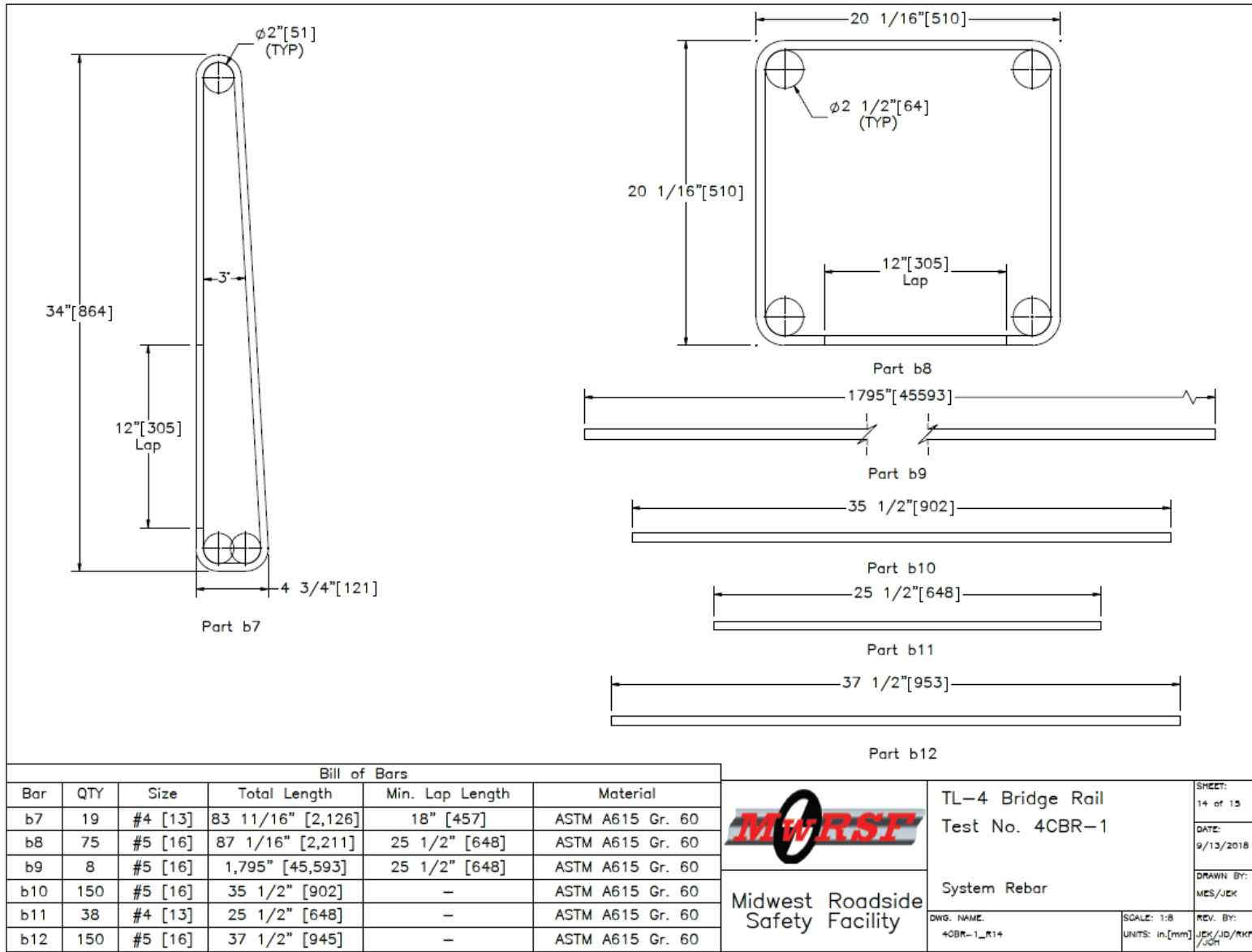


Figure 32. System Rebar, Test No. 4CBR-1

Item No.	QTY.	Description	Material Specification	Treatment Specification
a1	1	Bridge Deck Concrete	Min. f'c = 5,000 psi [34.5 MPa] NE Mix L5500	-
a2	1	Bridge Rail Concrete	Min. f'c = 5,000 psi [34.5 MPa] NE Mix L5500	-
a3	1	Grade Beam Concrete	Min. f'c = 4,000 psi [27.6 MPa] NE Mix 47BD	-
a4	1	Overlay	Concrete NE Mix 9019 CITY	-
b1	75	#4 [13] Rebar, 70 1/4" [1,784] Total Unbent Length	ASTM A615 Gr. 60	Epoxy Coated (ASTM A775 or A934)
b2	75	#4 [13] Rebar, 46 1/2" [1,181] Total Unbent Length	ASTM A615 Gr. 60	Epoxy Coated (ASTM A775 or A934)
b3	75	#4 [13] Rebar, 103 1/2" [2,629] Total Length	ASTM A615 Gr. 60	Epoxy Coated (ASTM A775 or A934)
b4	75	#5 [16] Rebar, 115 3/8" [2,931] Total Unbent Length	ASTM A615 Gr. 60	Epoxy Coated (ASTM A775 or A934)
b5	24	#4 [13] Rebar, 895" [22,733] Total Length	ASTM A615 Gr. 60	Epoxy Coated (ASTM A775 or A934)
b6	75	#5 [16] Bent Rebar, 56 1/4" [1,429] Total Unbent Length	ASTM A615 Gr. 60	Epoxy Coated (ASTM A775 or A934)
b7	19	#4 [13] Bent Rebar, 83 11/16" [2,126] Total Unbent Length	ASTM A615 Gr. 60	Epoxy Coated (ASTM A775 or A934)
b8	75	#5 [16] Bent Rebar, 87 1/16" [2,211] Total Unbent Length	ASTM A615 Gr. 60	Epoxy Coated (ASTM A775 or A934)
b9	8	#5 [16] Rebar, 1,795" [45,593] Total Length	ASTM A615 Gr. 60	Epoxy Coated (ASTM A775 or A934)
b10	150	#5 [16] Rebar, 35 1/2" [902] Total Length	ASTM A615 Gr. 60	Epoxy Coated (ASTM A775 or A934)
b11	38	#4 [13] Rebar, 25 1/2" [648] Total Length	ASTM A615 Gr. 60	Epoxy Coated (ASTM A775 or A934)
b12	150	#5 [16] Rebar, 37 1/2" [945] Total Length	ASTM A615 Gr. 60	Epoxy Coated (ASTM A775 or A934)
b13	149	#4 [13] Rebar, 112" [2,845] Total Unbent Length	ASTM A615 Gr. 60	Epoxy Coated (ASTM A775 or A934)
-	1	Epoxy	Min. bond strength = 1,450 psi [10.0 MPa]	-
-	1	Releasing Agent/Medium	1/4" [6] Thick Polyethylene Plastic ASTM D4397	-

 Midwest Roadside Safety Facility	TL-4 Bridge Rail Test No. 4CBR-1	SHEET: 15 of 15 DATE: 9/13/2018 DRAWN BY: MES/JEK
	DWG. NAME: 4CBR-1_R14	SCALE: 1:200 UNITS: in./mm

Figure 33. Bill of Materials, Test No. 4CBR-1



Figure 34. Test Installation Photographs, Test No. 4CBR-1

7 TEST CONDITIONS

7.1 Test Facility

The Outdoor Test Site is located at the Lincoln Air Park on the northwest side of the Lincoln Municipal Airport and is approximately 5 miles northwest of the University of Nebraska-Lincoln.

7.2 Vehicle Tow and Guidance System

A reverse-cable, tow system with a 1:2 mechanical advantage was used to propel the test vehicle. The distance traveled and the speed of the tow vehicle were one-half that of the test vehicle. The test vehicle was released from the tow cable before impact with the barrier system. A digital speedometer on the tow vehicle increased the accuracy of the test vehicle impact speed.

A vehicle guidance system developed by Hinch [40] was used to steer the test vehicle. A guide flag, attached to the left-front wheel and the guide cable, was sheared off before impact with the barrier system. The $\frac{3}{8}$ -in. diameter guide cable was tensioned to approximately 3,500 lb and supported both laterally and vertically every 100 ft by hinged stanchions. The hinged stanchions stood upright while holding up the guide cable, but as the vehicle was towed down the line, the guide flag struck and knocked each stanchion to the ground.

7.3 Test Vehicle

For test no. 4CBR-1, a 2005 International 4300 single-unit truck was used as the test vehicle. The curb, test inertial, and gross static vehicle weights were 14,742 lb, 22,198 lb, and 22,360 lb, respectively. The test vehicle and ballast are shown in Figures 35 through 37 and vehicle dimensions are shown in Figure 38.

The longitudinal component of the center of gravity (c.g.) was determined using the measured axle weights. The location of the c.g. is shown in Figures 38 and 39. Data used to calculate the location of the c.g. and ballast information are shown in Appendix B.

Square, black- and white-checked targets were placed on the vehicle for reference to be viewed from the high-speed digital video cameras and aid in the video analysis, as shown in Figure 39. Round, checked targets were placed at the c.g. on the left-side door, the right-side door, and the roof of the vehicle.

The front wheels of the test vehicle were aligned to vehicle standards except the toe-in value was adjusted to zero such that the vehicle would track properly along the guide cable. A 5B flash bulb was mounted under the vehicle's left-side windshield wiper and was fired by a pressure tape switch mounted at the impact corner of the bumper. The flash bulb was fired upon initial impact with the test article to create a visual indicator of the precise time of impact on the high-speed digital videos. A radio-controlled brake system was installed in the test vehicle so the vehicle could be brought safely to a stop after the test.



Figure 35. Test Vehicle, Test No. 4CBR-1



Figure 36. Test Vehicle Ballast, Test No. 4CBR-1



49

Figure 37. Test Vehicle's Interior Floorboards and Undercarriage, Test No. 4CBR-1

Date: <u>8/21/2018</u>		Test Name: <u>4CBR-1</u>		VIN No: <u>1HTMMAAN66H284494</u>	
Year: <u>2005</u>		Make: <u>International</u>		Model: <u>4300</u>	
Tire Size: <u>11r22.5</u>		Tire Inflation Pressure: <u>105 Psi</u>		Odometer: <u>324817</u>	

Vehicle Geometry - in. (mm)
Target Ranges listed below

A: <u>92 1/2 (2350)</u>	B: <u>98 7/8 (2511)</u>
C: <u>344 (8738)</u> <small>Max: 394 (10000)</small>	D: <u>41 (1041)</u>
E: <u>229 1/2 (5829)</u> <small>Max: 240 (6100)</small>	F: <u>82 1/2 (2096)</u>
G: <u>50 5/8 (1286)</u>	H: <u>140 1/2 (3569)</u>
I: <u>20 3/4 (527)</u>	J: <u>35 1/4 (895)</u>
K: <u>23 (584)</u>	L: <u>48 1/2 (1232)</u> <small>49±2 (1245±50)</small>
M: <u>79 3/4 (2026)</u>	N: <u>72 3/4 (1848)</u>
O: <u>59 (1499)</u>	P: <u>1 (25)</u>
Q: <u>34 3/8 (873)</u>	R: <u>23 3/8 (594)</u>
S: <u>37 7/8 (962)</u>	T: <u>69 (1753)</u>
U: <u>106 3/4 (2711)</u>	V: <u>223 (5664)</u>
W: <u>4 (102)</u>	X: <u>146 1/8 (3712)</u>
Y: <u>30 1/8 (765)</u>	Z: <u>47 1/2 (1207)</u>

Ballast		Weight: <u>7927 (3596)</u>		W: <u>4 (102)</u>	
CG height: <u>63 1/2 (1613)</u> <small>63±2 (1600±50)</small>				X: <u>146 1/8 (3712)</u>	
				Y: <u>30 1/8 (765)</u>	
				Z: <u>47 1/2 (1207)</u>	
				AA: <u>71 3/8 (1813)</u>	

Mass Distribution lb (kg)		IW (Impact Width): <u>90 1/4 (2292)</u>		AA: <u>71 3/8 (1813)</u>	
Gross Static	LF <u>4424 (2007)</u>	RF <u>4304 (1952)</u>			
	LR <u>6800 (3084)</u>	RR <u>6832 (3099)</u>			

Weights lb (kg)	Curb	Test Inertial	Gross Static	Wheel Center Height (Front):
W-front	<u>7636 (3464)</u>	<u>8606 (3904)</u>	<u>8728 (3959)</u>	<u>19 1/2 (495)</u>
W-rear	<u>7106 (3223)</u>	<u>13592 (6165)</u>	<u>13632 (6183)</u>	Wheel Center Height (Rear): <u>20 (508)</u>
W-total	<u>14742 (6687)</u> <small>13200±2200 (6000±1000)</small>	<u>22198 (10069)</u> <small>22046±660 (10000±300)</small>	<u>22360 (10142)</u>	Wheel Well Clearance (Front): <u>46 1/2 (1181)</u>
				Wheel Well Clearance (Rear): <u>43 1/2 (1105)</u>
				Bottom Frame Height (Front): <u>11 (279)</u>
				Bottom Frame Height (Rear): <u>27 (686)</u>

GVWR Ratings lb		Surrogate Occupant Data		Engine Type: <u>Diesel</u>	
Front	<u>14000</u>	Type:	<u>Hybrid II</u>	Engine Size: <u>7.6L V6</u>	
Rear	<u>23000</u>	Mass:	<u>162 lb</u>	Transmission Type: <u>Manual</u>	
Total	<u>37000</u>	Seat Position:	<u>Left/Driver</u>	Drive Type: <u>RWD</u>	

Note any damage prior to test: _____ None

Figure 38. Vehicle Dimensions, Test No. 4CBR-1

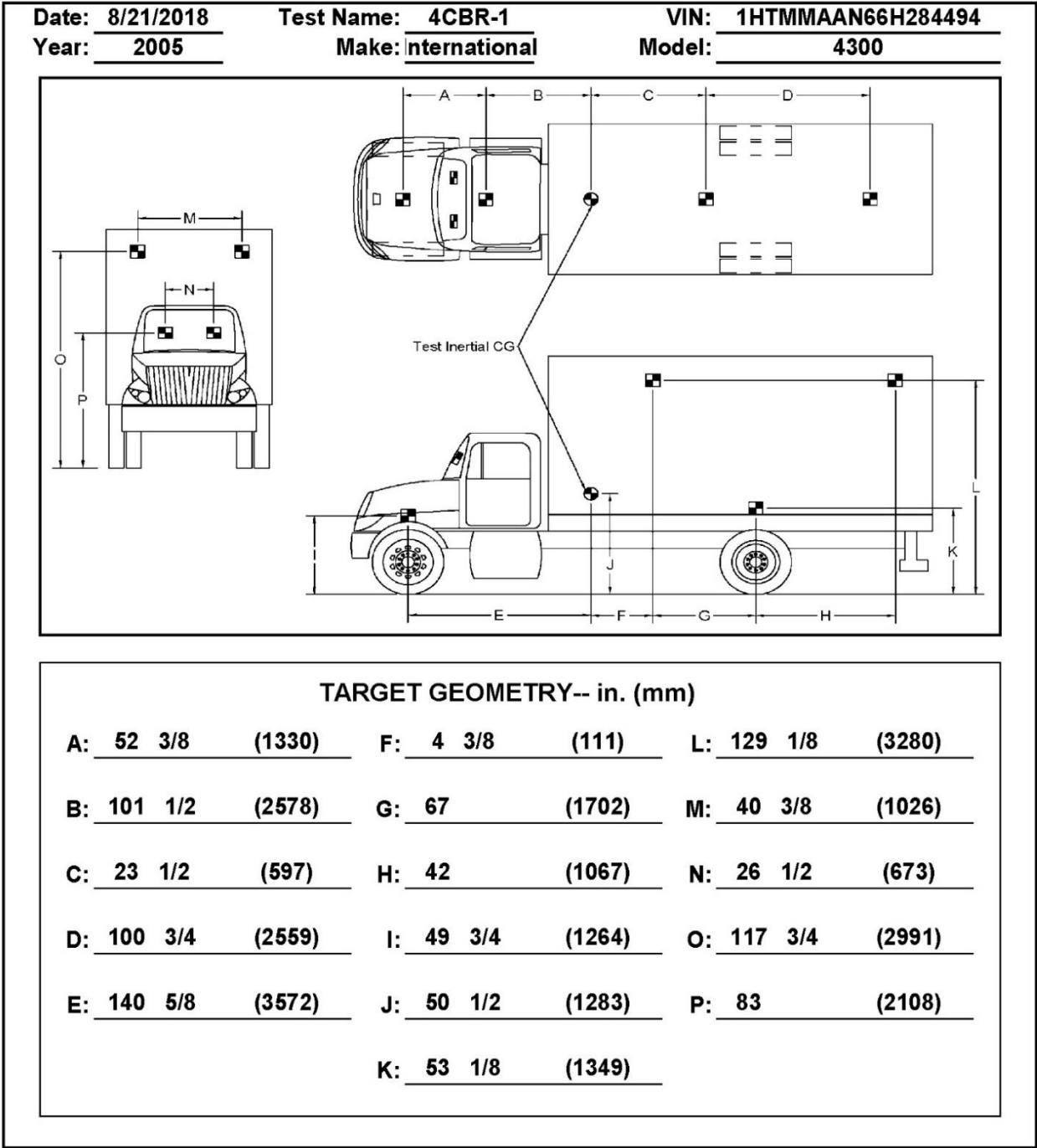


Figure 39. Target Geometry, Test No. 4CBR-1

7.4 Simulated Occupant

For test no. 4CBR-1, a Hybrid II 50th-Percentile, Adult Male Dummy, equipped with footwear, was placed in the right-front seat of the test vehicle with the seat belt fastened. The simulated occupant had a final weight of 162 lb. As recommended by MASH 2016, the simulated occupant weight was not included in calculating the c.g. location.

7.5 Data Acquisition Systems

7.5.1 Accelerometers

Two environmental shock and vibration sensor/recorder systems were used to measure the accelerations in the longitudinal, lateral, and vertical directions. The electronic accelerometer data obtained in dynamic testing was filtered using the SAE Class 60 and the SAE Class 180 Butterworth filters conforming to the SAE J211/1 specifications [41]. The two systems, the SLICE-1 and SLICE-2 units, were modular data acquisition systems manufactured by Diversified Technical Systems, Inc. (DTS) of Seal Beach, California. The SLICE-2 unit was mounted in the truck box near the c.g., while the SLICE-1 unit was mounted in the cab. The acceleration sensors were mounted inside the bodies of custom-built, SLICE 6DX event data recorders and recorded data at 10,000 Hz to the onboard microprocessor. Each SLICE 6DX was configured with 7 GB of non-volatile flash memory, a range of ± 500 g's, a sample rate of 10,000 Hz, and a 1,650 Hz (CFC 1000) anti-aliasing filter. The "SLICEWare" computer software program and a customized Microsoft Excel worksheet were used to analyze and plot the accelerometer data.

7.5.2 Rate Transducers

Two identical angular rate sensor systems mounted inside the bodies of the SLICE-1 and SLICE-2 event data recorders were used to measure the rates of rotation of the test vehicle. Each SLICE MICRO Triax ARS had a range of 1,500 degrees/sec in each of the three directions (roll, pitch, and yaw) and recorded data at 10,000 Hz to the onboard microprocessors. The raw data measurements were then downloaded, converted to the proper Euler angles for analysis, and plotted. The "SLICEWare" computer software program and a customized Microsoft Excel worksheet were used to analyze and plot the angular rate sensor data.

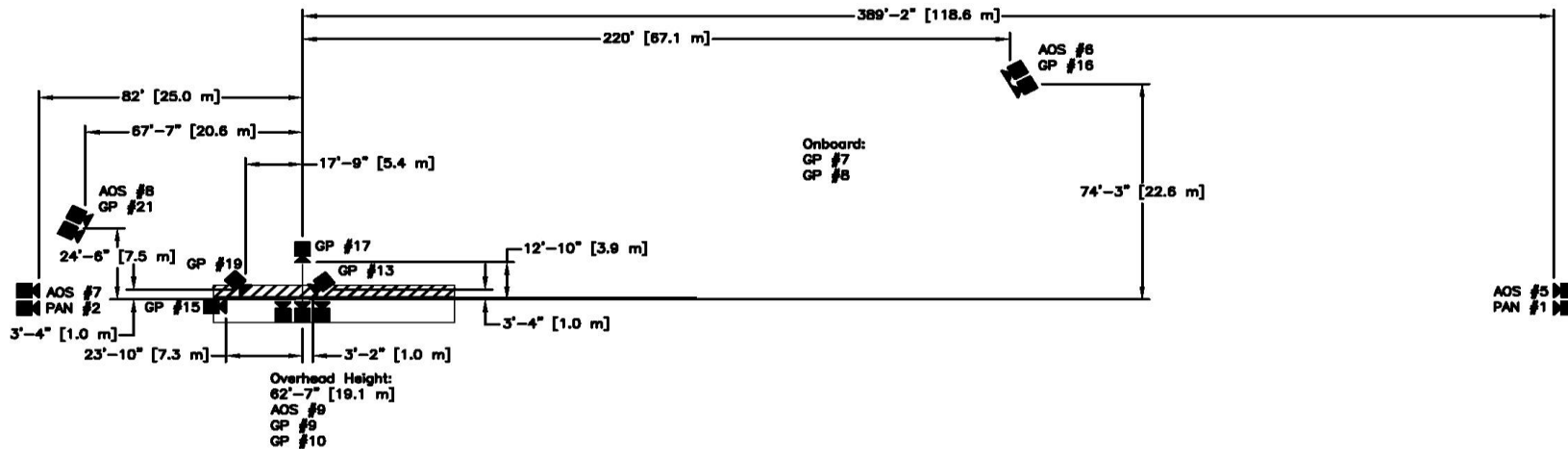
7.5.3 Retroreflective Optic Speed Trap

The retroreflective optic speed trap was used to determine the speed of the test vehicle before impact. Three retroreflective targets, spaced at approximately 18-in. intervals, were applied to the side of the vehicle. When the emitted beam of light was reflected by the targets and returned to the Emitter/Receiver, a signal was sent to the data acquisition computer, recording at 10,000 Hz, as well as the external LED box activating the LED flashes. The speed was then calculated using the spacing between the retroreflective targets and the time between the signals. LED lights and high-speed digital video analysis are only used as a backup in the event that vehicle speeds cannot be determined from the electronic data.

7.5.4 Digital Photography

Five AOS high-speed digital video cameras, ten GoPro digital video cameras, and two Panasonic digital video cameras were utilized to film test no. 4CBR-1. Camera details, camera operating speeds, lens information, and a schematic of the camera locations relative to the system are shown in Figure 40. Note, cameras AOS-9 and GP-9 experienced technical difficulties and did not record the impact event.

The high-speed videos were analyzed using TEMA Motion and Redlake MotionScope software programs. Actual camera speed and camera divergence factors were considered in the analysis of the high-speed videos. A digital still camera was also used to document pre- and post-test conditions for the test.



No.	Type	Operating Speed (frames/sec)	Lens	Lens Setting
AOS-5	AOS X-PRI Gigabit	500	100 mm Fixed	
AOS-6	AOS X-PRI Gigabit	500	Fujinon 35mm Fixed	
AOS-7	AOS X-PRI Gigabit	500	Fujinon 50 mm Fixed	
AOS-8	AOS S-VIT 1531	500	Sigma 28-70	Between 35 and 50
AOS-9	AOS TRI-VIT	1000	Kowa 12 mm fixed	
GP-7	GoPro Hero 4	30		
GP-8	GoPro Hero 4	120		
GP-9	GoPro Hero 4	120		
GP-10	GoPro Hero 4	120		
GP-13	GoPro Hero 4	240		
GP-15	GoPro Hero 4	240		
GP-16	GoPro Hero 4	240		
GP-17	GoPro Hero 4	240		
GP-19	GoPro Hero 6	120		
GP-21	GoPro Hero 6	120		
PAN-1	Panasonic (HC-V770)	60		
PAN-2	Panasonic (HC-V770)	60		

Figure 40. Camera Locations, Speeds, and Lens Settings, Test No. 4CBR-1

8 FULL-SCALE CRASH TEST NO. 4CBR-1

8.1 Weather Conditions

Test no. 4CBR-1 was conducted on August 21, 2018 at approximately 1:15 p.m. The weather conditions as per the National Oceanic and Atmospheric Administration (station 14939/LNK) were reported and are shown in Table 10.

Table 10. Weather Conditions, Test No. 4CBR-1

Temperature	72°F
Humidity	61%
Wind Speed	14 mph
Wind Direction	350° from True North
Sky Conditions	Clear
Visibility	8 Statute Miles
Pavement Surface	Dry
Previous 3-Day Precipitation	2.5 in.
Previous 7-Day Precipitation	2.9 in.

8.2 Test Description

Initial vehicle impact was to occur 27 ft – 8 in. downstream from the upstream end of barrier, as shown in Figure 41, which was selected to load the center of the simulated bridge deck and avoid loads transferring out close to the ends of the deck. During test no. 4CBR-1, the 22,198-lb SUT impacted the bridge rail 4 in. upstream from the targeted impact point at a speed of 57.6 mph and an angle of 16.0 degrees. The barrier contained and redirected the SUT with minimal system deflection and negligible system damage. The SUT reached a maximum roll angle of 35 degrees during redirection and exited the system with a speed and angle of 41.7 mph and 2.8 degrees, respectively. After exiting the system, the SUT rolled downstream, impacted a row of portable concrete barriers, ruptured a few of the barrier connections, and came to rest on top of one of the barrier segments approximately 350 ft downstream from impact. A detailed description of the sequential impact events is contained in Table 11, and sequential photographs of the impact event are shown in Figures 42 through 44. Documentary photographs are shown in Figure 45. Photographs of the vehicle trajectory and final position are shown in Figure 46.

Table 11. Sequential Description of Impact Events, Test No. 4CBR-1

Time (sec)	Event
0.000	Vehicle's front bumper contacted barrier 328 in. downstream from upstream end of barrier.
0.010	Vehicle's left-front tire contacted concrete barrier.
0.026	Vehicle's left-front fender deformed.
0.036	Vehicle's hood contacted concrete barrier.
0.042	Vehicle rolled toward system.
0.116	Vehicle yawed away from system.
0.136	Vehicle's right-front tire became airborne.
0.148	Vehicle gouged face of concrete barrier.
0.210	Vehicle's right-rear tire became airborne.
0.242	Vehicle's left-rear tire contacted concrete barrier.
0.262	Vehicle's left-rear lower box corner contacted concrete barrier.
0.290	Vehicle's grille became disengaged.
0.296	Vehicle was parallel to system at a speed of 48.7 mph.
0.366	Vehicle pitched downward.
0.520	Vehicle's box in contact with top of concrete barrier.
0.668	Vehicle reached a maximum roll angle of 35 degrees and began to roll away from barrier.
0.852	Vehicle's box gouged top-front corner of concrete barrier.
0.874	Vehicle's air tank became disengaged.
1.102	Vehicle's left-front tire re-contacted concrete barrier.
1.114	Vehicle's left headlight contacted concrete barrier.
1.166	Vehicle's right-front tire regained contact with ground.
1.292	Vehicle's right-rear tire regained contact with ground.
1.382	Vehicle's right box door lower hinge disengaged.
1.562	Vehicle's left-front tire became airborne.
1.626	Vehicle exited system at a speed of 41.7 mph and an angle of 2.8 degrees.
1.828	Vehicle's left-front tire regained contact with ground.
4.300	Vehicle impacted portable concrete barriers used for vehicle containment.
4.800	Vehicle overrode a portable concrete barrier segment.
8.000	Vehicle came to rest approximately 350 feet downstream from impact.



Figure 41. Impact Location, Test No. 4CBR-1



0.000 sec



1.000 sec



0.200 sec



1.200 sec



0.400 sec



1.400 sec



0.600 sec



1.600 sec



0.800 sec



1.800 sec

Figure 42. Sequential Photographs, Test No. 4CBR-1



0.000 sec



1.000 sec



0.200 sec



1.200 sec



0.400 sec



1.400 sec



0.600 sec



1.600 sec



0.800 sec



1.800 sec

Figure 43. Additional Sequential Photographs, Test No. 4CBR-1



0.000 sec



0.100 sec



0.200 sec



0.400 sec



0.600 sec



0.800 sec



0.000 sec



0.100 sec



0.200 sec



0.400 sec



0.600 sec



0.800 sec

Figure 44. Additional Sequential Photographs, Test No. 4CBR-1

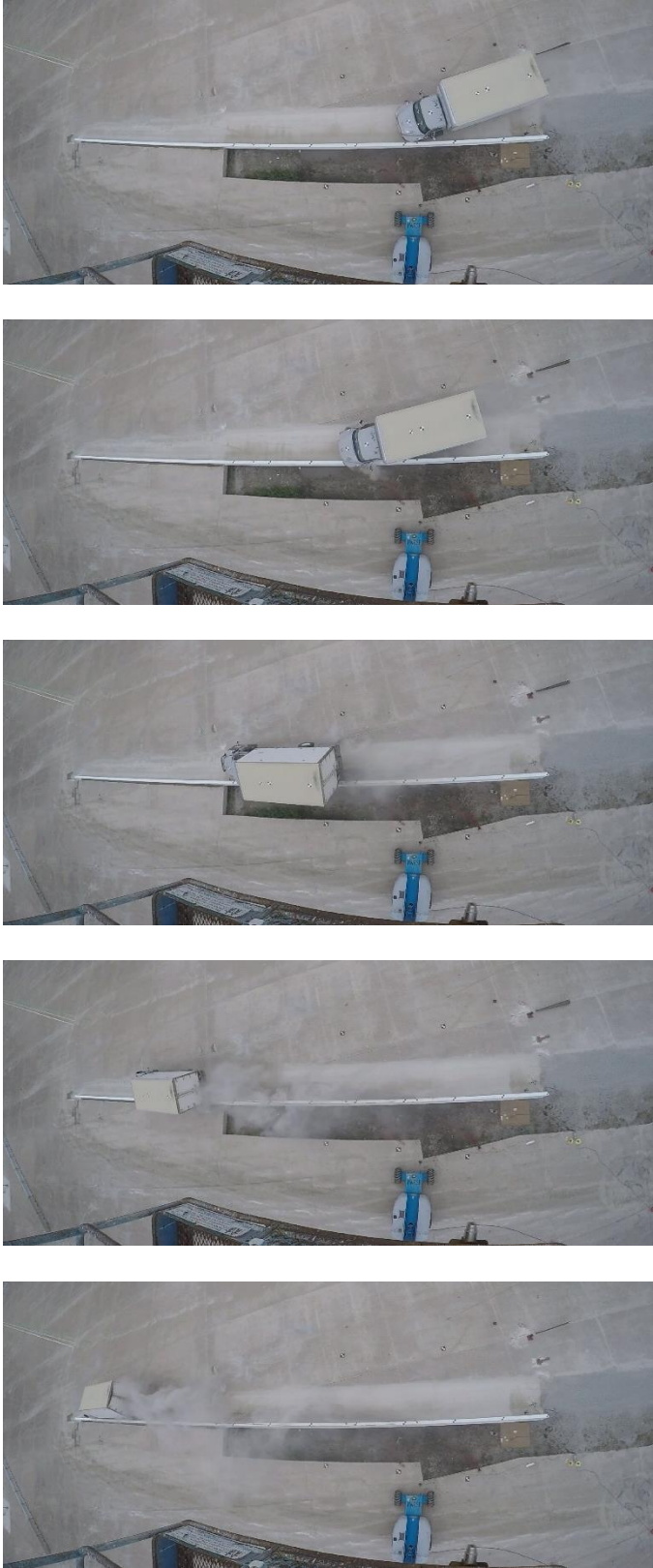


Figure 45. Documentary Photographs, Test No. 4CBR-1



Figure 46. Vehicle Final Position and Trajectory Marks, Test No. 4CBR-1

8.3 Barrier Damage

Damage to the barrier was minimal, as shown in Figures 47 through 50. Barrier damage consisted of contact marks, concrete gouges and spalling, and minor cracks. Shrinkage cracks present before testing were highlighted with a red marker, as can be seen in the damage documentation photographs.

The length of vehicle contact was approximately 112 ft. The primary contact mark on the face of the bridge rail began at the impact point and extended 25 ft downstream. Another significant contact mark was observed on the top face, starting 27 ft – 8 in. downstream from the impact point and spanning 17 ft – 8 in., coinciding with the cargo box leaning on the barrier. Less severe contact marks were observed on the top face of the barrier starting 45 ft – 7 in. from the impact point and extending 42 ft – 4 in. downstream. Additionally, minor contact marks were observed on the front face of the barrier beginning 44 ft – 3 in. downstream from impact and continuing to the downstream end of the system.

Significant gouging in the front face of the bridge rail occurred 3 ft – 8 in. downstream from the impact point and continued 9 ft downstream. Additionally, the top front edge of the railing experienced significant gouging where the cargo box leaned on the barrier beginning 46 ft – 2 in. downstream from the impact point and extending 10 ft – 10 in. downstream.

The bridge deck and overlay remained undamaged during the test. Even after the overlay was removed from the deck surface, only minor cracks were observed. However, these cracks were likely just shrinkage cracks, and none were thought to be structurally significant.

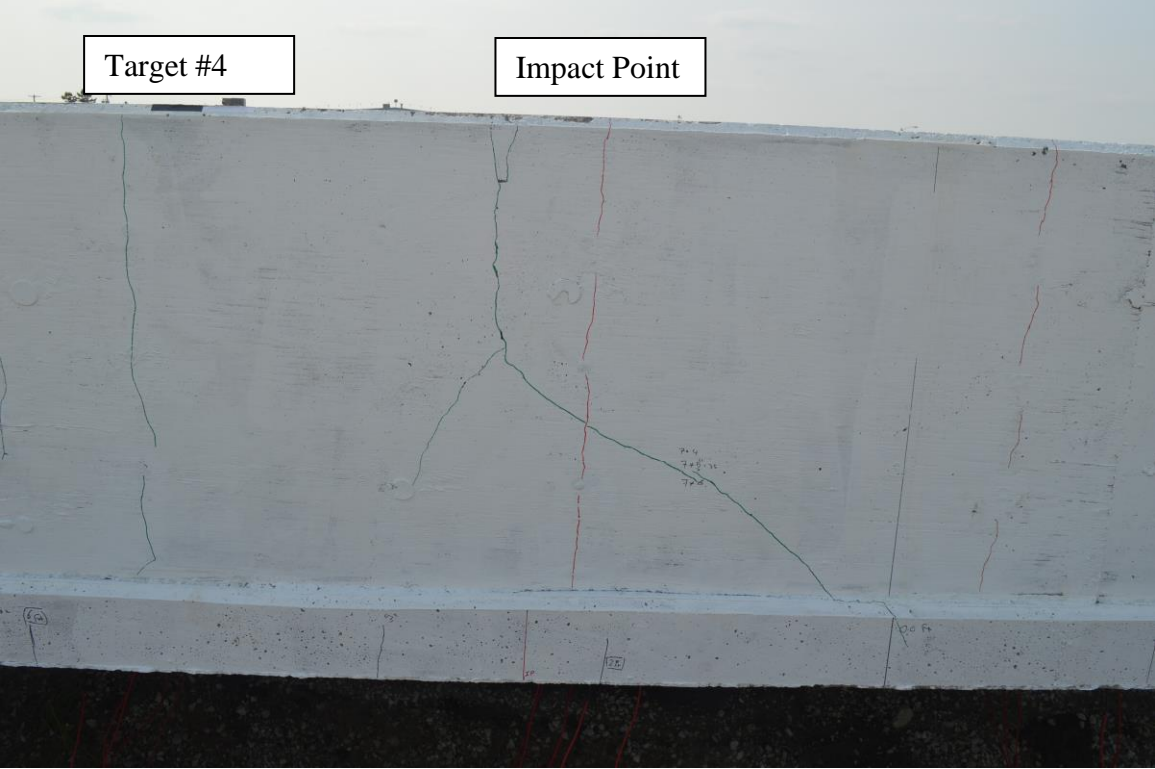
The maximum lateral dynamic barrier deflection, including flexure in the deck, was 1.0 in., which occurred 22 ft – 11 in. downstream from the impact point, as determined from high-speed digital video analysis. After the impact event, the deck overhang and barrier both returned to their original positions resulting in a permanent set of 0.0 in. The working width of the system was 53.7 in., also determined from high-speed digital video analysis. A schematic of the permanent set, dynamic deflection, and working width is shown in Figure 51.



Figure 47. Overall System Damage, Test No. 4CBR-1



Figure 48. System Damage, Downstream Gouge Details, Test No. 4CBR-1



Note: Red lines are shrinkage cracks present before testing. Green lines are cracks from impact.

Figure 49. System Damage, Backside of Bridge Rail, Test No. 4CBR-1



Figure 50. Deck Damage, Test No. 4CBR-1

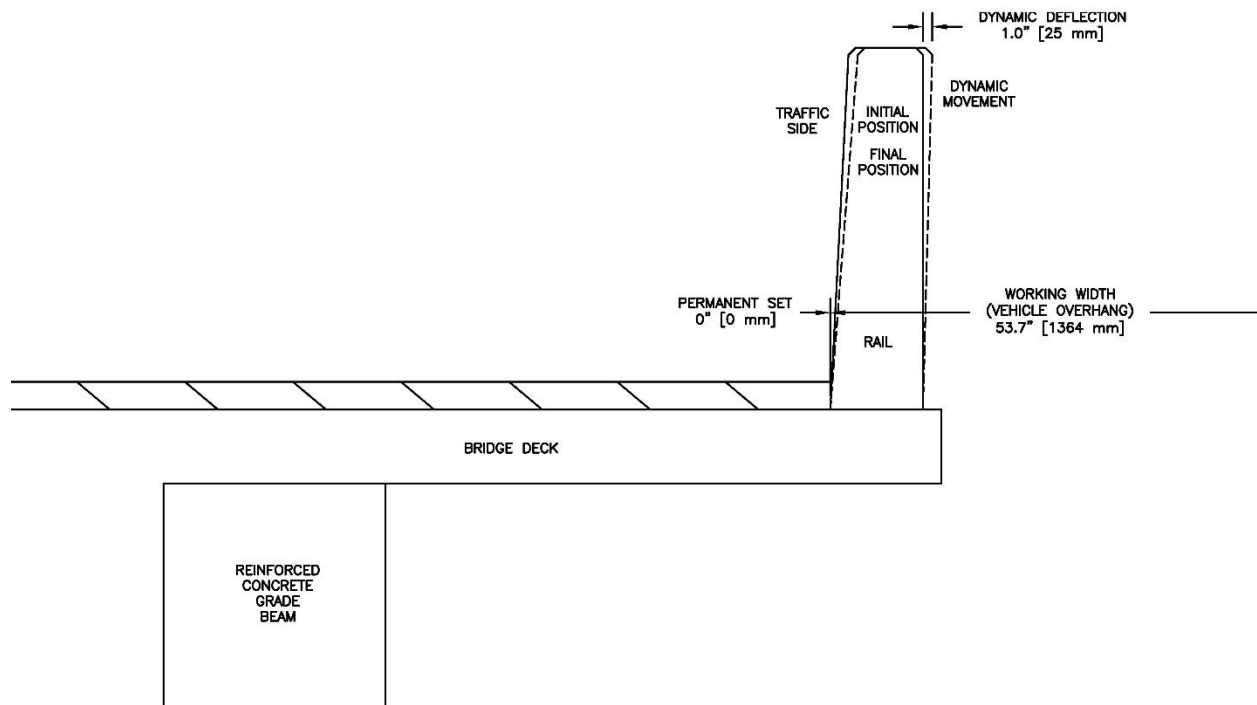


Figure 51. Permanent Set, Dynamic Deflection, and Working Width, Test No. 4CBR-1

8.4 Vehicle Damage

In test no. 4CBR-1, the test vehicle experienced two distinct impact sequences: (1) the impact with the concrete bridge rail and (2) a secondary impact with portable concrete barriers (PCBs) placed to contain the vehicle after exiting the system. The secondary impact was severe and resulted in most of the damage sustained by the vehicle. It is important to distinguish the damage sustained in each impact, as the secondary impact damage is irrelevant to the evaluation of the concrete bridge rail system.

In the impact with the concrete bridge rail system, the test vehicle sustained minimal damage concentrated on the left-front corner of the vehicle. The grille disengaged from the vehicle. The left side of the front bumper was deformed inward and backward. The left fender was pushed upward and dented inward. The left-front and left-rear wheel assemblies were deformed, and deformations and gouging were present on the left-side wheel rims. The left side of the rear bumper was dented and scuffed. Additionally, the right-side box door was removed from its hinges. The damage sustained by the vehicle in the impact with the bridge rail system, prior to its secondary impact with the PCBs, is shown in Figure 52. Note that the vehicle was rolling downstream on all tires.



Figure 52. Vehicle Damage after Primary Impact

After the test, the vehicle suffered severe damage in a secondary impact where the vehicle broke through and overrode a PCB installation. Severe damage was sustained by the front end and undercarriage of the vehicle, including complete disengagement of the front axle, severing of the brake lines, backward crushing of the engine compartment, and separation of the floor pan seam near the left-front corner of the occupant compartment. Less severe damage included tearing of the front tires and denting and gouging of the undercarriage in multiple locations.

The total damage sustained by the vehicle in both test no. 4CBR-1 and the subsequent impact with the arresting structure is shown in Figures 53 through 56. Overall, the damage to the vehicle was severe, although the damage sustained in the actual impact with the concrete bridge rail system was minimal. The maximum occupant compartment intrusions are listed in Table 12 along with the intrusion limits established in MASH 2016 [3] for various areas of the occupant compartment. Complete occupant compartment and vehicle deformations and the corresponding locations are provided in Appendix C. MASH 2016 defines intrusion or deformation as the occupant compartment being deformed and reduced in size with no observed penetration. The floor pan deformation and seam opening near the left-front corner of the heavily-corroded floor pan, as shown in Figure 56, were sustained during the secondary impact as the front axle and tire were driven backward and under the occupant compartment. Consequently, the floor pan seam opening was not included in the safety evaluation of the bridge rail system. Therefore, none of the established MASH 2016 deformation limits were violated in test no. 4CBR-1. Outward deformations, which are denoted as negative numbers in Appendix C, are not considered crush toward the occupant and are not evaluated by MASH 2016 criteria.



Figure 53. Left- and Right-Side Vehicle Damage, Test No. 4CBR-1



Figure 54. Rear Vehicle Damage, Test No. 4CBR-1



Figure 55. Post-Test Undercarriage Photos, Test No. 4CBR-1



Figure 56. Post-Test Floor Pan Photos, Test No. 4CBR-1

Table 12. Maximum Occupant Compartment Intrusion by Location, Test No. 4CBR-1

Location	Maximum Intrusion (in.)	MASH 2016 Allowable Intrusion (in.)
Wheel Well & Toe Pan	3.9	≤ 9
Floor Pan & Transmission Tunnel	5.7	≤ 12
A-Pillar	2.0	≤ 5
A-Pillar (Lateral)	2.0	≤ 3
B-Pillar	0.1	≤ 5
B-Pillar (Lateral)	0.0	≤ 3
Side Front Panel (in Front of A-Pillar)	3.9	≤ 12
Side Door (Above Seat)	2.1	≤ 9
Side Door (Below Seat)	1.8	≤ 12
Roof	0.1	≤ 4
Windshield	0.0	≤ 3
Side Window	Intact	No shattering resulting from contact with structural member of test article
Dash	7.0	N/A

N/A – Not Applicable

8.5 Occupant Risk

The calculated occupant impact velocities (OIVs) and maximum 0.010-sec average occupant ridedown accelerations (ORAs) in both the longitudinal and lateral directions and maximum Euler angles are shown in Table 13. Although MASH does not specify limits for OIVs, ORAs, or angular displacements, they are reported herein for comparison purposes. Additionally, THIV, PHD, and ASI values were calculated included in Table 13. The recorded data from the accelerometers and the rate transducers are shown graphically in Appendix D.

Table 13. Summary of OIV, ORA, THIV, PHD, and ASI Values, Test No. 4CBR-1

Evaluation Criteria		Transducer		MASH Limits
		SLICE-1 (in cab)	SLICE-2 (at c.g.)	
OIV ft/s	Longitudinal	-4.87	-7.54	not required
	Lateral	13.84	12.21	not required
ORA g's	Longitudinal	-7.89	-13.83	not required
	Lateral	7.42	14.90	not required
Maximum Angular Displacement deg.	Roll	-35.0	-32.8	not required
	Pitch	-5.2	-6.0	not required
	Yaw	18.2	17.1	not required
THIV – ft/s		36.45	18.60	not required
PHD – g's		8.61	16.87	not required
ASI		0.81	0.80	not required

8.6 Impact Loads

The longitudinal and lateral vehicle accelerations, as measured at the vehicle’s c.g., were processed using an SAE CFC-60 filter and a 50-msec moving average. The 50-msec moving average vehicle accelerations were then combined with the uncoupled yaw angle versus time data in order to estimate the vehicular loading applied to the barrier system. From the data analysis, the perpendicular impact forces were determined for the bridge rail, as shown in Figure 57. A maximum perpendicular (i.e., lateral) impact load equal to 153 kips was imparted on the barrier at 0.275 s after impact, as determined by the SLICE-2 unit. A peak frictional load of 50 kips was observed 0.244 s after impact. Note, these impact loads are significantly higher than expected. Previously measured impact loads from MASH TL-4 crash tests using this estimation procedure were typically between 95 kips and 110 kips [17-18].

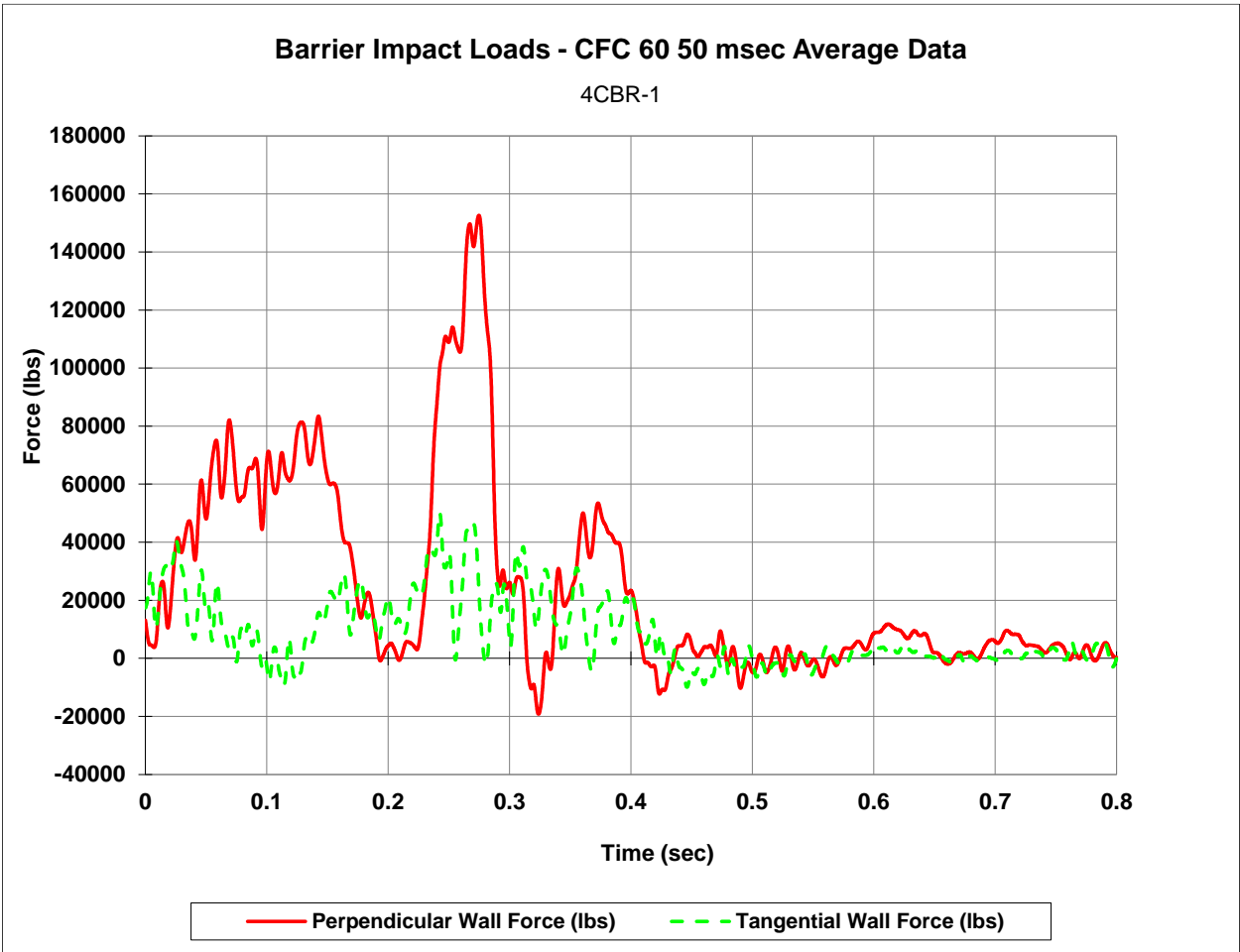
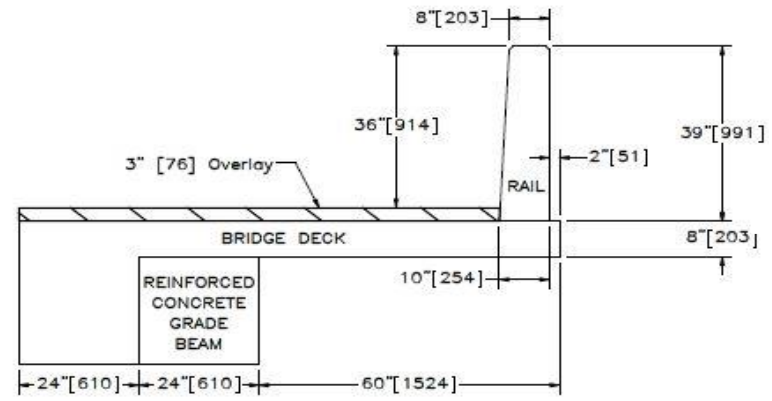
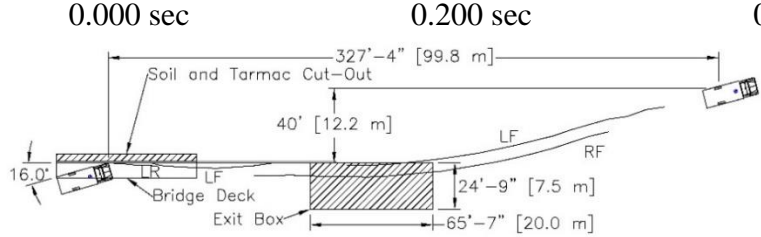


Figure 57. Perpendicular and Tangential Impact Forces, Test No. 4CBR-1

8.7 Discussion

A summary of the test results and sequential photographs are shown in Figure 58. The analysis of the test results for test no. 4CBR-1 showed that the system adequately contained and redirected the 10000S vehicle with minimal lateral displacements of the barrier. The test vehicle did not penetrate nor ride over the barrier and remained upright during and after the collision. Detached elements, fragments, or other debris from the test article did not penetrate or show potential for penetrating the occupant compartment, or present an undue hazard to other traffic, pedestrians, or work-zone personnel. Vehicle roll, pitch, and yaw angular displacements, as shown in Appendix D, were deemed acceptable, because they did not adversely influence occupant risk nor cause rollover. After impact, the vehicle exited the barrier at an angle of 2.8 degrees, and its trajectory did not violate the bounds of the exit box. Deformations of, or intrusions into, the occupant compartment that could have caused serious injury did not occur during the test, as the opening of the floor pan seam occurred during the secondary impact with the PCBs. Therefore, test no. 4CBR-1 was determined to be acceptable according to the MASH 2016 safety performance criteria for test designation no. 4-12.



- Test AgencyMwRSF
- Test Number.....4CBR-1
- Date 8/21/18
- MASH 2016 Test Designation No..... 4-12
- Test Article..... Optimized MASH TL-4 Concrete Bridge Rail
- Total Length 150 ft
- Key Component – Concrete Bridge Rail
 - Length 150 ft
 - Height 36 in. from top of existing tarmac
- Soil Type Well-Graded Gravel
- Vehicle Make /Model..... 2005 International 4300 single unit truck
 - Curb..... 14,742 lb
 - Test Inertial..... 22,198 lb
 - Gross Static..... 22,360 lb
- Impact Conditions
 - Speed 57.6 mph
 - Angle 16 deg.
 - Impact Location..... 332 in. downstream from upstream end of barrier
- Impact Severity 186.2 kip-ft > 142 kip-ft limit from MASH 2016
- Exit Conditions
 - Speed 41.7 mph
 - Angle 2.8 deg.
- Exit Box Criterion Pass
- Vehicle Stability.....Satisfactory
- Vehicle Stopping Distance 327 ft – 4 in.
- Vehicle Damage.....Minimal
 - VDS [42] 11-FL-6
 - CDC [43] 11-FLEW-3
 - Maximum Interior Deformation 5.7 in.
- Test Article Damage.....Minimal
- Maximum Test Article Deflections
 - Permanent Set..... 0.0 in.
 - Dynamic 1.0 in.
 - Working Width..... 53.7 in.

• Transducer Data

Evaluation Criteria		Transducer		MASH 2016 Limit
		SLICE-1 (in-cab)	SLICE-2 (at c.g.)	
OIV ft/s	Longitudinal	-4.87	-7.54	not required
	Lateral	13.84	12.21	not required
ORA g's	Longitudinal	-7.89	-13.83	not required
	Lateral	7.42	14.90	not required
Maximum Angular Displacement deg.	Roll	-35.0	-32.8	not required
	Pitch	-5.2	-6.0	not required
	Yaw	18.2	17.1	not required
THIV – ft/s		36.45	18.60	not required
PHD – g's		8.61	16.87	not required
ASI		0.81	0.80	not required

77

Figure 58. Summary of Test Results, Test No. 4CBR-1

9 SUMMARY, CONCLUSIONS, AND RECOMMENDATIONS

A new MASH TL-4, single-slope, reinforced-concrete bridge rail was designed, crash tested, and evaluated. The bridge rail was optimized to satisfy MASH TL-4 design loads, maximize vehicle stability, minimize installation costs, and minimize load transfer into the deck to mitigate the potential for deck damage. The new bridge rail was configured with an 8-in. wide top surface, a front face with a 2.9-degree slope from vertical, and 10-in. wide base, which was narrower than other, previously tested MASH TL-4 single-slope bridge rails. The narrow width and minimal reinforcement helped to minimize initial installation costs. Additionally, the barrier had a 39-in. design height, such that it would remain MASH TL-4 crashworthy after roadway overlays up to 3 in. thick.

One full-scale crash test, test no. 4CBR-1, was conducted on a concrete bridge rail in accordance with MASH test designation no. 4-12. The bridge rail was tested in combination with a critical deck configuration which featured an 8-in. thickness and a 5-ft overhang. The bridge rail was installed with a 39 in. height above the deck, and a 3-in. overlay was applied to the deck surface bringing the effective height of the bridge rail to 36 in. This critical rail configuration was used to evaluate potential override and maximize loading to the bridge rail and deck overhang.

During the test, the 22,198-lb single-unit truck impacted the MASH TL-4 concrete bridge rail system at a speed of 57.6 mph and an angle of 16.0 degrees, thus resulting in an impact severity of 186.3 kip-ft. The single-unit truck was successfully contained and redirected, and the vehicle exited the system at an angle of 2.8 degrees. The truck box leaned over the top of the bridge rail to establish a 53.7-in. working width, but the vehicle did not show any propensity for rollover during or after the test. After the crash test, minimal damage in the form of concrete gouges and hairline cracks was observed in the bridge rail near the impact region and along the top of the barrier. No damage related to the impact event was found on the top or bottom surfaces of the deck. A summary of the MASH evaluation of the bridge rail is shown in Table 14.

The bridge rail's roughly 3-degree sloped front face allowed the barrier to be installed using slipform operations while also ensuring vehicle stability. This slope fell between other existing MASH barriers that have been successfully tested with passenger vehicles at 0-degree, 9-degree, and 11-degree sloped front faces, effectively bracketing the performance of the barrier [23-24, 37-39]. As such, MASH test designation nos. 4-10 and 4-11 were deemed non-critical because occupant risk and passenger vehicle stability were not a concern and test designation no. 4-12 would apply higher magnitude impact loads to the bridge rail. Thus, the new concrete bridge rail was considered MASH 2016 TL-4 crashworthy.

Both interior and end region reinforcement configurations were developed for the new TL-4 bridge rail. The two configurations differ only in the spacing of the vertical steel rebar (12 in. for interior regions and 4 in. for end regions). The test installation comprised only the bridge rail's interior configuration as it was calculated as having a lower strength capacity than the end region configuration. Therefore, the test was conducted on the more critical of the two reinforcement configurations. Since the bridge rail's interior region showed no signs of structural damage, the end region should also be considered MASH crashworthy. Note, end section reinforcement should be used for at least 6 ft adjacent to any railing discontinuity or expansion/contraction gap. There could be vehicle snag concerns on the ends of barrier segments if the gaps between adjacent segments were large enough. However, anchored portable concrete barrier systems have been

successfully MASH tested with 4-in. gaps between segments [44], so limiting the gaps to a maximum width of 4 in. would alleviate this snag potential. Additionally, it is recommended that chamfering barrier edges adjacent to gaps can further reduce snagging potential [45-46].

Although the barrier was designed with an increased height to account for future overlays, some state DOTs do not apply overlays to their bridge decks, while others mill down the wearing surface before an overlay is applied to keep the roadway at a relatively constant height. Thus, some state DOTs may not desire to increase the height of their bridge rails above the nominal 36 in. height for MASH TL-4 barriers. In these situations, the bridge rail could be installed with a 36-in. nominal height without changing any other design features. The same reinforcement configuration should be used, only the longitudinal bars would be spaced slightly closer to one another. Maintaining the 2-in. setback with this shorter version of the barrier would result in only a 0.3-degree increase to the slope of the barrier face. The resulting 3.2-degree slope is well below the 11.0-degree slope that was previously successfully tested to MASH TL-4 with a 36-in. tall single slope barrier [9]. Thus, the 36-in. tall version of the bridge rail should also be considered crashworthy to MASH TL-4 criteria. Additionally, if the barrier is properly anchored to a moment slab or foundation, the new TL-4 design could be used as a median or roadside barrier, especially in its double-sided, or symmetric, configuration shown previously in Figure 14.

It is recognized that different transportation agencies may prefer to use a different deck thickness and/or cantilever distance. The deck design methodology described herein can be utilized to supplement the design specifications within AASHTO LFRD BDS [15]. Thus, bridge engineers can design and analyze various deck configurations in combination with concrete bridge rails. Similarly, yield-line theory could be utilized to evaluate potential modifications to the reinforcement configuration, if desired. Configurations with a minimum capacity equal to the capacity of the at-tested bridge rail, 84.4 kips, would be considered crashworthy.

Table 14. Summary of Safety Performance Evaluation

Evaluation Factors	Evaluation Criteria	Test No. 4CBR-1
Structural Adequacy	A. Test article should contain and redirect the vehicle or bring the vehicle to a controlled stop; the vehicle should not penetrate, underride, or override the installation although controlled lateral deflection of the test article is acceptable.	S
Occupant Risk	D. 1. Detached elements, fragments or other debris from the test article should not penetrate or show potential for penetrating the occupant compartment, or present an undue hazard to other traffic, pedestrians, or personnel in a work zone. 2. Deformations of, or intrusions into, the occupant compartment should not exceed limits set forth in Section 5.2.2 and Appendix E of MASH 2016.	S
	G. It is preferable, although not essential, that the vehicle remain upright during and after collision.	S
MASH 2016 Test Designation No.		4-12
Final Evaluation (Pass or Fail)		Pass

S – Satisfactory

U – Unsatisfactory

N/A – Not Applicable

10 MASH EVALUATION

The new MASH TL-4, single-slope, reinforced-concrete bridge rail detailed herein was optimized to satisfy MASH TL-4 design loads, maximize vehicle stability, minimize installation costs, minimize the potential for deck damage, and be compatible with roadway overlays up to 3 in. thick. The new bridge rail was 39 in. tall, 8 in. wide at the top, and 10 in. wide at the base. The bridge rail was configured with a near-vertical front face with a 2-in. batter that resulted in a slope of 2.9 degrees from vertical. Reinforcement consisted of eight #5 rebar divided equally between the front and back faces of the rail and #4 vertical U-bars spaced at 12 in. on-center.

For the full-scale testing and evaluation, the bridge rail was mounted to an 8-in. thick reinforced-concrete deck with a 5-ft overhang distance. A 3-in. overlay consisting of a weak concrete slurry was applied to the surface of the deck bringing the effective height of the bridge rail down to 36 in. This configuration was determined to be the most critical in terms of loading to the barrier and bridge deck, vehicle stability, and potential for the vehicle to roll over the barrier.

The new MASH TL-4 bridge rail was subjected to one full scale crash test in accordance with MASH test designation no. 4-12. The single-unit truck (SUT) was successfully contained and redirected, and the vehicle exited the system rolling on all wheels. Damage to the system consisted only of concrete gouging, hairline cracks, and cosmetic contact marks. The deck remained undamaged during the test. Thus, the bridge rail satisfied all safety performance criteria for MASH test designation no. 4-12.

A review of previous crash testing into concrete barrier systems led to the conclusion that only MASH test designation no. 4-12 was critical for evaluating the TL-4 concrete bridge rail. The impact severity of the 10000S SUT test was 34 percent higher than the 2700P pickup test and 278 percent higher than the 1100C small car test. NCHRP Project 22-20(2) found that the increased impact severity translated to increased impact loads for the 10000S SUT as compared to the passenger vehicles, as observed in the recommended impact loads for TL-3 and TL-4 MASH impacts [19]. Subsequently, the 10000S SUT test would impart the highest lateral impact load to the barrier and be the critical test for evaluating the strength of both the bridge rail and the bridge deck overhang.

Vehicle stability was not considered to be critical for either of the passenger vehicle tests. Previous crash testing of the 2270P pickup into an 11-degree single-slope concrete bridge rail and vertical-faced concrete bridge rails resulted in successful MASH tests with minimal vehicle roll and pitch displacements [37-39]. Similarly, previous 1100C small car tests have been successfully conducted on both single slope and vertical face concrete bridge rails [23-24]. The 3-degree slope of the new concrete TL-4 bridge rail was between those of typical single slope barriers and vertical parapets, so vehicle performance had been effectively bracketed by previous crash tests and there were no concerns for vehicle instability or excessive occupant risk values. Therefore, MASH test designation nos. 4-10 and 4-11 were deemed non-critical.

Although the full-scale crash test was conducted on a bridge railing interior section, end section reinforcement was designed by decreasing the vertical U-bar spacing to 4 in. on-center. The strength of this end section design was shown to be greater than that of the tested interior section using AASHTO recommended evaluation methods [15]. As such, the new TL-4 barrier's

end sections should also be considered MASH TL-4 crashworthy. Note, end section reinforcement should be used within 6 ft of any railing discontinuity or expansion/contraction gap.

Finally, the new bridge railing was developed with a nominal height of 39 in. to account for future roadway overlays up to 3 in. thick and still satisfy the 36-in. minimum height requirement for MASH TL-4 barriers. The bridge rail was tested and evaluated in the critical configuration with a 3-in. overlay placed on the deck in order to maximize loading and moment demands on the system. Since the test successfully redirected the vehicle while sustaining only cosmetic damage, the railing should be considered crashworthy at heights between 36 and 39 in. Therefore, the new concrete bridge rail has been determined to be crashworthy to MASH 2016 TL-4 standards at its nominal height of 39 in. and after roadway overlays up to 3 in. thick. Further, a 36-in. tall version of the new bridge rail (without deck overlays) consisting of the same reinforcement pattern was also determined to be MASH 2016 TL-4 crashworthy.

11 REFERENCES

1. Ross, H.E., Sicking, D.L., Zimmer, R.A., and Michie, J.D., *Recommended Procedures for the Safety Performance Evaluation of Highway Features*, National Cooperative Highway Research Program (NCHRP) Report 350, Transportation Research Board, Washington, D.C., 1993.
2. *Manual for Assessing Safety Hardware*, American Association of State Highway and Transportation Officials (AASHTO), Washington, D.C., 2009.
3. *Manual for Assessing Safety Hardware, Second Edition*, American Association of State Highway and Transportation Officials (AASHTO), Washington, D.C., 2016.
4. Polivka, K.A., Faller, R.K., Sicking, D.L., Rohde, J.R., Bielenberg, R.W., Reid, J.D., and Coon, B.A., *Performance Evaluation of the Permanent New Jersey Safety Shape Barrier - Update to NCHRP 350 Test No. 4-12*, Report No. TRP-03-178-06, Midwest Roadside Safety Facility, University of Nebraska-Lincoln, Lincoln, Nebraska, October 13, 2006.
5. Bullard, D.L., Bligh, R.P., Menges, W.L., and Haug, R.R., *Volume I: Evaluation of Existing Roadside Safety Hardware Using Updated Criteria*, NCHRP Project 22-14(03), Texas A&M Transportation Institute, Texas A&M University, College Station, Texas, March 2010.
6. Albuquerque, F.D.B. and Sicking, D.L., *Evaluation of the In-Service Safety Performance of Safety-Shape and Vertical Concrete Barriers*, Report No. TRP-03-259-11, Midwest Roadside Safety Facility, University of Nebraska-Lincoln, Lincoln, Nebraska, December 2011.
7. Rosenbaugh, S.K., Sicking, D.L., and Faller, R.K., *Development of a TL-5 Vertical Face Concrete Median Barrier Incorporating Head Ejection Criteria*, Report No. TRP-03-194-07, Midwest Roadside Safety Facility, University of Nebraska-Lincoln, Lincoln, Nebraska, December 2007.
8. Hallquist, J.O., *LS-DYNA: Keyword User's Manual, Version 971*, Livermore Software Technology Corporation, Livermore, CA, 2007.
9. Sheikh, N.M., Bligh, R.P., and Menges, W.L., *Determination of Minimum Height and Lateral Design Load for MASH Test Level 4 Bridge Rails*, Test Report 9-1002-5, Texas A&M Transportation Institute, Texas A&M University, College Station, Texas, December 2011.
10. Olson, R.M., Post, E.R., and McFarland, W.F., *Tentative Service Requirements for Bridge Rail Systems*, NCHRP Report 86, Texas A&M Transportation Institute, Texas A&M University, College Station, Texas, 1970.
11. Hirsch, T.J., *Analytical Evaluation of Texas Bridge Rails to Contain Buses and Trucks*, Research Report 230-2, Texas A&M Transportation Institute, Texas A&M University, College Station, Texas, August 1978.

12. Ritter, M.A., Faller, R.K., and Sicking, D.L., *Development of Low-Volume Curb-Type Bridge Railings for Timber Bridge Decks*, Report No. TRP-03-31-93, Midwest Roadside Safety Facility, University of Nebraska-Lincoln, Lincoln, Nebraska, December 1993.
13. Noel, J.S., Hirsch, T.J., Buth, C.E., and Arnold, A., *Loads on Bridge Railings*, Transportation Research Record, Volume 796, Texas A&M Transportation Institute, Texas A&M University, College Station, Texas, 1981.
14. Beason, W.L., Hirsch, T.J., and Campise, W.L., *Measurement of Heavy Vehicle Impact Forces and Inertia Properties*, Texas A&M Transportation Institute, Texas A&M University, College Station, Texas, January 1989.
15. AASHTO, *AASHTO LRFD Bridge Design Specifications*, 8th Edition, Washington, D.C., 2017.
16. Eller, C.M. and Reid, J.D., *Determination of Impact Forces from Vehicle-to-Barrier Crashes*, University Honors Program Thesis, Midwest Roadside Safety Facility, University of Nebraska-Lincoln, April 23, 2007.
17. Schmidt, J.D., Schmidt, T.L., Rosenbaugh, S.K., Faller, R.K., Bielenberg, R.W., Reid, J.D., Holloway, J.C., and Lechtenberg, K.A., *MASH TL-4 Crash Testing and Evaluation of the RESTORE Barrier*, Report No. TRP 03-318-15, Midwest Roadside Safety Facility, University of Nebraska Lincoln, Lincoln, Nebraska, November 3, 2015.
18. Pena, O., Faller, R.K., Rasmussen, J.D., Steelman, J.S., Rosenbaugh, S.K., Bielenberg, R.W., Mauricio, P., and Duren, J.T., *Development of a MASH Test Level 4 Steel, Side-Mounted, Beam-and-Post, Bridge Rail*, Report No. TRP 03-410-20, Midwest Roadside Safety Facility, University of Nebraska Lincoln, Lincoln, Nebraska, July 20, 2020.
19. Bligh, R.P., Briaud, J., Abu-Odeh, A., Saez, D.O., Maddah, L.S., and Kim, K.M., *Design Guidelines for Test Level 3 through Test Level 5 Roadside Barrier Systems Placed on MSE Retaining Wall*, NCHRP Project 22-20(2), Texas A&M Transportation Institute, Texas A&M University, College Station, Texas, June 2017.
20. Albuquerque, F.D. and Sicking, D.L., *Evaluation of the In-Service Performance of Safety-Shape and Vertical Concrete Barriers*, Report No. TRP-03-259-11, Midwest Roadside Safety Facility, University of Nebraska-Lincoln, Lincoln, NE, December 16, 2011.
21. Rosenbaugh, S.K., Sicking, D.L., and Faller R.K., *Development of a TL-5 Vertical Face Concrete Median Barrier Incorporating Head Ejection Criteria*, Report No. TRP-03-194-07, Midwest Roadside Safety Facility, University of Nebraska-Lincoln, Lincoln, Nebraska, December 2007.
22. Polivka, K.A., Faller, R.K., Sicking, D.L., Rohde, J.R., Bielenberg, R.W., Reid, J.D., and Coon, B.A., *Performance Evaluation of the Permanent New Jersey Safety Shape Barrier - Update to NCHRP 350 Test No. 3-10 (2214NJ-1)*, Report No. TRP-03-177-06, Midwest Roadside Safety Facility, University of Nebraska-Lincoln, Lincoln, Nebraska, October 13, 2006.

23. Whitesel, D., Jewell, J., and Meline, R., *Compliance Crash Testing of the Type 60 Median Barrier, Test 140MASH3C16-04*, FHWA Report CA17-2654, Caltrans: California Department of Transportation, Sacramento, California, May 2018.
24. Bielenberg, R.W., Yoo, S., Faller, R.K., and Urbank, E.L., *Crash Testing and Evaluation of the HDOT 34-in. Tall Aesthetic Concrete Bridge Rail: MASH Test Designation Nos. 3-10 nad 3-11*, Report No. TRP-03-420-19, Midwest Roadside Safety Facility, University of Nebraska-Lincoln, Lincoln, Nebraska, October 21, 2019.
25. Silvestri-Dobrovolny, C., Schulz, N., Moran, S., Skinner, T., Bligh, R., and Williams, W., *MASH Equivalency of NCHRP Report 350-Approved Bridge Railings*, NCHRP Project 20-07(395), Texas A&M Transportation Institute, Texas A&M University, College Station, Texas, November 2017.
26. Loken, A.E., Steelman, J.S., Rosenbaugh, S.K., and Faller, R.F., *Establishing Safe Operating Speeds for Autonomous Vehicles on the Automated Skyway Express in Jacksonville, Florida*, Report No. TRP-03-422-20, Midwest Roadside Safety Facility, University of Nebraska-Lincoln, Lincoln, Nebraska, November 18, 2020.
27. Frosch, R.J. and Morel, A.J., *Bridge Deck Overhang Design, Volume 2: Guardrails for Use on Historic Bridges*, FHWA Report IN/JTRP-2016/34, Purdue University, West Lafayette, Indiana, November 2016.
28. Alberson, D.C., Williams, W.F., and Menges, W.L., *Testing and Evaluation of the Florida F-Shape Bridge Rail with Reduced Deck Thickness*, Report No. 9-8132-3, Texas A&M Transportation Institute, Texas A&M University, College Station, Texas, March 2005.
29. Williams, W.F., Buth, C.E., and Menges, W.L., *Repair/Retrofit Anchorage Designs for Bridge Rails*, Report No. 0-4823-T1-1, Texas A&M Transportation Institute, Texas A&M University, College Station, Texas, March 2007.
30. American Concrete Institute, *ACI 318-14 Building Code Requirements for Structural Concrete (ACI 318-14) and Commentary (ACI 318R-14)*, American Concrete Institute, 2014.
31. Grubb, M.A., Wilson, K.E., White, C.D., and Nickas, W.N., *NHI Course No. 130081, 130081A, and 130081B: Load and Resistance Factor Design (LRFD) for Highway Bridge Superstructures – Reference Manual*. Report No. FHWA-NHI-15-047, FHWA, Washington DC, July 2015.
32. Wilson, K.E., Bouscher, J.W., Amrhein, W.A., and Modjeski and Masters, Inc., *NHI Course No. 130081: Load and Resistance Factor Design (LRFD) for Highway Bridge Superstructures – Design Examples*. Report No. FHWA-NHI-15-058, FHWA, Washington DC, August 2015.
33. Alberson, D.C., Williams, W.F., and Menges, W.L., *Testing and Evaluation of the Florida F-Shape Bridge Rail with Reduced Deck Thickness*, Report No. 9-8132-3, Texas A&M Transportation Institute, Texas A&M University, College Station, Texas, March 2005.

34. Rosenbaugh, S.K., Schmidt, J.D., Regier, E.M., and Faller, R.K., *Development of the Manitoba Constrained-Width, Tall Wall Barrier*, Report No. TRP-03-356-16, Midwest Roadside Safety Facility, University of Nebraska-Lincoln, Lincoln, Nebraska, September 26, 2016.
35. Washington State Department of Transportation, *WSDOT Bridge Design Manual LRFD*, Olympia, Washington, July 2019.
36. Precast/Prestressed Concrete Institute, *Bridge Design Manual, 3rd Edition, Second Release*, Precast/Prestressed Concrete Institute, Chicago, Illinois, 2014.
37. Williams, W.F., Bligh, R.P., and Menges, W.L., *MASH Test 3-11 of the TxDOT Single Slope Bridge Rail (Type SSTR) on Pan-Formed Bridge Deck*, Report No. 9-1002-3, Texas A&M Transportation Institute, Texas A&M University, College Station, Texas, March 2011.
38. Schmidt, J.D., Faller, R.K., Lechtenberg, K.A., Sicking, D.L., and Reid, J.D., *Development and Testing of a New Vertical-Faced Temporary Concrete Barrier for Use on Composite Panel Bridge Decks*, Report No. TRP-03-220-09, Midwest Roadside Safety Facility, University of Nebraska-Lincoln, Lincoln, Nebraska, October 13, 2009.
39. Williams, W.F., Bligh, R.P., and Menges, W.L., *MASH Test 3-11 of the TxDOT T222 Bridge Rail*, Report No. 9-1002-12-13, Texas A&M Transportation Institute, Texas A&M University, College Station, Texas, August 2014.
40. Hinch, J., Yang, T.L., and Owings, R., *Guidance Systems for Vehicle Testing*, ENSCO, Inc., Springfield, Virginia, 1986.
41. Society of Automotive Engineers (SAE), *Instrumentation for Impact Test – Part 1 – Electronic Instrumentation*, SAE J211/1 MAR95, New York City, NY, July 2007.
42. *Vehicle Damage Scale for Traffic Investigators*, Second Edition, Technical Bulletin No. 1, Traffic Accident Data (TAD) Project, National Safety Council, Chicago, Illinois, 1971.
43. *Collision Deformation Classification – Recommended Practice J224 March 1980*, Handbook Volume 4, Society of Automotive Engineers (SAE), Warrendale, Pennsylvania, 1985.
44. Bielenberg, R.W., Asselin, N., and Faller, R.K., *MASH TL-3 Evaluation of Concrete and Asphalt Tied-Down Anchorage for Portable Concrete Barrier*, Report No. TRP-03-386-19, Midwest Roadside Safety Facility, Lincoln, April 2019.
45. Bullard, D.L., Sheikh, N.M., Bligh, R.P., Haug, R.R., Schutt, J.R., Storey, B.J., *Aesthetic Concrete Barrier Design*, NCHRP Report 554, Texas A&M Transportation Institute, Texas A&M University, College Station, Texas, 2006.
46. *Expansion Gap Joint Width*, MwRSF Consulting Site, Question ID No. 1118, <https://mwrsf.unl.edu/q&a/view.php?id=1118>, November 2, 2016.

12 APPENDICES

Appendix A. Material Specifications

Table A-1. Bill of Materials, Test No. 4CBR-1

Item No.	Description	Material Specification	Reference
a1	Bridge Deck Concrete	Min. $f'_c = 5,000$ psi NE Mix L5500	Ticket#1225627 Report#2147370256
a2	Bridge Rail Concrete	Min. $f'_c = 5,000$ psi NE Mix L5500	Ticket#4206579, Ticket#420777
a3	Grade Beam Concrete	Min. $f'_c = 4,000$ psi NE Mix 47BD	Ticket#1222757 Report#2147370255
a4	Overlay	Concrete NE Mix 9019 CITY	Ticket#1228878
b1	#4 Rebar, 70¼" Total Unbent Length	ASTM A615 Gr. 60	H#KN1810005601
b2	#4 Rebar, 46½" Total Unbent Length	ASTM A615 Gr. 60	H#KN1810005601
b3	#4 Rebar, 103½" Total Length	ASTM A615 Gr. 60	H#KN1810005601
b4	#5 Rebar, 115⅜" Total Unbent Length	ASTM A615 Gr. 60	H#1810025501
b5	#4 Rebar, 895" Total Length	ASTM A615 Gr. 60	H#62139028
b6	#5 Bent Rebar, 56¼" Total Unbent Length	ASTM A615 Gr. 60	H#1810025501
b7	#4 Bent Rebar, 83⅙" Total Unbent Length	ASTM A615 Gr. 60	H#KN1810005601
b8	#5 Bent Rebar, 87⅙" Total Unbent Length	ASTM A615 Gr. 60	H#KN17101723
b9	#5 Rebar, 1,795" Total Length	ASTM A615 Gr. 60	H#1810025501
b10	#5 Rebar, 35½" Total Length	ASTM A615 Gr. 60	H#KN17101723
b11	#4 Rebar, 25½" Total Length	ASTM A615 Gr. 60	H#KN1810005601
b12	#5 Rebar, 37½" Total Unbent Length	ASTM A615 Gr. 60	H#1810025501
b13	#4 Rebar, 112" Total Unbent Length	ASTM A615 Gr. 60	H#57169166
-	Epoxy	Min. bond strength = 1,450 psi	N/A
-	Releasing Agent/Medium	¼ " Thick Polyethylene Plastic, ASTM D4397	N/A



Ready Mixed Concrete Company
6200 Cornhusker Hwy, Lincoln, NE 68529
Phone: (402) 434-1844 Fax: (402) 434-1877

Customer's Signature: _____

PLANT	TRUCK	DRIVER	CUSTOMER	PROJECT	TAX	PO NUMBER	DATE	TIME	TICKET	
01	223	7596	3	3		??	5/30/18	7:16 AM	1225627	
Customer CIA--MWRSF			Delivery Address 4630 NW 36TH ST			Special Instructions AIRPARK / NORTH OF GOODYEAR HANGERS				
LOAD QUANTITY	CUMULATIVE QUANTITY	ORDERED QUANTITY	PRODUCT CODE	PRODUCT DESCRIPTION		UOM	UNIT PRICE	EXTENDED PRICE		
10.50	10.50	31.50	25513000	L5500 (HE) .40		yd	\$127.91	\$1,343.06		
Water Added On Job At Customer's Request:		SLUMP 3.00 in	Notes:				TICKET SUBTOTAL		\$1,343.06	
						SALES TAX		\$0.00		
						TICKET TOTAL		\$1,343.06		
						PREVIOUS TOTAL				
						GRAND TOTAL		\$1,343.06		



CAUTION FRESH CONCRETE
KEEP CHILDREN AWAY

Contains Portland cement. Freshly mixed cement, mortar, concrete or grout may cause skin injury. Avoid prolonged contact with skin. Always wear appropriate Personal Protective Equipment (PPE). In case of contact with eyes or skin, flush thoroughly with water. If irritation persists, seek medical attention promptly.

Terms & Conditions

This concrete is produced with the ASTM standard specifications for ready mix concrete. Strengths are based on a 3" slump. Drivers are not permitted to add water to the mix to exceed this slump, except under the authorization of the customer and their acceptance of any decrease in compressive strength and any risk of loss as a result thereof. Cylinder tests must be handled according to ACI/ASTM specifications and drawn by a licensed testing lab and/or certified technician. Ready Mixed Concrete Company will not deliver any product beyond any curb lines unless expressly told to do so by customer and customer assumes all liability for any personal or property damage that may occur as a result of any such directive. The purchaser's exceptions and claims shall be deemed waived unless made in writing within 3 days from time of delivery. In such a case, seller shall be given full opportunity to investigate any such claim. Seller's liability shall in no event exceed the purchase price of the materials against which any claims are made.

MATERIAL	DESCRIPTION	DESIGN QTY	REQUIRED	BATCHED	% VAR	% MOISTURE	ACTUAL WATER
CEM1	CEM 1/2	752 lb	7896 lb	7860 lb	-0.46%		
G47B	47B GRAVEL	1915 lb	20437 lb	20400 lb	-0.18%	1.64% A	39 gl
L47B	47B ROCK	833 lb	8866 lb	8840 lb	-0.09%	1.36% E	14 gl
LRWR	POZZ 322N LOV	23.00 oz	241.50 oz	241.00 oz	-0.21%		
AIR	MICRO AIR 200	4.00 oz	42.00 oz	42.00 oz	0.00%		
WATER	WATER	34.0 GL	303.2 GL	300.5 GL	-0.87%		300.5 gl

Actual Num Batches: 1 Manual

Load: 39626 lb Design W/C: 0.38 Water/Cement: 0.38 T Design Water: 357.0 gl Actual: 354.3 gl

Slump: 3.00 in Water in Truck: 0.0 GL Adjust Water: 0.0 GL / Load Trim Water: 0.0 GL / CYDS

Actual W/C Ratio 0.38 Actual Water: 354 gl Batched Cement: 7860 lb Allowable Water: 9 lb To Add: 2.7 gl

Figure A-1. Bridge Deck Concrete Material Specification, Test No. 4CBR-1 (Item No. a1)



LINCOLN OFFICE
 825 "M" Street Suite 100
 Lincoln, NE 68508
 Phone: (402) 479-2200
 Fax: (402) 479-2276

COMPRESSION TEST OF CYLINDRICAL CONCRETE SPECIMENS - 6x12

ASTM Designation: C 39

Client Name: Midwest Roadside Safety Facility
Project Name: Miscellaneous Concrete Testing
Placement Location: 4CBR-1 DECK

Date 13-Jun-18

Mix Designation:

Required Strength:

Laboratory Test Data

Laboratory Identification	Field Identification	Date Cast	Date Received	Date Tested	Days Cured in Field	Days Cured in Laboratory	Age of Test, Days	Length of Specimen, in.	Diameter of Specimen, in.	Cross-Sectional Area, sq.in.	Maximum Load, lbf	Compressive Strength, psi.	Required Strength, psi.	Type of Fracture	ASTM Practice for Capping Specimen
URR- 61	A	5/30/2018	6/13/2018	6/13/2018	14	0	14	12	6.01	28.40	140,928	4,960		6	C 1231
URR- 62	B	5/30/2018	6/13/2018	6/13/2018	14	0	14	12	6.04	28.62	144,378	5,040		6	C 1231
URR- 63	C	5/30/2018	6/13/2018	6/13/2018	14	0	14	12	6.02	28.50	150,186	5,270		5	C 1231

1 cc: Ms. Karla Lechtenberg
 Midwest Roadside Safety Facility

91

Remarks: Truck 1 +5 gal.

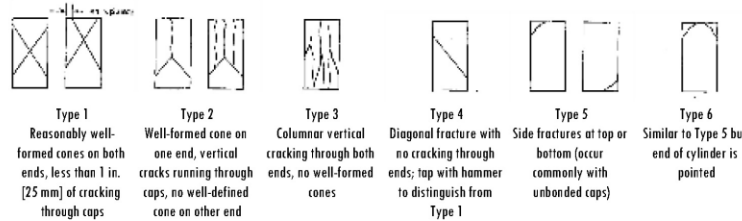
Concrete test specimens along with documentation and test data were submitted by Midwest Roadside Safety Facility.

Test results presented relate only to the concrete specimens as received from Midwest Roadside Safety Facility.

This report shall not be reproduced except in full, without the written approval of Alfred Benesch & Company.

Report Number 2147370256
 Page 1

Sketches of Types of Fractures



**ALFRED BENESCH & COMPANY
 CONSTRUCTION MATERIALS LABORATORY**

By Brant Wells
 Brant Wells, Field/Lab Operations Manager

Figure A-2. Bridge Deck, Concrete Strength Tests, Test No. 4CBR-1 (Item No. a1)

MWRSSF Report No. TRP-03-415-21
 March 26, 2021



Ready Mixed Concrete Company
6200 Cornhusker Hwy, Lincoln, NE 68529
Phone: (402) 434-1844 Fax: (402) 434-1877

Customer's Signature: _____

PLANT	TRUCK	DRIVER	CUSTOMER	PROJECT	TAX	PO NUMBER	DATE	TIME	TICKET
4	225	9516	3	3		BUNKY 5601716	7/2/18	9:53 AM	4206579
Customer CIA--MWRSS			Delivery Address 4630 NW 36TH ST			Special Instructions MIDWEST ROADSIDE SAFETY / NORTHOF GOODYEAR HANGERS			
LOAD QUANTITY	CUMULATIVE QUANTITY	ORDERED QUANTITY	PRODUCT CODE	PRODUCT DESCRIPTION		UOM	UNIT PRICE	EXTENDED PRICE	
7.50	7.50	7.50	25513000	L5500 (HE) .40		yd	\$127.91	\$959.33	
Water Added On Job At Customer's Request:		SLUMP 3.00 in	Notes:		TICKET SUBTOTAL			\$959.33	
					SALES TAX			\$0.00	
					TICKET TOTAL			\$959.33	
					PREVIOUS TOTAL				
					GRAND TOTAL			\$959.33	

CAUTION FRESH CONCRETE
KEEP CHILDREN AWAY

Contains Portland cement. Freshly mixed cement, mortar, concrete or grout may cause skin injury. Avoid prolonged contact with skin. Always wear appropriate Personal Protective Equipment (PPE). In case of contact with eyes or skin, flush thoroughly with water. If irritation persists, seek medical attention promptly.

Terms & Conditions

This concrete is produced with the ASTM standard specifications for ready mix concrete. Strengths are based on a 3" slump. Drivers are not permitted to add water to the mix to exceed this slump, except under the authorization of the customer and their acceptance of any decrease in compressive strength and any risk of loss as a result thereof. Cylinder tests must be handled according to ACI/ASTM specifications and drawn by a licensed testing lab and/or certified technician. Ready Mixed Concrete Company will not deliver any product beyond any curb lines unless expressly told to do so by customer and customer assumes all liability for any personal or property damage that may occur as a result of any such directive. The purchaser's exceptions and claims shall be deemed waived unless made in writing within 3 days from time of delivery. In such a case, seller shall be given full opportunity to investigate any such claim. Seller's liability shall in no event exceed the purchase price of the materials against which any claims are made.

MATERIAL	DESCRIPTION	DESIGN QTY	REQUIRED	BATCHED	% VAR	% MOISTURE	ACTUAL WATER
CEM1	TYPE I/II CEME1	752.0 lb	5640.0 lb	5655.0 lb	0.27%		
G47B	47B GRAVEL	1915.0 lb	14624.9 lb	14580.0 lb	-0.31%	1.83% A	31.4 gl
L47B	47B ROCK	833.0 lb	6424.9 lb	6420.0 lb	-0.02%	2.84% A	21.2 gl
LRWR	POZZ 322N LOV	28.0 oz	210.0 oz	210.0 oz	0.00%		
AIR	MB AE 200 air ei	3.3 oz	24.8 oz	25.0 oz	1.01%		
WATER	WATER	30.5 gl	176.0 gl	175.2 gl	-0.48%		175.2 gl

Actual Num Batches: 1 Manual

Load: 28132 lb Design W/C: 0.34 Water/Cement: 0.34 T Design Water: 228.8 gl Actual: 227.8 gl

Slump: 3.00 in Water in Truck: 0.0 gl Adjust Water: 0.0 gl / Load Trim Water: 0.0 gl / CYDS

Actual W/C Ratio 0.34 Actual Water: 228 gl Batched Cement: 5655 lb Allowable Water: 13 lb To Add: 1.0 gl

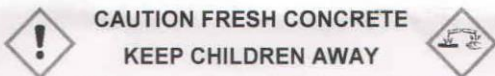
Figure A-3. Bridge Rail Concrete Material Specification, Test No. 4CBR-1 (Item No. a2)



Ready Mixed Concrete Company
6200 Cornhusker Hwy, Lincoln, NE 68529
Phone: (402) 434-1844 Fax: (402) 434-1877

Customer's Signature: _____

PLANT	TRUCK	DRIVER	CUSTOMER	PROJECT	TAX	PO NUMBER	DATE	TIME	TICKET
4	138	8544	3	3		BUNKY 5601716	7/30/18	11:29 AM	4207777
Customer CIA---MWRSS			Delivery Address 4630 NW 36TH ST			Special Instructions MIDWEST ROADSIDE SAFETY / NORTHOF GOODYEAR HANGERS			
LOAD QUANTITY	CUMULATIVE QUANTITY	ORDERED QUANTITY	PRODUCT CODE	PRODUCT DESCRIPTION		UOM	UNIT PRICE	EXTENDED PRICE	
10.00	10.00	10.00	25513000	L5500 (HE) .40		yd	\$127.91	\$1,279.10	
Water Added On Job At Customer's Request:		SLUMP 4.00 in	Notes:		TICKET SUBTOTAL		\$1,279.10		
					SALES TAX		\$0.00		
					TICKET TOTAL		\$1,279.10		
					PREVIOUS TOTAL				
					GRAND TOTAL		\$1,279.10		



Contains Portland cement. Freshly mixed cement, mortar, concrete or grout may cause skin injury. Avoid prolonged contact with skin. Always wear appropriate Personal Protective Equipment (PPE). In case of contact with eyes or skin, flush thoroughly with water. If irritation persists, seek medical attention promptly.

Terms & Conditions

This concrete is produced with the ASTM standard specifications for ready mix concrete. Strengths are based on a 3" slump. Drivers are not permitted to add water to the mix to exceed this slump, except under the authorization of the customer and their acceptance of any decrease in compressive strength and any risk of loss as a result thereof. Cylinder tests must be handled according to ACI/ASTM specifications and drawn by a licensed testing lab and/or certified technician. Ready Mixed Concrete Company will not deliver any product beyond any curb lines unless expressly told to do so by customer and customer assumes all liability for any personal or property damage that may occur as a result of any such directive. The purchaser's exceptions and claims shall be deemed waived unless made in writing within 3 days from time of delivery. In such a case, seller shall be given full opportunity to investigate any such claim. Seller's liability shall in no event exceed the purchase price of the materials against which any claims are made.

MATERIAL	DESCRIPTION	DESIGN QTY	REQUIRED	BATCHED	% VAR	% MOISTURE	ACTUAL WATER
CEM1	TYPE I/II CEMENT	752.0 lb	7520.0 lb	7500.0 lb	-0.27%		
G47B	47B GRAVEL	1915.0 lb	19500.1 lb	19460.0 lb	-0.21%	1.83% A	41.9 gl
L47B	47B ROCK	833.0 lb	8499.1 lb	8460.0 lb	-0.14%	2.03% A	20.2 gl
LRWR	POZZ 322N LOV	28.0 oz	280.0 oz	279.0 oz	-0.36%		
AIR	MB AE 200 air ei	3.3 oz	33.0 oz	33.0 oz	0.00%		
WATER	WATER	30.5 gl	252.8 gl	251.6 gl	-0.45%		251.6 gl

Figure A-4. Bridge Rail Concrete Material Specification, Test No. 4CBR-1 (Item No. a2)



Ready Mixed Concrete Company
6200 Cornhusker Hwy, Lincoln, NE 68529
Phone: (402) 434-1844 Fax: (402) 434-1877

Customer's Signature: _____

PLANT	TRUCK	DRIVER	CUSTOMER	PROJECT	TAX	PO NUMBER	DATE	TIME	TICKET
01	0134	7142	3	3		4CBR-1	3/30/18	10:30 AM	1222757
Customer CIA---MIDWEST ROADSIDE SAFETY			Delivery Address 4630 NW 36TH STREET			Special Instructions NORTH OF THE GOODYEAR HANGER			
LOAD QUANTITY	CUMULATIVE QUANTITY	ORDERED QUANTITY	PRODUCT CODE	PRODUCT DESCRIPTION		UOM	UNIT PRICE	EXTENDED PRICE	
6.00	12.00	12.00	470031PF	47BD (1PF) WO/R		yd	\$118.91	\$713.46	
				MINIMUM HAUL				\$10.00	
Water Added On Job At Customer's Request: <u>5</u>		SLUMP 3.00 in	Notes:		TICKET SUBTOTAL		\$723.46		
					SALES TAX		\$0.00		
					TICKET TOTAL		\$723.46		
					PREVIOUS TOTAL		\$723.46		
					GRAND TOTAL		\$1,446.92		



CAUTION FRESH CONCRETE
KEEP CHILDREN AWAY

Contains Portland cement. Freshly mixed cement, mortar, concrete or grout may cause skin injury. Avoid prolonged contact with skin. Always wear appropriate Personal Protective Equipment (PPE). In case of contact with eyes or skin, flush thoroughly with water. If irritation persists, seek medical attention promptly.

Terms & Conditions

This concrete is produced with the ASTM standard specifications for ready mix concrete. Strengths are based on a 3" slump. Drivers are not permitted to add water to the mix to exceed this slump, except under the authorization of the customer and their acceptance of any decrease in compressive strength and any risk of loss as a result thereof. Cylinder tests must be handled according to ACI/ASTM specifications and drawn by a licensed testing lab and/or certified technician. Ready Mixed Concrete Company will not deliver any product beyond any curb lines unless expressly told to do so by customer and customer assumes all liability for any personal or property damage that may occur as a result of any such directive. The purchaser's exceptions and claims shall be deemed waived unless made in writing within 3 days from time of delivery. In such a case, seller shall be given full opportunity to investigate any such claim. Seller's liability shall in no event exceed the purchase price of the materials against which any claims are made.

MATERIAL	DESCRIPTION	DESIGN QTY	REQUIRED	BATCHED	% VAR	% MOISTURE	ACTUAL WATER
G47B	47B GRAVEL	1975 lb	12063 lb	12080 lb	0.14%	1.80% M	26 gl
L47B	47B ROCK	840 lb	5085 lb	5040 lb	-0.26%	0.90% M	5 gl
CEM1PF	EAGLE PAVE	658 lb	3948 lb	3930 lb	-0.46%		
WATER	WATER	31.5 GL	158.0 GL	157.2 GL	-0.50%		157.2 gl
LRWR	POZZ 322N LOV	20.00 oz	120.00 oz	120.00 oz	0.00%		
AIR	MICRO AIR 200	6.80 oz	40.80 oz	41.00 oz	0.49%		

Actual	Num Batches: 1	Manual
Load: 22372 lb	Design W/C: 0.40	Water/Cement: 0.40 T Design Water: 189.0 gl
Slump: 3.00 in	Water in Truck: 0.0 GL	Adjust Water: 0.0 GL / Load Trim Water: 0.0 GL / CYDS
Actual W/C Ratio 0.40	Actual Water: 188 gl	Batched Cement: 3930 lb Allowable Water: 0 lb To Add: 0.8 gl

Figure A-5. Grade Beam Concrete Material Specification, Test No. 4CBR-1 (Item No. a3)



LINCOLN OFFICE
 825 "M" Street Suite 100
 Lincoln, NE 68508
 Phone: (402) 479-2200
 Fax: (402) 479-2276

COMPRESSION TEST OF CYLINDRICAL CONCRETE SPECIMENS - 6x12

ASTM Designation: C 39

Client Name: Midwest Roadside Safety Facility
Project Name: Miscellaneous Concrete Testing
Placement Location: 4CBR-1 Grade Beam

Date 15-Jun-18

Mix Designation:

Required Strength:

Laboratory Test Data

Laboratory Identification	Field Identification	Date Cast	Date Received	Date Tested	Days Cured in Field	Days Cured in Laboratory	Age of Test, Days	Length of Specimen, in.	Diameter of Specimen, in.	Cross-Sectional Area, sq.in.	Maximum Load, lbf	Compressive Strength, psi.	Required Strength, psi.	Type of Fracture	ASTM Practice for Capping Specimen
URR- 58	A	3/30/2018	6/13/2018	6/14/2018	75	1	76	12	5.97	28.01	166,675	5,950		5	C 1231
URR- 59	B	3/30/2018	6/13/2018	6/14/2018	75	1	76	12	5.96	27.90	174,078	6,240		5	C 1231
URR- 60	C	3/30/2018	6/13/2018	6/14/2018	75	1	76	12	5.94	27.67	174,604	6,310		3	C 1231

1 cc: Ms. Karla Lechtenberg
 Midwest Roadside Safety Facility

95

Remarks:

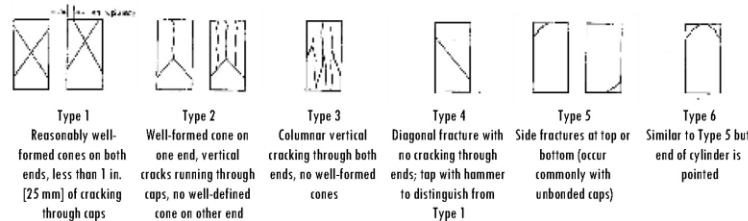
Concrete test specimens along with documentation and test data were submitted by Midwest Roadside Safety Facility.

Test results presented relate only to the concrete specimens as received from Midwest Roadside Safety

This report shall not be reproduced except in full, without the written approval of Alfred Benesch & Company.

Report Number 2147370255
 Page 1

Sketches of Types of Fractures



**ALFRED BENESCH & COMPANY
 CONSTRUCTION MATERIALS LABORATORY**

By Brant Wells
 Brant Wells, Field/Lab Operations Manager

Figure A-6. Grade Beam, Concrete Strength Tests, Test No. 4CBR-1 (Item No. a3)

MWRSSF Report No. TRP-03-415-21
 March 26, 2021

RM
Ready Mixed Concrete Company
 6200 Cornhusker Hwy, Lincoln, NE 68529
 Phone: (402) 434-1844 Fax: (402) 434-1877

Customer's Signature: _____

PLANT	TRUCK	DRIVER	CUSTOMER	PROJECT	TAX	PO NUMBER	DATE	TIME	TICKET
01	121	10364	3	3			8/13/18	10:14 AM	1228878
Customer CIA---MIDWEST ROADSIDE SAFETY			Delivery Address 4630 NW 36TH STREET			Special Instructions NORTH OF THE NORTH GOODYEAR HANGER			
LOAD QUANTITY	CUMULATIVE QUANTITY	ORDERED QUANTITY	PRODUCT CODE	PRODUCT DESCRIPTION		UOM	UNIT PRICE	EXTENDED PRICE	
5.00	5.00	10.00	9019CITY	CITY OF LINC 8"		yd	\$90.00	\$450.00	
Water Added On Job At Customer's Request:		SLUMP 3.00 in	Notes:		TICKET SUBTOTAL		\$450.00		
					SALES TAX		\$0.00		
					TICKET TOTAL		\$450.00		
					PREVIOUS TOTAL				
					GRAND TOTAL		\$450.00		



Terms & Conditions

CAUTION FRESH CONCRETE
KEEP CHILDREN AWAY

Contains Portland cement. Freshly mixed cement, mortar, concrete or grout may cause skin injury. Avoid prolonged contact with skin. Always wear appropriate Personal Protective Equipment (PPE). In case of contact with eyes or skin, flush thoroughly with water. If irritation persists, seek medical attention promptly.

This concrete is produced with the ASTM standard specifications for ready mix concrete. Strengths are based on a 3" slump. Drivers are not permitted to add water to the mix to exceed this slump, except under the authorization of the customer and their acceptance of any decrease in compressive strength and any risk of loss as a result thereof. Cylinder tests must be handled according to ACI/ASTM specifications and drawn by a licensed testing lab and/or certified technician. Ready Mixed Concrete Company will not deliver any product beyond any curb lines unless expressly told to do so by customer and customer assumes all liability for any personal or property damage that may occur as a result of any such directive. The purchaser's exceptions and claims shall be deemed waived unless made in writing within 3 days from time of delivery. In such a case, seller shall be given full opportunity to investigate any such claim. Seller's liability shall in no event exceed the purchase price of the materials against which any claims are made.

MATERIAL	DESCRIPTION	DESIGN QTY	REQUIRED	BATCHED	% VAR	% MOISTURE	ACTUAL WATER
CEM1	CEM 1/2	60 lb	300 lb	325 lb	8.33%		
FLYA	FLY ASH	200 lb	1000 lb	1010 lb	0.75%		
C33	C33 SAND	2887 lb	14695 lb	14640 lb	-0.37%	1.80% M	31 gl
AIR	MICRO AIR 200	15.00 oz	75.00 oz	75.00 oz	0.00%		
WATER	WATER	37.0 GL	153.9 GL	153.4 GL	-0.31%		153.4 gl

Actual	Num Batches: 1				Manual
Load: 17260 lb	Design W/C: 1.19	Water/Cement: 1.16	T	Design Water: 195.0 gl	Actual: 184.4 gl
Slump: 3.00 in	Water in Truck: 0.0 GL	Adjust Water: 0.0 GL / Load	Trim Water: 0.0 GL / CYDS		
Actual W/C Ratio 1.15	Actual Water: 184 gl	Batched Cement: 1335 lb	Allowable Water: 46 lb	To Add: 0.6 gl	

Figure A-7. Overlay Material Specification, Test No. 4CBR-1 (Item No. a4)

SOLD ADELPHIA METALS I LLC
411 MAIN ST E
TO: NEW PRAGUE, MN 56071-



CERTIFIED MILL TEST REPORT

Page: 1

SHIP ADELPHIA METALS LLC
ABC COATING
TO: 1160 BOUDREAU RD
MANTENO, IL 60950-

Ship from:
MTR #: 0000211730
Nucor Steel Kankakee, Inc.
One Nucor Way
Bourbonnais, IL 60914
815-937-3131

Date: 16-Jan-2018
B.L. Number: 561520
Load Number: 283881

Material Safety Data Sheets are available at www.nucorbar.com or by contacting your inside sales representative.

NBMG 08 January 1, 2012

LOT # HEAT #	DESCRIPTION	PHYSICAL TESTS					CHEMICAL TESTS												
		YIELD P.S.I.	TENSILE P.S.I.	ELONG % IN 8"	BEND	WT% DEF	C	Ni	Mn	Cr	P	Mo	S	V	Si	Cb	Cu	Sn	C.E.
PO# => KN1810005901	822711 Nucor Steel - Kankakee Inc 13#4 Rebar 40' A615M GR420 (Gr60) ASTM A615/A615M-16 GR 60 AASHT O M31-15 Melted 01/04/18 Rolled 01/07/18	70,065	106,862	13.8%	OK	-3.9%	.38	.99	.013	.055	.19	.33							
KN18100058		483MPa	737MPa			.035	.23	.17	.088	.008	.001								
PO# => KN1810005901	822711 Nucor Steel - Kankakee Inc 13#4 Rebar 40' A615M GR420 (Gr60) ASTM A615/A615M-16 GR 60 AASHT O M31-15 Melted 01/04/18 Rolled 01/07/18	70,101	106,526	12.9%	OK	-3.3%	.37	.96	.016	.050	.19	.33							
KN18100058		483MPa	734MPa			.036	.25	.20	.073	.008	.001								
PO# => KN18100059	822711 Nucor Steel - Kankakee Inc 13#4 Rebar 40' A615M GR420 (Gr60) ASTM A615/A615M-16 GR 60 AASHT O M31-15 Melted 01/04/18 Rolled 01/07/18	68,720	105,364	15.1%	OK	-3.9%	.38	.95	.018	.051	.20	.31							
KN18100059		474MPa	726MPa			.035	.23	.20	.071	.008	.001								

I hereby certify that the material described herein has been manufactured in accordance with the specifications and standards listed above and that it satisfies those requirements.
1) Yield repair was not performed on this material.
2) Melted and Manufactured in the United States.
3) Mercury, Pladium, or Alpha Source materials in any form have not been used in the production of this material.

QUALITY ASSURANCE: Caitlin Widdicombe

Caitlin Widdicombe

Figure A-8. #4 Rebar Material Specification, Test No. 4CBR-1 (Item Nos. b1, b2, b3, b7, and b11)

SOLD ADELPHIA METALS I LLC
411 MAIN ST E
TO: NEW PRAGUE, MN 56071-



CERTIFIED MILL TEST REPORT

Page: 1

SHIP ADELPHIA METALS LLC
ABC COATING
TO: 1160 BOUDREAU RD
MANTENO, IL 60950-

Ship from:
MTR #: 0000212259
Nucor Steel Kankakee, Inc.
One Nucor Way
Bourbonnais, IL 60914
815-937-3131

Date: 17-Jan-2018
B.L. Number: 561716
Load Number: 293988

Material Safety Data Sheets are available at www.nucorbar.com or by contacting your inside sales representative.

NBMG 08 January 1, 2012

LOT # HEAT #	DESCRIPTION	PHYSICAL TESTS					CHEMICAL TESTS												
		YIELD P.S.I.	TENSILE P.S.I.	ELONG % IN 8"	BEND	WT% DEF	C	Ni	Mn	Cr	P	Mo	S	V	Si	Cb	Cu	Sn	C.E.
PO# => KN1810025501	822711 Nucor Steel - Kankakee Inc 16#5 Rebar 40' A615M GR420 (Gr60) ASTM A615/A615M-16 GR 60 AASHT O M31-15 Melted 01/12/18 Rolled 01/16/18	67,589	103,912	15.6%	OK	-3.2%	.37	.98	.014	.051	.17	.31							
KN18100255		466MPa	716MPa			.039	.18	.18	.065	.008	.001								
PO# => KN1810025602	822711 Nucor Steel - Kankakee Inc 16#5 Rebar 40' A615M GR420 (Gr60) ASTM A615/A615M-16 GR 60 AASHT O M31-15 Melted 01/12/18 Rolled 01/16/18	67,177	104,692	15.6%	OK	-3.5%	.38	1.01	.016	.058	.19	.34							
KN18100256		463MPa	722MPa			.039	.19	.17	.060	.009	.001								

I hereby certify that the material described herein has been manufactured in accordance with the specifications and standards listed above and that it satisfies those requirements.
1) Yield repair was not performed on this material.
2) Melted and Manufactured in the United States.
3) Mercury, Pladium, or Alpha Source materials in any form have not been used in the production of this material.

QUALITY ASSURANCE: Caitlin Widdicombe

Caitlin Widdicombe

Figure A-9. #5 Rebar Material Specification, Test No. 4CBR-1 (Item Nos. b4, b6, b9, and b12)

GERDAU
US-ML-ST PAUL
1678 RED ROCK ROAD
SAINT PAUL, MN 55119
USA

CUSTOMER SHIP TO SIMCOTE INC 1645 RED ROCK RD SAINT PAUL, MN 55119 USA	CUSTOMER BILL TO SIMCOTE INC 1645 RED ROCK ROAD SAINT PAUL, MN 55119-6014 USA	GRADE 60 (420)	SHAPE / SIZE Rebar / #4 (13MM)
SALES ORDER 2492020/000040	CUSTOMER MATERIAL N°	LENGTH 60'00"	WEIGHT 12,786 LB
SPECIFICATION / DATE of REVISION ASTM A615/A615M-14		HEAT / BATCH 62139028/03	
CUSTOMER PURCHASE ORDER NUMBER 3621	BILL OF LADING 1332-0906031875	DATE 08/14/2015	

CHEMICAL COMPOSITION	C	Mn	P	S	Si	Cr	Ni	Cu	Mo	Sn	V	Nb
	0.41	1.16	0.009	0.020	0.20	0.27	0.11	0.12	0.018	0.012	0.004	0.002

MECHANICAL PROPERTIES	YS PSI	YS MPa	UTS PSI	UTS MPa	Elong %	Bend
	67000	462	102500	707	15.00	OK

MECHANICAL PROPERTIES
Bend Test
OK

GEOMETRIC CHARACTERISTICS

Yield	Def 1/8"	Def Gap	Def/Rate
0.00	0.004	0.150	0.331

COMMENTS / NOTES
Material 100% melted and rolled in the USA. Manufacturing process for this steel, which may include strip melted in an electric arc furnace and hot rolling, has been performed at Gerdau St. Paul Mill, 1678 Red Rock Rd., St. Paul, Minnesota, USA. All products produced from strand cast 50kcs. Silicon killed (deoxidized) steel. No weld repair performed. Steel not exposed to mercury or any liquid alloy which is liquid at ambient temperatures during processing or while in Gerdau St. Paul Mill's possession. Any modification to this certification as provided by Gerdau St. Paul Mill without the expressed written consent of Gerdau St. Paul Mill negates the validity of this test report. This report shall not be reproduced except in full, without the expressed written consent of Gerdau St. Paul Mill. Gerdau St. Paul Mill is not responsible for the suitability of this material to meet specific applications.
level track 62139028/03 roll id #4/2015

The above figures are certified chemical and physical test records as contained in the permanent records of company. We certify that these data are correct and in compliance with specified requirements. This material, including the billets, was melted and manufactured in the USA. CMTR complies with EN 10204 3.1.

Mhaskar BHASKAR YALAMANCHIL
QUALITY DIRECTOR

M ALEX BALDRENBURG
QUALITY ASSURANCE MGR

Figure A-10. #4 Rebar Material Specification, Test No. 4CBR-1 (Item No. b5)

SOLD SIMCOTE INC
1645 RED ROCK RD
ST PAUL, MN 55119

NUCOR
NUCOR STEEL KANKAKEE, INC.

CERTIFIED MILL TEST REPORT

Page: 1

Ship from:
MTR #: 0000172529
Nucor Steel Kankakee, Inc.
One Nucor Way
Bourbonnais, IL 60914
815-937-3131

Date: 23-May-2017
B.L. Number: 538613
Load Number: 285402

Material Safety Data Sheets are available at www.nucor.com or by contacting your inside sales representative.

LOT # HEAT #	DESCRIPTION	PHYSICAL TESTS				CHEMICAL TESTS										
		YIELD P.S.I.	TENSILE P.S.I.	ELONG % IN 8"	BEND	C	Mn	P	S	Si	Cr	Mo	V	Nb	Sn	C.E.
PO# => KN1710172001	MN-3669 Nucor Steel - Kankakee Inc 16#S Rebar	66,130	104,206	15.1%	OK	-4.1%	.38	.92	.019	.048	.17	.45				
KN17101720	40' A615M GR420 (Gr60) ASTM A615/A615M-16 GR 60 AASHT O M31-15 Melted 03/24/17 Rolled 04/14/17	456MPa	718MPa			.037	.19	.17	.056	.008	.001					
PO# => KN1710172101	MN-3669 Nucor Steel - Kankakee Inc 16#S Rebar	66,090	104,589	15.0%	OK	-4.4%	.38	.99	.018	.046	.19	.36				
KN17101721	40' A615M GR420 (Gr60) ASTM A615/A615M-16 GR 60 AASHT O M31-15 Melted 03/24/17 Rolled 04/14/17	456MPa	721MPa			.037	.17	.17	.050	.009	.00					
PO# => KN1710172301	MN-3669 Nucor Steel - Kankakee Inc 16#S Rebar	65,424	105,869	14.5%	OK	-4.1%	.38	.97	.020	.051	.17	.32				
KN17101723	40' A615M GR420 (Gr60) ASTM A615/A615M-16 GR 60 AASHT O M31-15 Melted 03/24/17 Rolled 04/14/17	472MPa	730MPa			.036	.16	.16	.047	.008	.00					

I hereby certify that the material described herein has been manufactured in accordance with the specifications and standards listed above and that it satisfies those requirements.

1) Weld repair was not performed on this material.
2) Melted and manufactured in the United States.
3) Mercury, Radium, or Alpha source materials in any form have not been used in the production of this material.

QUALITY ASSURANCE: Caitlin Widdicombe
Caitlin Widdicombe

Figure A-11. #5 Rebar Material Specification, Test No. 4CBR-1 (Item Nos. b8 and b10)

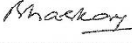
CERTIFIED MATERIAL TEST REPORT												Page 1/1	
 US-ML-KNOXVILLE 1919 TENNESSEE AVENUE N. W. KNOXVILLE, TN 37921 USA			CUSTOMER SHIP TO SIMCOTE INC 1645 RED ROCK SAINT PAUL, MN 55119 USA			CUSTOMER BILL TO SIMCOTE INC 1645 RED ROCK ROAD SAINT PAUL, MN 55119-6014 USA			GRADE 60 (420) TMX		SHAPE / SIZE Rebar / #4 (13MM)		DOCUMENT ID: 0000000000
			SALES ORDER 3749568/000990			CUSTOMER MATERIAL N°			LENGTH 60'00"		WEIGHT 94,262 LB		HEAT / BATCH 57149156/02
CUSTOMER PURCHASE ORDER NUMBER MN-3676				BILL OF LADING 1326-000074465		DATE 11/10/2017		SPECIFICATION / DATE of REVISION ASTM A615/A615M-15 E1					
CHEMICAL COMPOSITION													
C	Mn	P	S	Si	Cr	Ni	Cu	Mo	Sn	V	CE _{eq} A706		
0.26	0.57	0.006	0.040	0.21	0.32	0.10	0.13	0.009	0.011	0.002	0.38		
MECHANICAL PROPERTIES													
YS ksi			YS MPa			UTS ksi			UTS MPa			G/L Inch	
83730			577			98550			680			8.000	
MECHANICAL PROPERTIES													
Elong.			Bend Test										
10.60			OK										
GEOMETRIC CHARACTERISTICS													
%Light	Def Hat	Def Gap	Def Space										
4.49	Inch 0.032	Inch 0.115	Inch 0.320										
COMMENTS / NOTES													
<p>The above figures are certified chemical and physical test records as contained in the permanent records of company. We certify that these data are correct and in compliance with specified requirements. This material, including the billets, was melted and manufactured in the USA. CMTR complies with EN 10204 3.1.</p> <div style="display: flex; justify-content: space-between;"> <div style="text-align: center;">  BHASKAR YALAMANCHILI QUALITY DIRECTOR Phone: (409) 769-1014 Email: bhaskar.yalamanchili@gerdau.com </div> <div style="text-align: center;">  JIM HALL QUALITY ASSURANCE MGR. Phone: 855-202-5972 Email: jim.hall@gerdau.com </div> </div>													

Figure A-12. #4 Rebar Material Certification, Test No. 4CBR-1 (Item No. b13)

Appendix B. Vehicle Center of Gravity Determination

Date: <u>8/21/2018</u>	Test Name: <u>4CBR-1</u>	VIN: <u>1HTMMAAN66H284494</u>	
Year: <u>2005</u>	Make: <u>International</u>	Model: <u>4300</u>	

Vehicle CG Determination

VEHICLE	Equipment	Weight (lb)	Vertical CG (in.)	Vertical M (lb-in.)
+	Unballasted Truck (Curb)	14742	43.068	634909.15
+	Hub	44	19.5	858.0
+	Brake activation cylinder & frame	8	51.0	408.0
+	Pneumatic tank (Nitrogen)	22	45.5	1001.0
+	Strobe/Brake Battery	5	49.0	245.0
+	Tow Pin Plate	9	13.5	121.5
+	Brake Receiver/Wires	6	95.75	574.5
+	Cab DAS Unit & Plate	15	44.625	669.375
+	CG DAS Units & Enclosure	19	38.0	722.0
-	Battery	-161	29.5	-4749.5
-	Oil	-47	22.25	-1045.75
-	Interior	-73	76.0	-5548.0
-	Fuel	-368	27.25	-10028.0
-	Coolant	-62	49.75	-3084.5
-	Washer fluid	-6	38.5	-231.0
+	Onboard supplemental	17	50.0	850.0
+	Plate hardware	0	0	0
BALLAST				
+	Barrier	4648	67.25	312578.0
+	Ballast Hardware	213	45.25	9638.25
+	1/2" metal plate A/Left/Driver	202.5	65.75	13314.375
	1/2 " metal plate B/Right/Passenger	202.5	63.0	12757.5
	Husker plates	90	65.25	5872.5
+	Foam	57	52.0	2964.0
+	Chic Rail	1224	63.0	77112.0
+	Concrete Blocks	1290	53.5	69015.0
				1118923.4

Note: (+) is added equipment to vehicle, (-) is removed equipment from vehicle

Estimated Total Weight (lb) 22097	Total Ballast Weight (lb) 7927
Vertical CG Location (in.) 50.637	Ballast Vertical CG Location (in.) 63.486

Vehicle Dimensions for C.G. Calculations

Wheel Base: <u>229.5</u> in.	Front Track Width: <u>79.75</u> in.
	Rear Track Width: <u>72.75</u> in.

Center of Gravity	10000S MASH Targets	Test Inertial	Difference
Test Inertial Weight (lb)	22046 ± 660	22198	152.0
Longitudinal CG (in.)	NA	140.525	NA
Lateral CG (in.)	NA	0.031	NA
Vertical CG (in.)	NA	50.637	NA
Ballast Vertical CG (in.)	63 ± 2	63.486	0.48576

Note: Long. CG is measured from front axle of test vehicle
Note: Lateral CG measured from centerline - positive to vehicle right (passenger) side

CURB WEIGHT (lb)		
	Left	Right
Front	3818	3818
Rear	3491	3615
FRONT	7636	lb
REAR	7106	lb
TOTAL	14742	lb

TEST INERTIAL WEIGHT (lb)		
	Left	Right
Front	4342	4264
Rear	6748	6844
FRONT	8606	lb
REAR	13592	lb
TOTAL	22198	lb

Figure B-1. Vehicle Mass Distribution, Test No. 4CBR-1

Appendix C. Vehicle Deformation Records

The following figures and tables describe all occupant compartment measurements taken on the test vehicle used in full-scale crash testing herein. MASH 2016 defines intrusion as the occupant compartment being deformed and reduced in size with no penetration. Outward deformations, which are denoted as negative numbers within this Appendix, are not considered as crush toward the occupant, and are not subject to evaluation by MASH 2016 criteria.

Date: 8/21/2018 Test Name: 4CBR-1 VIN: 1HTMMAAN66H284494
Year: 2005 Make: International Model: 4300

**VEHICLE DEFORMATION
FLOOR PAN - SET 1**

	POINT	Pretest X (in.)	Pretest Y (in.)	Pretest Z (in.)	Posttest X (in.)	Posttest Y (in.)	Posttest Z (in.)	ΔX^A (in.)	ΔY^A (in.)	ΔZ^A (in.)	Total Δ (in.)	Crush ^B (in.)	Directions for Crush ^C
TOE PAN - WHEEL WELL (X, Z)	1	36.4674	-49.4055	-3.8975	36.0225	-49.6101	-5.0601	0.4449	-0.2046	1.1626	1.2615	1.2448	X, Z
	2	37.1384	-46.2370	-2.2706	36.0534	-46.1612	-3.9265	1.0850	0.0758	1.6559	1.9812	1.9797	X, Z
	3	36.9255	-42.4163	-2.0493	36.3315	-42.4893	-3.0751	0.5940	-0.0730	1.0258	1.1876	1.1854	X, Z
	4	37.1555	-39.8293	-2.0993	36.8666	-40.1810	-2.1020	0.2889	-0.3517	0.0027	0.4552	0.2889	X, Z
	5	37.0105	-37.2942	-2.0110	36.7456	-37.7292	-1.9355	0.2649	-0.4350	-0.0755	0.5149	0.2649	X
	6	33.4570	-49.3363	-1.9941	32.5222	-49.1660	-5.1023	0.9348	0.1703	3.1082	3.2502	3.2457	X, Z
	7	33.7813	-46.4843	-0.9770	32.6526	-45.8970	-4.5738	1.1287	0.5873	3.5968	3.8152	3.7697	X, Z
	8	34.5511	-42.2567	-1.1871	33.9144	-42.2179	-2.7200	0.6367	0.0388	1.5329	1.6603	1.6599	X, Z
	9	34.9671	-39.2787	-1.2749	34.5601	-39.6360	-1.4772	0.4070	-0.3573	0.2023	0.5781	0.4545	X, Z
	10	34.9578	-36.4047	-1.2270	34.6199	-36.7357	-1.3254	0.3379	-0.3310	0.0984	0.4831	0.3519	X, Z
FLOOR PAN (Z)	11	27.3817	-50.4422	0.5615	25.6040	-49.3542	-4.9448	1.7777	1.0880	5.5063	5.8876	5.5063	Z
	12	27.5931	-46.3698	0.5475	26.2425	-45.6236	-3.3423	1.3506	0.7462	3.8898	4.1847	3.8898	Z
	13	27.5615	-41.4376	0.5311	26.8511	-41.4418	-1.2576	0.7104	-0.0042	1.7887	1.9246	1.7887	Z
	14	27.9270	-37.1558	0.6001	27.4918	-37.3775	-0.0501	0.4352	-0.2217	0.6502	0.8132	0.6502	Z
	15	27.9657	-33.0454	0.6238	27.7049	-33.3648	0.1032	0.2608	-0.3194	0.5206	0.6641	0.5206	Z
	16	21.3825	-51.6320	0.6660	20.1293	-51.1378	-2.4487	1.2532	0.4942	3.1147	3.3935	3.1147	Z
	17	21.4321	-46.9891	0.7668	20.3942	-46.7433	-1.5795	1.0379	0.2458	2.3463	2.5774	2.3463	Z
	18	21.7415	-42.8400	0.6011	21.0786	-42.6160	-0.9412	0.6629	0.2240	1.5423	1.6936	1.5423	Z
	19	22.0778	-38.3065	0.6243	21.5877	-38.3986	-0.2812	0.4901	-0.0921	0.9055	1.0337	0.9055	Z
	20	22.8684	-31.5904	0.7294	22.6789	-31.7671	0.1373	0.1895	-0.1767	0.5921	0.6463	0.5921	Z
	21	15.1470	-51.7476	0.6341	14.3092	-51.6159	-0.5086	0.8378	0.1317	1.1427	1.4230	1.1427	Z
	22	15.2197	-45.5853	0.4869	14.3868	-45.4443	-0.8454	0.8329	0.1410	1.3323	1.5775	1.3323	Z
	23	15.4531	-40.2479	0.7139	14.9049	-40.3155	-0.0638	0.5482	-0.0676	0.7777	0.9539	0.7777	Z
	24	16.1517	-33.5081	0.7614	15.8169	-33.5339	0.0432	0.3348	-0.0258	0.7182	0.7928	0.7182	Z
	25	16.5787	-28.1840	0.7312	16.3698	-28.0943	0.3159	0.2089	0.0897	0.4153	0.4735	0.4153	Z
	26	5.0714	-50.7364	0.5619	4.4269	-50.4451	0.4381	0.6445	0.2913	0.1238	0.7180	0.1238	Z
	27	4.6939	-43.9596	0.5901	4.0861	-43.6630	0.2181	0.6078	0.2966	0.3720	0.7719	0.3720	Z
	28	5.0197	-35.8360	0.6169	4.5954	-35.6086	0.1447	0.4243	0.2274	0.4722	0.6743	0.4722	Z
	29	4.8988	-30.2646	0.6621	4.8067	-30.0528	0.3587	0.0921	0.2118	0.3034	0.3813	0.3034	Z
	30	4.8519	-25.7293	0.1543	4.7603	-25.4408	-0.0528	0.0916	0.2885	0.2071	0.3668	0.2071	Z

^A Positive values denote deformation as inward toward the occupant compartment, negative values denote deformations outward away from the occupant compartment.

^B Crush calculations that use multiple directional components will disregard components that are negative and only include positive values where the component is deforming inward toward the occupant compartment.

^C Direction for Crush column denotes which directions are included in the crush calculations. If "NA" then no intrusion is recorded, and Crush will be 0.

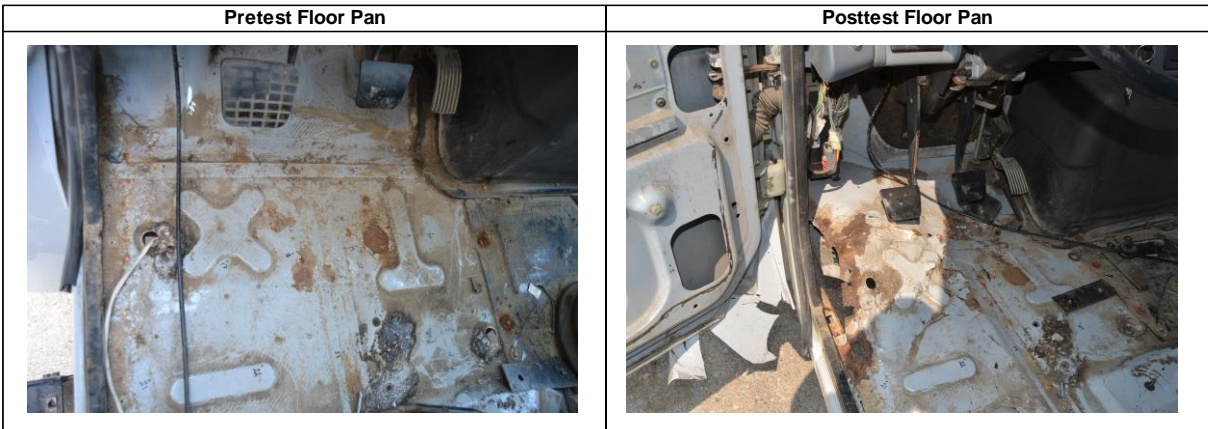


Figure C-1. Floor Pan Deformation Data – Set 1, Test No. 4CBR-1

Date: 8/21/2018 Test Name: 4CBR-1 VIN: 1HTMMAAN66H284494
Year: 2005 Make: International Model: 4300

**VEHICLE DEFORMATION
FLOOR PAN - SET 2**

	POINT	Pretest X (in.)	Pretest Y (in.)	Pretest Z (in.)	Posttest X (in.)	Posttest Y (in.)	Posttest Z (in.)	ΔX^A (in.)	ΔY^A (in.)	ΔZ^A (in.)	Total Δ (in.)	Crush ^B (in.)	Directions for Crush ^C
TOE PAN - WHEEL WELL (X, Z)	1	23.1809	-59.5010	-4.8098	22.8613	-59.6978	-6.1647	0.3196	-0.1968	1.3549	1.4059	1.3921	X, Z
	2	23.7668	-56.3246	-3.1655	22.7721	-56.2584	-5.0055	0.9947	0.0662	1.8400	2.0927	2.0917	X, Z
	3	23.4529	-52.5121	-2.9241	22.9217	-52.5854	-4.1271	0.5312	-0.0733	1.2030	1.3171	1.3151	X, Z
	4	23.6147	-49.9197	-2.9602	23.3762	-50.2670	-3.1371	0.2385	-0.3473	0.1769	0.4569	0.2969	X, Z
	5	23.4028	-47.3897	-2.8586	23.1694	-47.8222	-2.9523	0.2334	-0.4325	0.0937	0.5003	0.2515	X, Z
	6	20.1682	-59.5213	-2.9090	19.3476	-59.3763	-6.2026	0.8206	0.1450	3.2936	3.3974	3.3943	X, Z
	7	20.4163	-56.6672	-1.8764	19.3637	-56.1087	-5.6499	1.0526	0.5585	3.7735	3.9572	3.9176	X, Z
	8	21.0745	-52.4198	-2.0635	20.4968	-52.4015	-3.7692	0.5777	0.0183	1.7057	1.8010	1.8009	X, Z
	9	21.4118	-49.4313	-2.1350	21.0523	-49.8078	-2.5075	0.3595	-0.3765	0.3725	0.6401	0.5177	X, Z
	10	21.3267	-46.5589	-2.0719	21.0105	-46.9084	-2.3342	0.3162	-0.3495	0.2623	0.5394	0.4108	X, Z
FLOOR PAN (Z)	11	14.1220	-60.8007	-0.3651	12.4403	-59.8081	-6.0443	1.6817	0.9926	5.6792	6.0056	5.6792	Z
	12	14.2260	-56.7241	-0.3573	12.9486	-56.0693	-4.4144	1.2774	0.6548	4.0571	4.3036	4.0571	Z
	13	14.0643	-51.7944	-0.3476	13.4115	-51.8842	-2.2990	0.6528	-0.0898	1.9514	2.0597	1.9514	Z
	14	14.3166	-47.5048	-0.2556	13.9100	-47.8090	-1.0616	0.4066	-0.3042	0.8060	0.9526	0.8060	Z
	15	14.2469	-43.3951	-0.2101	13.9824	-43.7926	-0.8786	0.2645	-0.3975	0.6685	0.8215	0.6685	Z
	16	8.1563	-62.1487	-0.2727	7.0330	-61.8009	-3.5599	1.1233	0.3478	3.2872	3.4912	3.2872	Z
	17	8.0832	-57.5067	-0.1473	7.1441	-57.4063	-2.6582	0.9391	0.1004	2.5109	2.6826	2.5109	Z
	18	8.2832	-53.3501	-0.2907	7.6838	-53.2623	-1.9895	0.5994	0.0878	1.6988	1.8036	1.6988	Z
	19	8.4999	-48.8096	-0.2431	8.0452	-49.0347	-1.2985	0.4547	-0.2251	1.0554	1.1710	1.0554	Z
	20	9.1129	-42.0756	-0.1017	8.9036	-42.3723	-0.8312	0.2093	-0.2967	0.7295	0.8149	0.7295	Z
	21	1.9260	-62.4286	-0.3111	1.2343	-62.4970	-1.6216	0.6917	-0.0684	1.3105	1.4834	1.3105	Z
	22	1.8363	-56.2658	-0.4257	1.0953	-56.3241	-1.9126	0.7410	-0.0583	1.4869	1.6623	1.4869	Z
	23	1.9286	-50.9254	-0.1701	1.4338	-51.1862	-1.0933	0.4948	-0.2608	0.9232	1.0794	0.9232	Z
	24	2.4492	-44.1699	-0.0863	2.1077	-44.3778	-0.9362	0.3415	-0.2079	0.8499	0.9392	0.8499	Z
	25	2.7355	-38.8363	-0.0879	2.4697	-38.9243	-0.6234	0.2658	-0.0880	0.5355	0.6043	0.5355	Z
	26	-8.1727	-61.6831	-0.3878	-8.6825	-61.6803	-0.6632	0.5098	0.0028	0.2754	0.5794	0.2754	Z
	27	-8.7289	-54.9188	-0.3240	-9.2608	-54.9129	-0.8328	0.5319	0.0059	0.5088	0.7361	0.5088	Z
	28	-8.6175	-46.7897	-0.2539	-9.0342	-46.8452	-0.8468	0.4167	-0.0555	0.5929	0.7268	0.5929	Z
	29	-8.8853	-41.2238	-0.1792	-9.0176	-41.2872	-0.5916	0.1323	-0.0634	0.4124	0.4377	0.4124	Z
	30	-9.0514	-36.6887	-0.6631	-9.2259	-36.6767	-0.9689	0.1745	0.0120	0.3058	0.3523	0.3058	Z

^A Positive values denote deformation as inward toward the occupant compartment, negative values denote deformations outward away from the occupant compartment.

^B Crush calculations that use multiple directional components will disregard components that are negative and only include positive values where the component is deforming inward toward the occupant compartment.

^C Direction for Crush column denotes which directions are included in the crush calculations. If "NA" then no intrusion is recorded, and Crush will be 0.

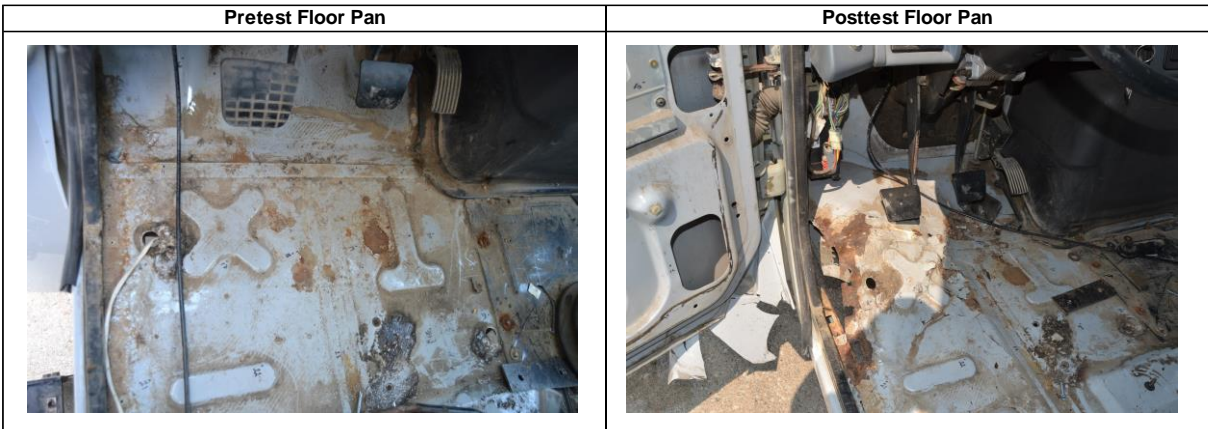


Figure C-2. Floor Pan Deformation Data – Set 2, Test No. 4CBR-1

Date: 8/21/2018		Test Name: 4CBR-1		VIN: 1HTMMAAN66H284494									
Year: 2005		Make: International		Model: 4300									
VEHICLE DEFORMATION INTERIOR CRUSH - SET 1													
	POINT	Pretest X (in.)	Pretest Y (in.)	Pretest Z (in.)	Posttest X (in.)	Posttest Y (in.)	Posttest Z (in.)	ΔX^A (in.)	ΔY^A (in.)	ΔZ^A (in.)	Total Δ (in.)	Crush ^B (in.)	Directions for Crush ^C
DASH (X, Y, Z)	1	29.1538	-50.9629	-29.9524	34.5101	-46.4510	-30.0170	-5.3563	4.5119	-0.0646	7.0037	7.0037	X, Y, Z
	2	30.3065	-39.7248	-32.4891	33.7970	-35.3169	-32.5755	-3.4905	4.4079	-0.0864	5.6232	5.6232	X, Y, Z
	3	29.6650	-22.7405	-31.6411	30.0804	-19.0287	-31.7985	-0.4154	3.7118	-0.1574	3.7383	3.7383	X, Y, Z
	4	26.8354	-33.5796	-21.1215	29.4199	-30.3657	-20.8811	-2.5845	3.2139	0.2404	4.1312	4.1312	X, Y, Z
	5	24.9393	-22.7839	-21.0696	26.0113	-19.9206	-20.7670	-1.0720	2.8633	0.3026	3.0723	3.0723	X, Y, Z
	6	25.1003	-18.1382	-20.7677	25.1757	-15.1847	-20.8119	-0.0754	2.9535	-0.0442	2.9548	2.9548	X, Y, Z
SIDE PANEL (Y)	7	30.8961	-54.5767	-3.1454	35.7475	-51.1738	-3.9732	-4.8514	3.4029	-0.8278	5.9834	3.4029	Y
	8	34.0631	-54.6666	-4.4477	38.8612	-50.7252	-4.7548	-4.7981	3.9414	-0.3071	6.2170	3.9414	Y
	9	30.7911	-54.4937	-7.5939	35.6948	-50.9447	-7.8308	-4.9037	3.5490	-0.2369	6.0579	3.5490	Y
IMPACT SIDE DOOR (Y)	10	23.0413	-55.0877	-18.4315	27.4633	-52.9715	-18.7188	-4.4220	2.1162	-0.2873	4.9107	2.1162	Y
	11	13.3546	-54.7910	-20.7538	17.7352	-53.9820	-21.1236	-4.3806	0.8090	-0.3698	4.4700	0.8090	Y
	12	0.8676	-54.5837	-18.9719	5.3553	-55.1197	-19.3011	-4.4877	-0.5360	-0.3292	4.5316	-0.5360	Y
	13	-2.7949	-53.2041	-6.1865	1.6899	-54.1485	-6.4922	-4.4848	-0.9444	-0.3057	4.5933	-0.9444	Y
	14	9.3095	-57.3932	-4.1510	14.1483	-56.9429	-4.4406	-4.8388	0.4503	-0.2896	4.8683	0.4503	Y
	15	21.4945	-54.4265	-6.2498	25.8752	-52.6156	-6.5921	-4.3807	1.8109	-0.3423	4.7526	1.8109	Y
ROOF - (Z)	16	21.9033	-46.6572	-52.9040	25.3864	-43.9711	-53.1530	-3.4831	2.6861	-0.2490	4.4056	-0.2490	Z
	17	23.7688	-40.8017	-53.2521	26.5505	-37.9345	-53.4509	-2.7817	2.8672	-0.1988	3.9998	-0.1988	Z
	18	25.1102	-35.2438	-53.4245	27.2282	-32.2965	-53.5585	-2.1180	2.9473	-0.1340	3.6319	-0.1340	Z
	19	25.9011	-28.2507	-53.5640	27.2887	-25.1805	-53.5724	-1.3876	3.0702	-0.0084	3.3692	-0.0084	Z
	20	26.8919	-19.1910	-53.3965	27.2671	-16.0465	-53.2977	-0.3752	3.1445	0.0988	3.1683	0.0988	Z
	21	5.7987	-45.0054	-55.8523	9.0339	-44.2084	-56.0656	-3.2352	0.7970	-0.2133	3.3387	-0.2133	Z
	22	6.1383	-38.2353	-56.1346	8.6084	-37.3836	-56.2692	-2.4701	0.8517	-0.1546	2.6174	-0.1546	Z
	23	6.3392	-33.3018	-56.3688	8.3032	-32.4601	-56.4655	-1.9640	0.8417	-0.0967	2.1389	-0.0967	Z
	24	6.4976	-28.1402	-56.5376	7.8789	-27.2625	-56.5811	-1.3813	0.8777	-0.0435	1.6371	-0.0435	Z
	25	6.7127	-21.9575	-56.6170	7.5235	-21.0980	-56.5957	-0.8108	0.8595	0.0213	1.1818	0.0213	Z
	26	-9.2407	-45.6611	-57.0471	-5.8563	-46.5278	-57.2041	-3.3844	-0.8667	-0.1570	3.4971	-0.1570	Z
	27	-8.8979	-38.7920	-57.6738	-6.3092	-39.6902	-57.7699	-2.5887	-0.8982	-0.0961	2.7418	-0.0961	Z
	28	-8.3940	-31.5643	-58.0045	-6.6039	-32.4072	-58.0759	-1.7901	-0.8429	-0.0714	1.9799	-0.0714	Z
	29	-8.3266	-24.9032	-57.8342	-7.2680	-25.7618	-57.7921	-1.0586	-0.8586	0.0421	1.3637	0.0421	Z
	30	-8.3213	-20.4467	-58.3001	-7.7673	-21.4349	-58.1769	-0.5540	-0.9882	0.1232	1.1396	0.1232	Z
A-PILLAR Maximum (X, Y, Z)	31	21.1428	-51.2517	-48.1255	23.6649	-49.9473	-48.2343	-2.5221	1.3044	-0.1088	2.8415	1.3044	Y
	32	23.7451	-51.8520	-43.3197	26.4324	-50.3510	-43.3676	-2.6873	1.5010	-0.0479	3.0785	1.5010	Y
	33	25.3644	-52.2930	-39.3050	28.0979	-50.6526	-39.3357	-2.7335	1.6404	-0.0307	3.1881	1.6404	Y
	34	26.7067	-52.7268	-36.7783	29.5419	-51.0254	-36.8467	-2.8352	1.7014	-0.0684	3.3072	1.7014	Y
	35	28.3513	-53.1280	-33.5640	30.8379	-51.2301	-34.1567	-2.4866	1.8979	-0.5927	3.1838	1.8979	Y
	36	29.4524	-53.5731	-30.7335	32.3405	-51.6128	-30.8496	-2.8881	1.9603	-0.1161	3.4925	1.9603	Y
A-PILLAR Lateral (Y)	31	21.1428	-51.2517	-48.1255	23.6649	-49.9473	-48.2343	-2.5221	1.3044	-0.1088	2.8415	1.3044	Y
	32	23.7451	-51.8520	-43.3197	26.4324	-50.3510	-43.3676	-2.6873	1.5010	-0.0479	3.0785	1.5010	Y
	33	25.3644	-52.2930	-39.3050	28.0979	-50.6526	-39.3357	-2.7335	1.6404	-0.0307	3.1881	1.6404	Y
	34	26.7067	-52.7268	-36.7783	29.5419	-51.0254	-36.8467	-2.8352	1.7014	-0.0684	3.3072	1.7014	Y
	35	28.3513	-53.1280	-33.5640	30.8379	-51.2301	-34.1567	-2.4866	1.8979	-0.5927	3.1838	1.8979	Y
	36	29.4524	-53.5731	-30.7335	32.3405	-51.6128	-30.8496	-2.8881	1.9603	-0.1161	3.4925	1.9603	Y
B-PILLAR Maximum (X, Y, Z)	37	-9.2086	-51.5540	-51.5706	-6.5492	-52.3789	-51.4785	-2.6594	-0.8249	0.0921	2.7859	0.0921	Z
	38	-9.2640	-52.0593	-46.1715	-6.5194	-52.9905	-46.0229	-2.7446	-0.9312	0.1486	2.9021	0.1486	Z
	39	-8.9858	-52.6077	-41.1394	-6.3349	-53.5675	-41.0209	-2.6509	-0.9598	0.1185	2.8218	0.1185	Z
	40	-9.2456	-53.1929	-34.6196	-6.3708	-54.1926	-34.5670	-2.8748	-0.9997	0.0526	3.0441	0.0526	Z
B-PILLAR Lateral (Y)	37	-9.2086	-51.5540	-51.5706	-6.5492	-52.3789	-51.4785	-2.6594	-0.8249	0.0921	2.7859	-0.8249	Y
	38	-9.2640	-52.0593	-46.1715	-6.5194	-52.9905	-46.0229	-2.7446	-0.9312	0.1486	2.9021	-0.9312	Y
	39	-8.9858	-52.6077	-41.1394	-6.3349	-53.5675	-41.0209	-2.6509	-0.9598	0.1185	2.8218	-0.9598	Y
	40	-9.2456	-53.1929	-34.6196	-6.3708	-54.1926	-34.5670	-2.8748	-0.9997	0.0526	3.0441	-0.9997	Y

^A Positive values denote deformation as inward toward the occupant compartment, negative values denote deformations outward away from the occupant compartment.
^B Crush calculations that use multiple directional components will disregard components that are negative and only include positive values where the component is deforming inward toward the occupant compartment.
^C Direction for Crush column denotes which directions are included in the crush calculations. If "NA" then no intrusion is recorded, and Crush will be 0.

Figure C-3. Occupant Compartment Deformation Data – Set 1, Test No. 4CBR-1

Date: 8/21/2018 Year: 2005		Test Name: 4CBR-1 Make: International		VIN: 1HTMMAAN66H284494 Model: 4300									
VEHICLE DEFORMATION INTERIOR CRUSH - SET 2													
	POINT	Pretest X (in.)	Pretest Y (in.)	Pretest Z (in.)	Posttest X (in.)	Posttest Y (in.)	Posttest Z (in.)	ΔX^A (in.)	ΔY^A (in.)	ΔZ^A (in.)	Total Δ (in.)	Crush ^B (in.)	Directions for Crush ^C
DASH PANEL (X, Y, Z)	1	15.3500	-61.5137	-30.9137	20.5151	-56.9495	-31.0617	-5.1651	4.5642	-0.1480	6.8944	6.8944	X, Y, Z
	2	16.3974	-50.2507	-33.3850	19.6351	-45.8065	-33.5278	-3.2377	4.4442	-0.1428	5.5004	5.5004	X, Y, Z
	3	15.5962	-33.2784	-32.4389	15.6616	-29.5856	-32.6239	-0.0654	3.6928	-0.1850	3.6980	3.6980	X, Y, Z
	4	12.8668	-44.2043	-21.9828	15.1468	-41.0244	-21.8052	-2.2800	3.1799	0.1776	3.9168	3.9168	X, Y, Z
	5	10.8694	-33.4274	-21.8689	11.5747	-30.6352	-21.6129	-0.7053	2.7922	0.2560	2.8913	2.8913	X, Y, Z
	6	10.9867	-28.7822	-21.5401	10.6951	-25.9127	-21.6201	0.3216	2.8695	-0.0800	2.8886	2.8886	X, Y, Z
SIDE PANEL (Y)	7	17.1217	-65.2660	-4.1276	21.7500	-61.8746	-5.0553	-4.6283	3.3914	-0.9277	5.8123	3.3914	Y
	8	20.2896	-65.3185	-5.4297	24.8586	-61.3706	-5.8235	-4.5690	3.9479	-0.3938	6.0512	3.9479	Y
	9	17.0167	-65.1583	-8.5756	21.7050	-61.6134	-8.9109	-4.6883	3.5449	-0.3353	5.8872	3.5449	Y
IMPACT SIDE DOOR (Y)	10	9.2745	-65.7623	-19.4181	13.5382	-63.6756	-19.8409	-4.2637	2.0867	-0.4228	4.7657	2.0867	Y
	11	-0.4141	-65.5432	-21.7409	3.8342	-64.8176	-22.2840	-4.2483	0.7256	-0.5431	4.3439	0.7256	Y
	12	-12.9028	-65.4636	-19.9606	-8.5316	-66.1643	-20.5091	-4.3712	-0.7007	-0.5485	4.4609	-0.7007	Y
	13	-16.5802	-64.1925	-7.1683	-12.2493	-65.3599	-7.7036	-4.3309	-1.1674	-0.5353	4.5173	-1.1674	Y
	14	-4.4374	-68.2794	-5.1543	0.2453	-67.9765	-5.6377	-4.6827	0.3029	-0.4834	4.7173	0.3029	Y
	15	7.7196	-65.1862	-7.2332	11.9092	-63.4481	-7.7165	-4.1896	1.7381	-0.4833	4.5615	1.7381	Y
ROOF - (Z)	16	8.0632	-57.1436	-53.8416	11.4214	-54.4152	-54.2037	-3.3582	2.7284	-0.3621	4.3420	-0.3621	Z
	17	9.8737	-51.2689	-54.1554	12.4917	-48.3588	-54.4467	-2.6180	2.9101	-0.2913	3.9252	-0.2913	Z
	18	11.1628	-45.6977	-54.2954	13.0813	-42.7102	-54.5044	-1.9185	2.9875	-0.2090	3.5566	-0.2090	Z
	19	11.8880	-38.6968	-54.3942	13.0304	-35.5942	-54.4577	-1.1424	3.1026	-0.0635	3.3068	-0.0635	Z
	20	12.7936	-29.6292	-54.1741	12.8649	-26.4644	-54.1055	-0.0713	3.1648	0.0686	3.1663	0.0686	Z
	21	-8.0657	-55.6261	-56.7838	-4.9167	-54.8833	-57.1682	-3.1390	0.7428	-0.3844	3.2485	-0.3844	Z
	22	-7.7797	-48.8516	-57.0269	-5.4484	-48.0643	-57.3351	-2.3313	0.7873	-0.3082	2.4799	-0.3082	Z
	23	-7.6252	-43.9151	-57.2326	-5.8302	-43.1449	-57.4706	-1.7950	0.7702	-0.2380	1.9677	-0.2380	Z
	24	-7.5153	-38.7514	-57.3714	-6.3356	-37.9537	-57.5434	-1.1797	0.7977	-0.1720	1.4344	-0.1720	Z
	25	-7.3682	-32.5666	-57.4150	-6.7875	-31.7957	-57.5067	-0.5707	0.7709	-0.0917	0.9635	-0.0917	Z
	26	-23.0880	-56.4161	-57.9858	-19.7654	-57.4255	-58.3719	-3.3226	-1.0094	-0.3861	3.4939	-0.3861	Z
	27	-22.8097	-49.5406	-58.5727	-20.3237	-50.5912	-58.8811	-2.4860	-1.0506	-0.3084	2.7164	-0.3084	Z
	28	-22.3738	-42.3067	-58.8614	-20.7316	-43.3114	-59.1261	-1.6422	-1.0047	-0.2647	1.9433	-0.2647	Z
	29	-22.3689	-35.6464	-58.6526	-21.5005	-36.6799	-58.7879	-0.8684	-1.0335	-0.1353	1.3567	-0.1353	Z
	30	-22.4055	-31.1874	-59.0927	-22.0663	-32.3582	-59.1375	-0.3392	-1.1708	-0.0448	1.2198	-0.0448	Z
A-PILLAR Maximum (X, Y, Z)	31	7.3452	-61.7726	-49.0900	9.7793	-60.4594	-49.3411	-2.4341	1.3132	-0.2511	2.7771	1.3132	Y
	32	9.9522	-62.3761	-44.2871	12.5386	-60.8612	-44.4696	-2.5864	1.5149	-0.1825	3.0029	1.5149	Y
	33	11.5748	-62.8252	-40.2746	14.1968	-61.1712	-40.4353	-2.6220	1.6540	-0.1607	3.1043	1.6540	Y
	34	12.9357	-63.2730	-37.7078	15.6391	-61.5426	-37.9452	-2.7034	1.7304	-0.2374	3.2185	1.7304	Y
	35	14.6042	-63.7023	-34.5083	16.9303	-61.7500	-35.2530	-2.3261	1.9523	-0.7447	3.1268	1.9523	Y
	36	15.6332	-64.0757	-31.7012	18.4290	-62.1374	-31.9447	-2.7958	1.9383	-0.2435	3.4107	1.9383	Y
A-PILLAR Lateral (Y)	31	7.3452	-61.7726	-49.0900	9.7793	-60.4594	-49.3411	-2.4341	1.3132	-0.2511	2.7771	1.3132	Y
	32	9.9522	-62.3761	-44.2871	12.5386	-60.8612	-44.4696	-2.5864	1.5149	-0.1825	3.0029	1.5149	Y
	33	11.5748	-62.8252	-40.2746	14.1968	-61.1712	-40.4353	-2.6220	1.6540	-0.1607	3.1043	1.6540	Y
	34	12.9357	-63.2730	-37.7078	15.6391	-61.5426	-37.9452	-2.7034	1.7304	-0.2374	3.2185	1.7304	Y
	35	14.6042	-63.7023	-34.5083	16.9303	-61.7500	-35.2530	-2.3261	1.9523	-0.7447	3.1268	1.9523	Y
	36	15.6332	-64.0757	-31.7012	18.4290	-62.1374	-31.9447	-2.7958	1.9383	-0.2435	3.4107	1.9383	Y
B-PILLAR Maximum (X, Y, Z)	37	-23.0326	-62.3445	-52.4497	-20.3833	-63.3354	-52.6984	-2.6493	-0.9909	-0.2487	2.8395	0.0000	NA
	38	-23.0278	-62.8797	-47.1035	-20.3600	-63.9930	-47.2481	-2.6678	-1.1133	-0.1446	2.8944	0.0000	NA
	39	-22.8174	-63.4504	-42.0810	-20.1811	-64.6097	-42.2506	-2.6363	-1.1593	-0.1696	2.8849	0.0000	NA
	40	-23.0611	-64.0750	-35.6340	-20.2260	-65.2904	-35.8024	-2.8351	-1.2154	-0.1684	3.0892	0.0000	NA
B-PILLAR Lateral (Y)	37	-23.0326	-62.3445	-52.4497	-20.3833	-63.3354	-52.6984	-2.6493	-0.9909	-0.2487	2.8395	-0.9909	Y
	38	-23.0278	-62.8797	-47.1035	-20.3600	-63.9930	-47.2481	-2.6678	-1.1133	-0.1446	2.8944	-1.1133	Y
	39	-22.8174	-63.4504	-42.0810	-20.1811	-64.6097	-42.2506	-2.6363	-1.1593	-0.1696	2.8849	-1.1593	Y
	40	-23.0611	-64.0750	-35.6340	-20.2260	-65.2904	-35.8024	-2.8351	-1.2154	-0.1684	3.0892	-1.2154	Y

^A Positive values denote deformation as inward toward the occupant compartment, negative values denote deformations outward away from the occupant compartment.

^B Crush calculations that use multiple directional components will disregard components that are negative and only include positive values where the component is deforming inward toward the occupant compartment.

^C Direction for Crush column denotes which directions are included in the crush calculations. If "NA" then no intrusion is recorded, and Crush will be 0.

Figure C-4. Occupant Compartment Deformation Data – Set 2, Test No. 4CBR-1

Date: 8/21/2018
 Year: 2005

Test Name: 4CBR-1
 Make: International

VIN: 1HTMMAAN66H284494
 Model: 4300

Reference Set 1			
Location	Maximum Deformation ^{A,B} (in.)	MASH Allowable Deformation (in.)	Directions of Deformation ^C
Roof	0.1	≤ 4	Z
Windshield ^D	0.0	≤ 3	X, Z
A-Pillar Maximum	2.0	≤ 5	Y
A-Pillar Lateral	2.0	≤ 3	Y
B-Pillar Maximum	0.1	≤ 5	Z
B-Pillar Lateral	-0.8	≤ 3	Y
Toe Pan - Wheel Well	3.8	≤ 9	X, Z
Side Front Panel	3.9	≤ 12	Y
Side Door (above seat)	2.1	≤ 9	Y
Side Door (below seat)	1.8	≤ 12	Y
Floor Pan	5.5	≤ 12	Z
Dash - no MASH requirement	7.0	NA	X, Y, Z

Reference Set 2			
Location	Maximum Deformation ^{A,B} (in.)	MASH Allowable Deformation (in.)	Directions of Deformation ^C
Roof	0.1	≤ 4	Z
Windshield ^D	NA	≤ 3	X, Z
A-Pillar Maximum	2.0	≤ 5	Y
A-Pillar Lateral	2.0	≤ 3	Y
B-Pillar Maximum	0.0	≤ 5	NA
B-Pillar Lateral	-1.0	≤ 3	Y
Toe Pan - Wheel Well	3.9	≤ 9	X, Z
Side Front Panel	3.9	≤ 12	Y
Side Door (above seat)	2.1	≤ 9	Y
Side Door (below seat)	1.7	≤ 12	Y
Floor Pan	5.7	≤ 12	Z
Dash - no MASH requirement	7.0	NA	X, Y, Z

^A Items highlighted in red do not meet MASH allowable deformations.

^B Positive values denote deformation as inward toward the occupant compartment, negative values denote deformations outward away from the occupant compartment.

^C For Toe Pan - Wheel Well the direction of deformation may include X and Z direction. For A-Pillar Maximum and B-Pillar Maximum the direction of deformation may include X, Y, and Z directions. The direction of deformation for Toe Pan -Wheel Well, A-Pillar Maximum, and B-Pillar Maximum only include components where the deformation is positive and intruding into the occupant compartment. If direction of deformation is "NA" then no intrusion is recorded and deformation will be 0.

^D If deformation is observed for the windshield then the windshield deformation is measured posttest with an exemplar vehicle, therefore only one set of reference is measured and recorded.

Notes on vehicle interior crush:

The negative Z values are not correct due excell equation issues with signage limits. Please look directly at the crush pages for maximums.

Figure C-5. Maximum Occupant Compartment Deformation, Test No. 4CBR-1

Appendix D. Accelerometer and Rate Transducer Data Plots, Test No. 4CBR-1

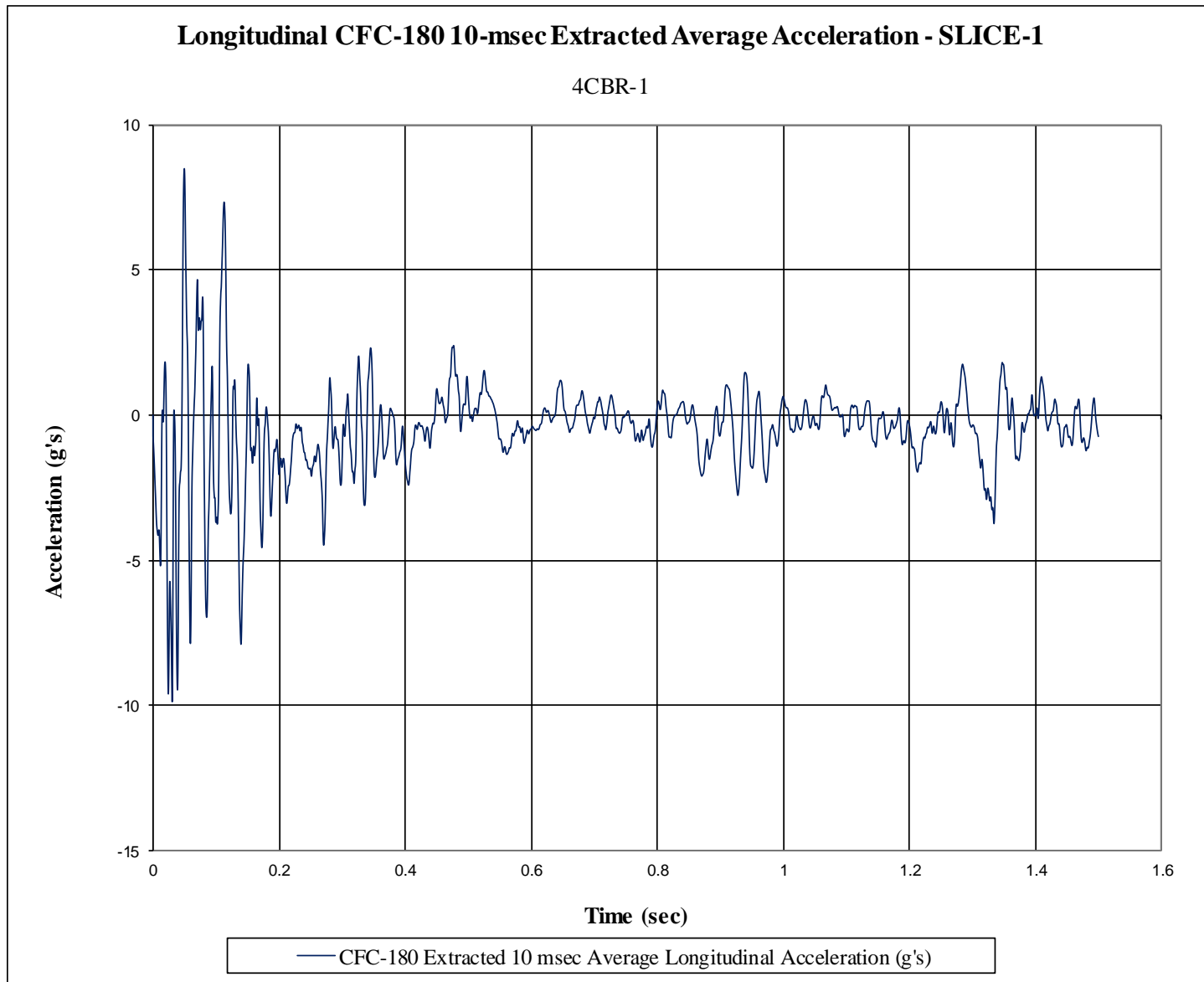


Figure D-1. 10-ms Average Longitudinal Acceleration (SLICE-1, cab), Test No. 4CBR-1

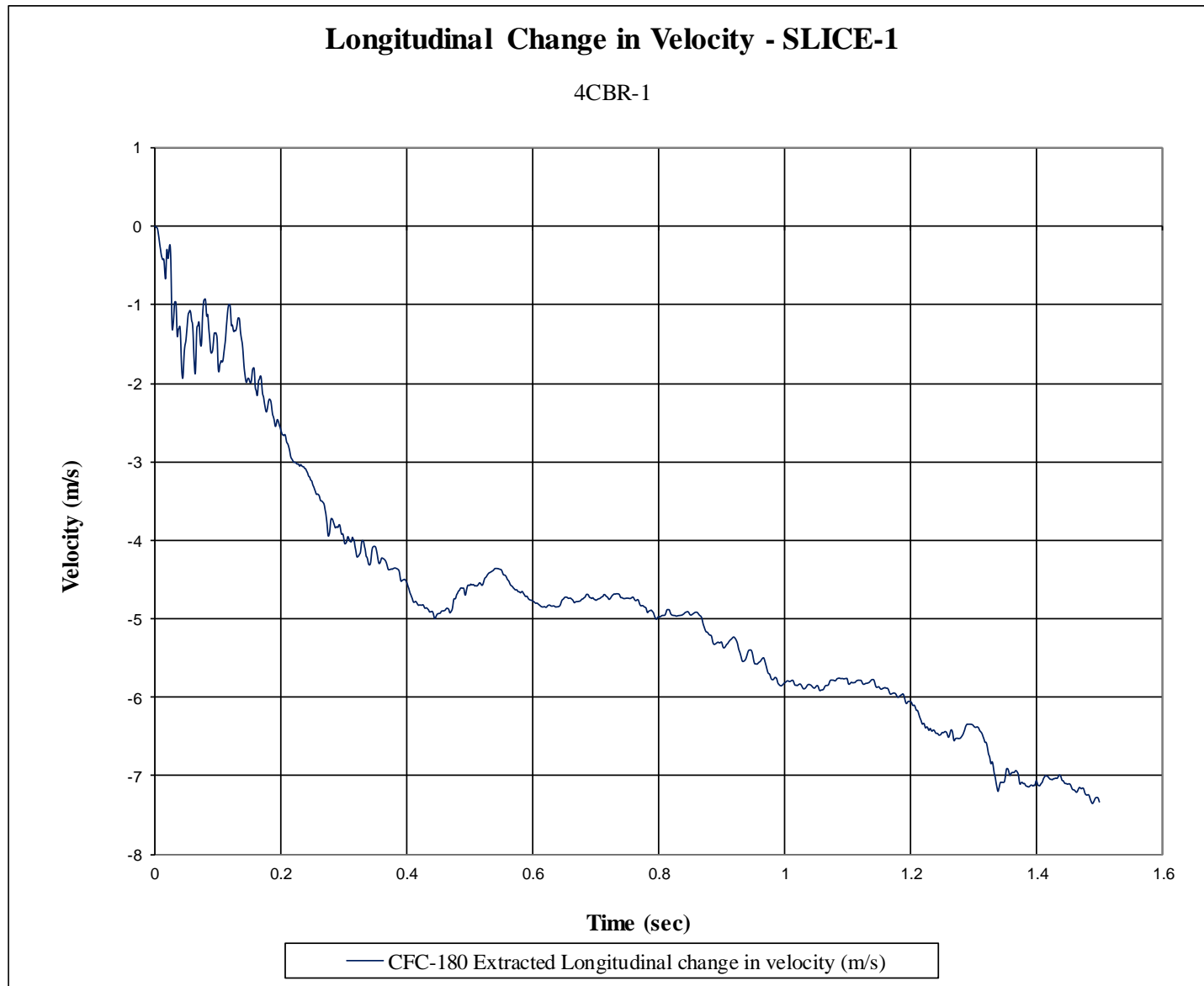


Figure D-2. Longitudinal Change in Velocity (SLICE-1, cab), Test No. 4CBR-1

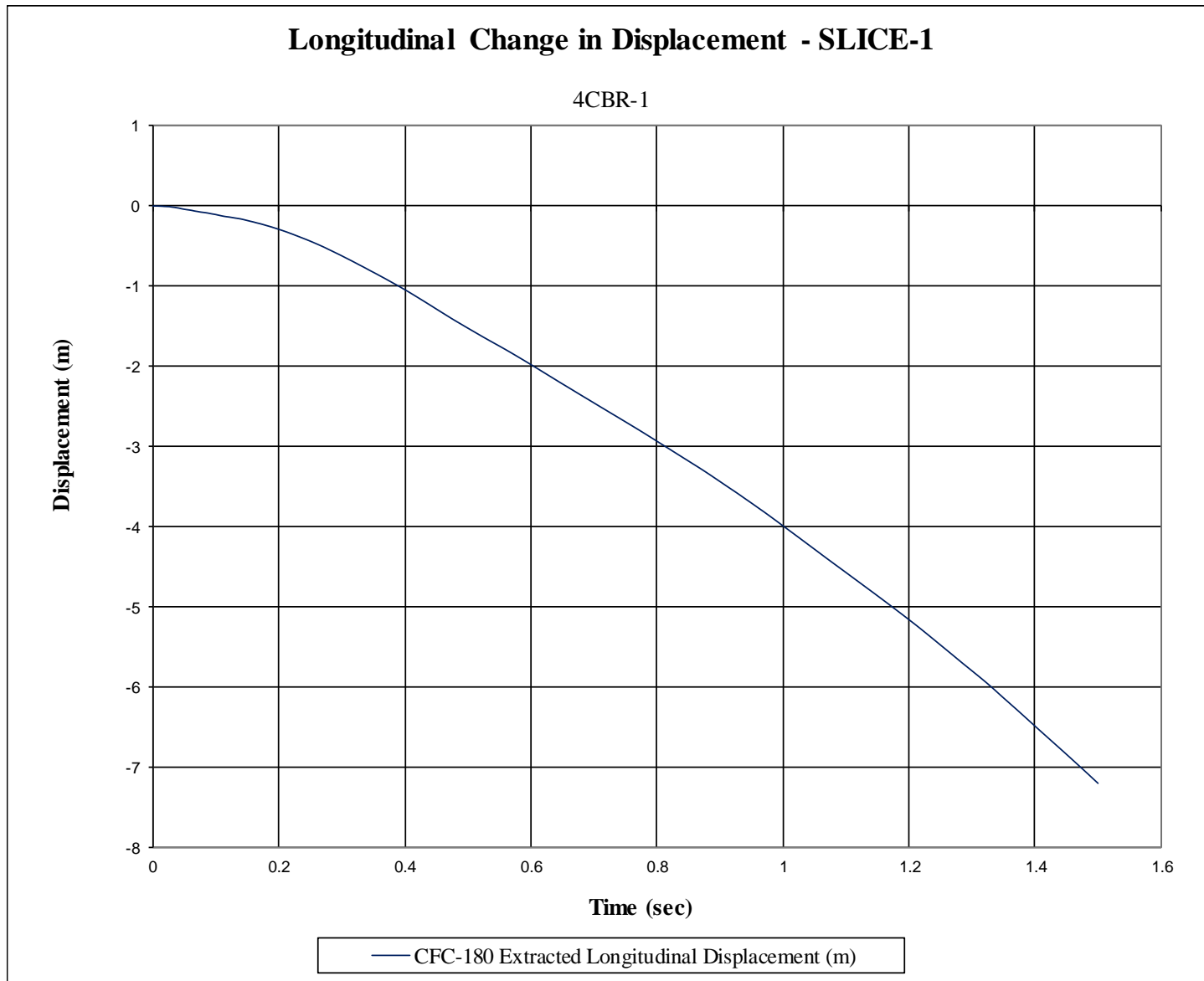


Figure D-3. Longitudinal Occupant Displacement (SLICE-1, cab), Test No. 4CBR-1

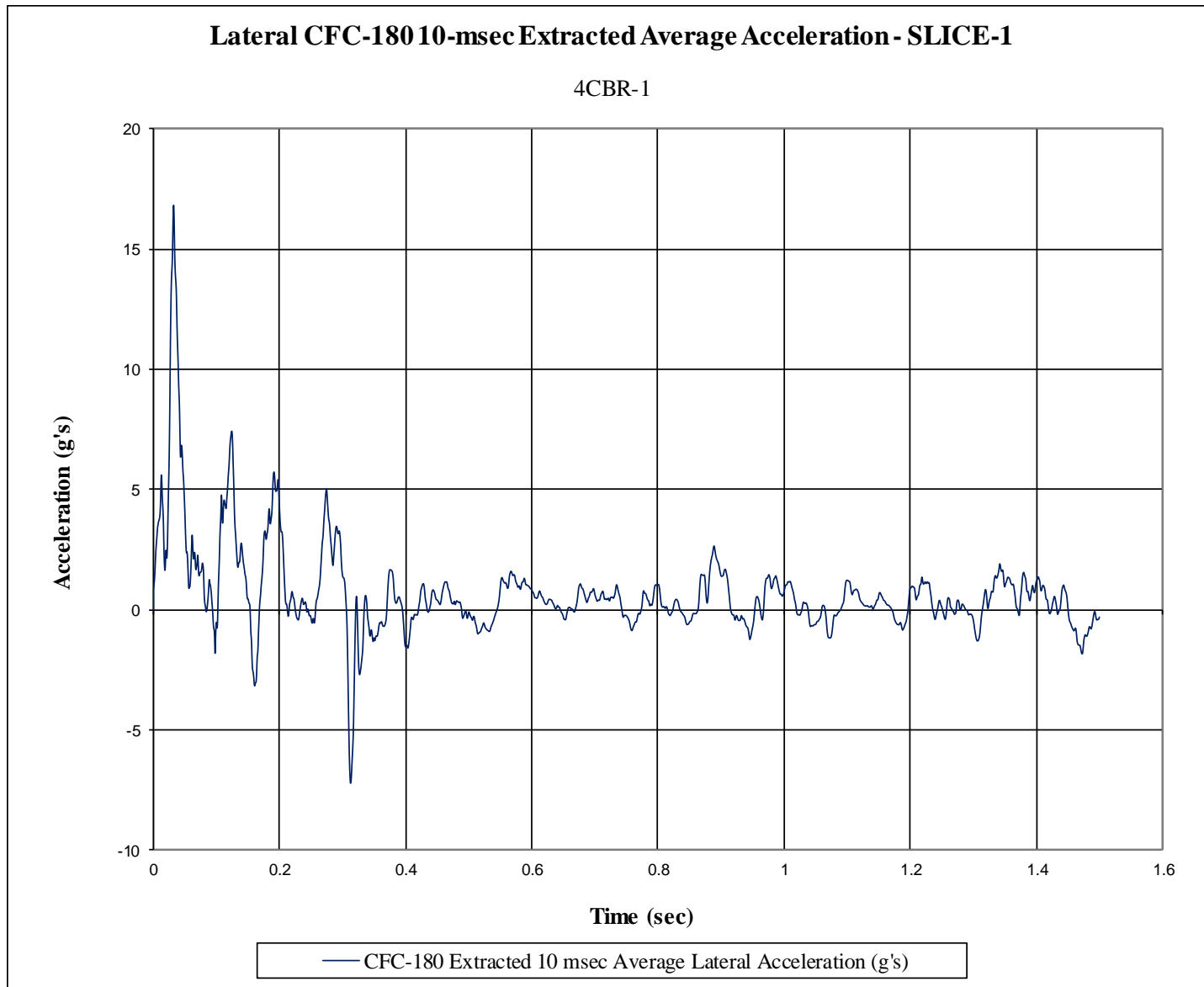


Figure D-4. 10-ms Average Lateral Acceleration (SLICE-1, cab), Test No. 4CBR-1

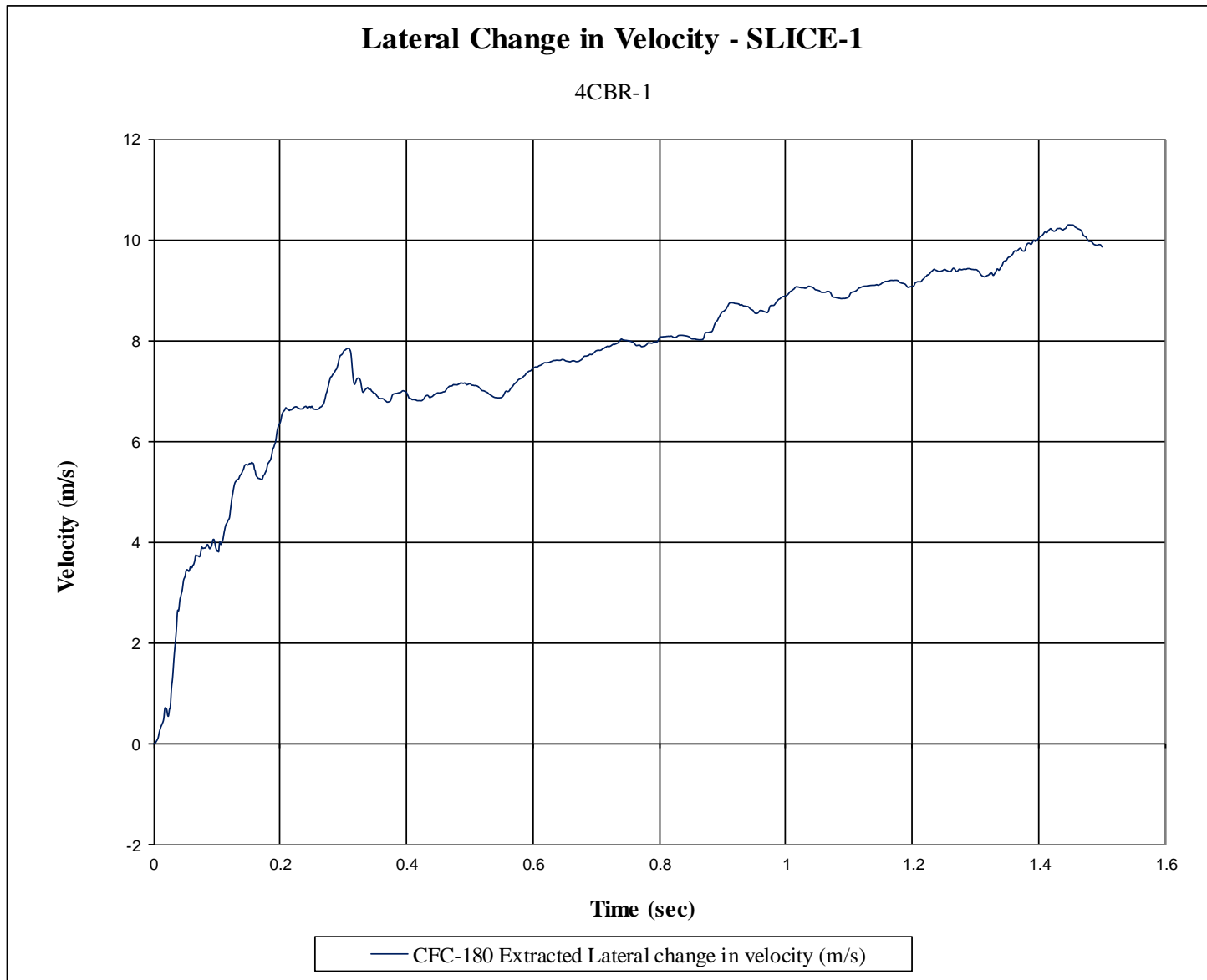


Figure D-5. Lateral Change in Velocity (SLICE-1, cab), Test No. 4CBR-1

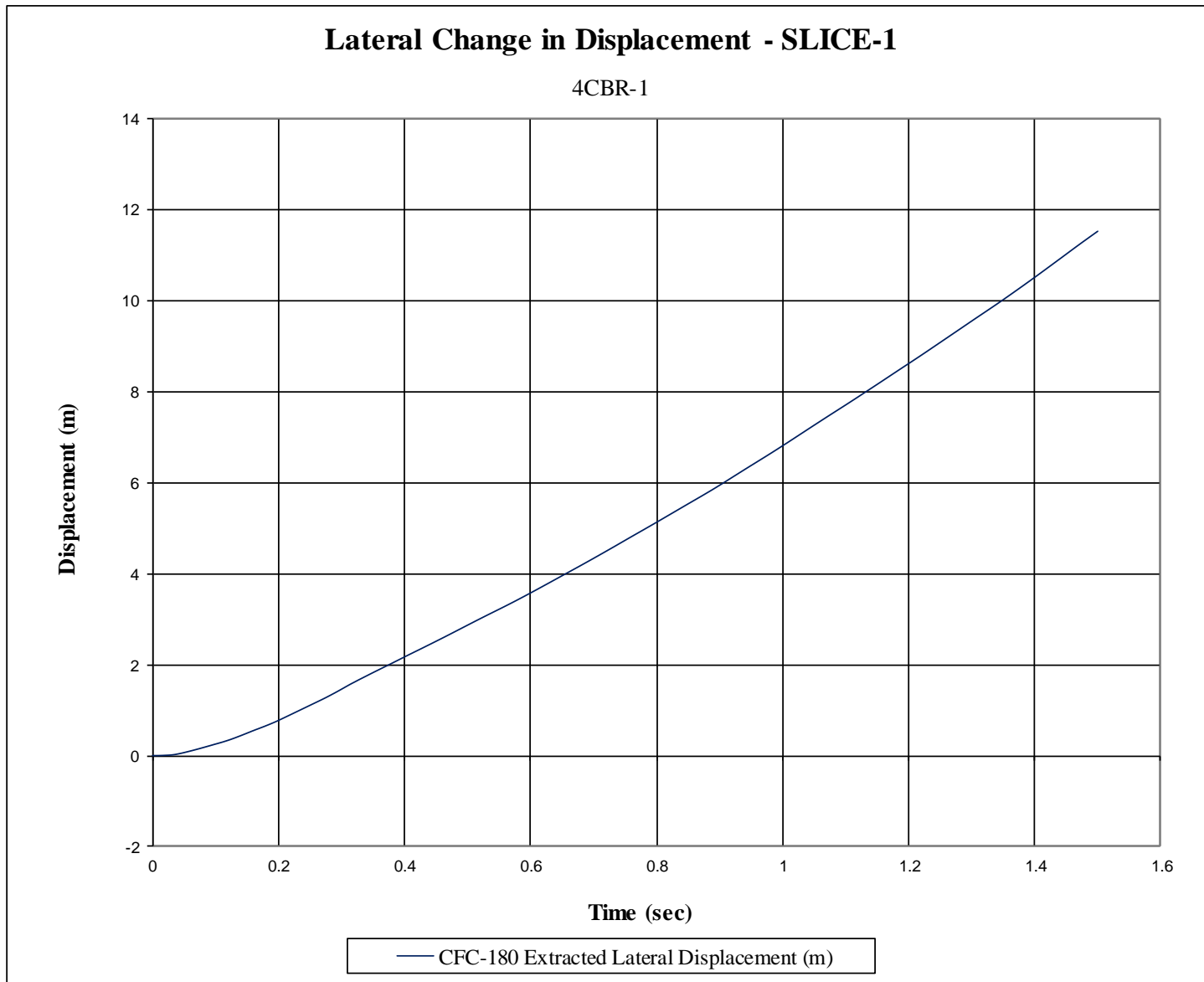


Figure D-6. Lateral Occupant Displacement (SLICE-1, cab), Test No. 4CBR-1

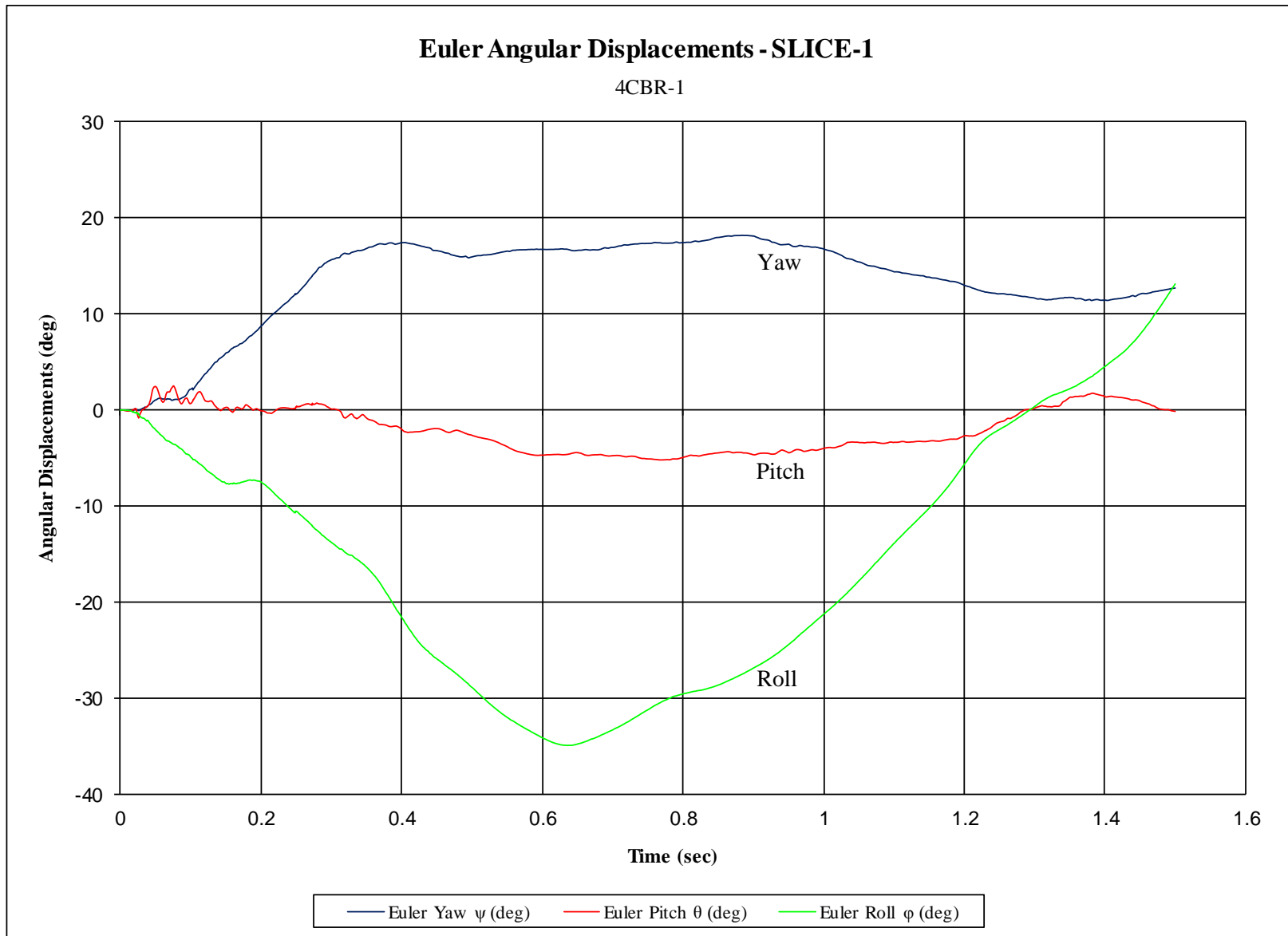


Figure D-7. Vehicle Angular Displacements (SLICE-1, cab), Test No. 4CBR-1

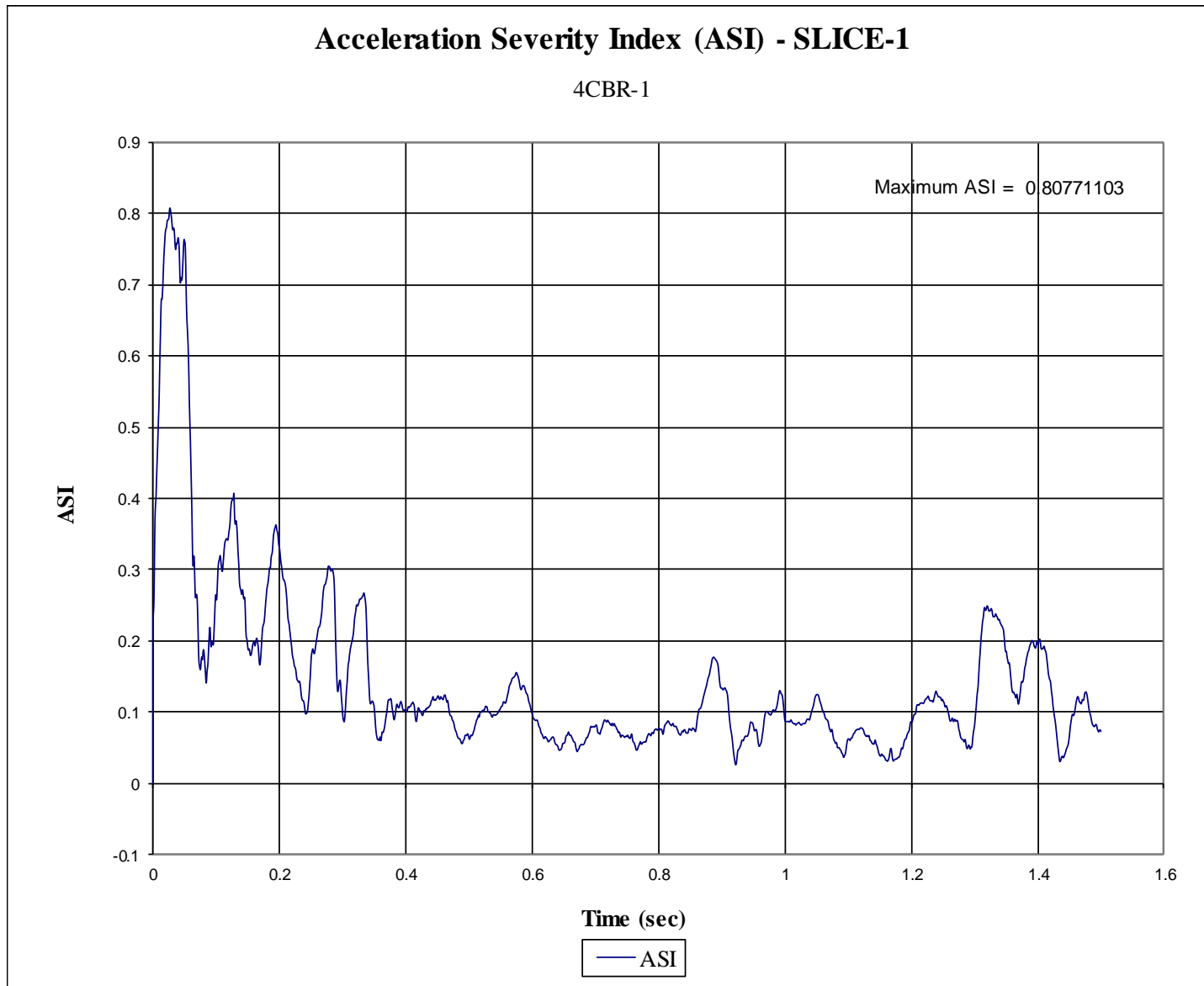


Figure D-8. Acceleration Severity Index (SLICE-1, cab), Test No. 4CBR-1

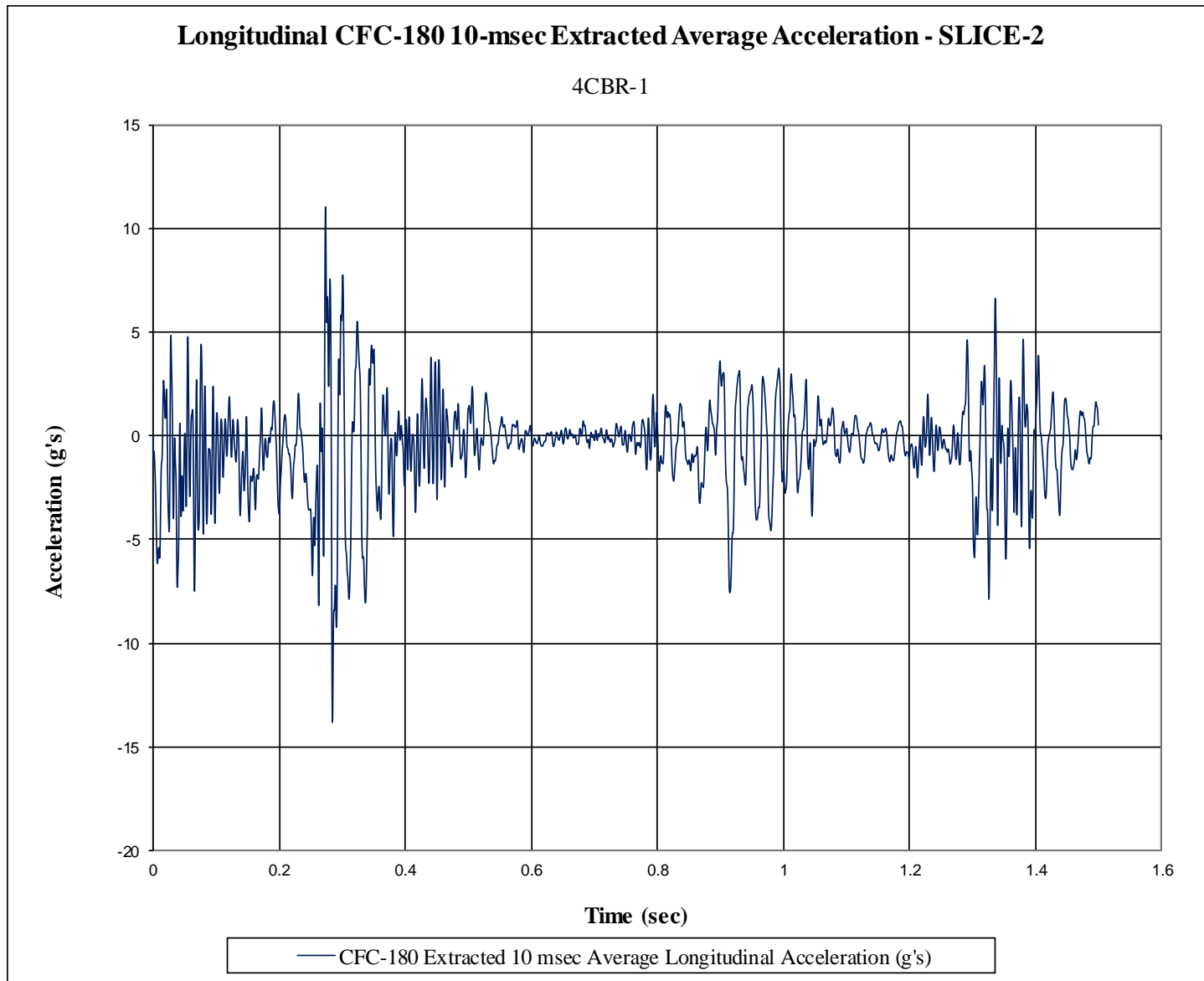


Figure D-9. 10-ms Average Longitudinal Acceleration (SLICE-2, c.g.), Test No. 4CBR-1

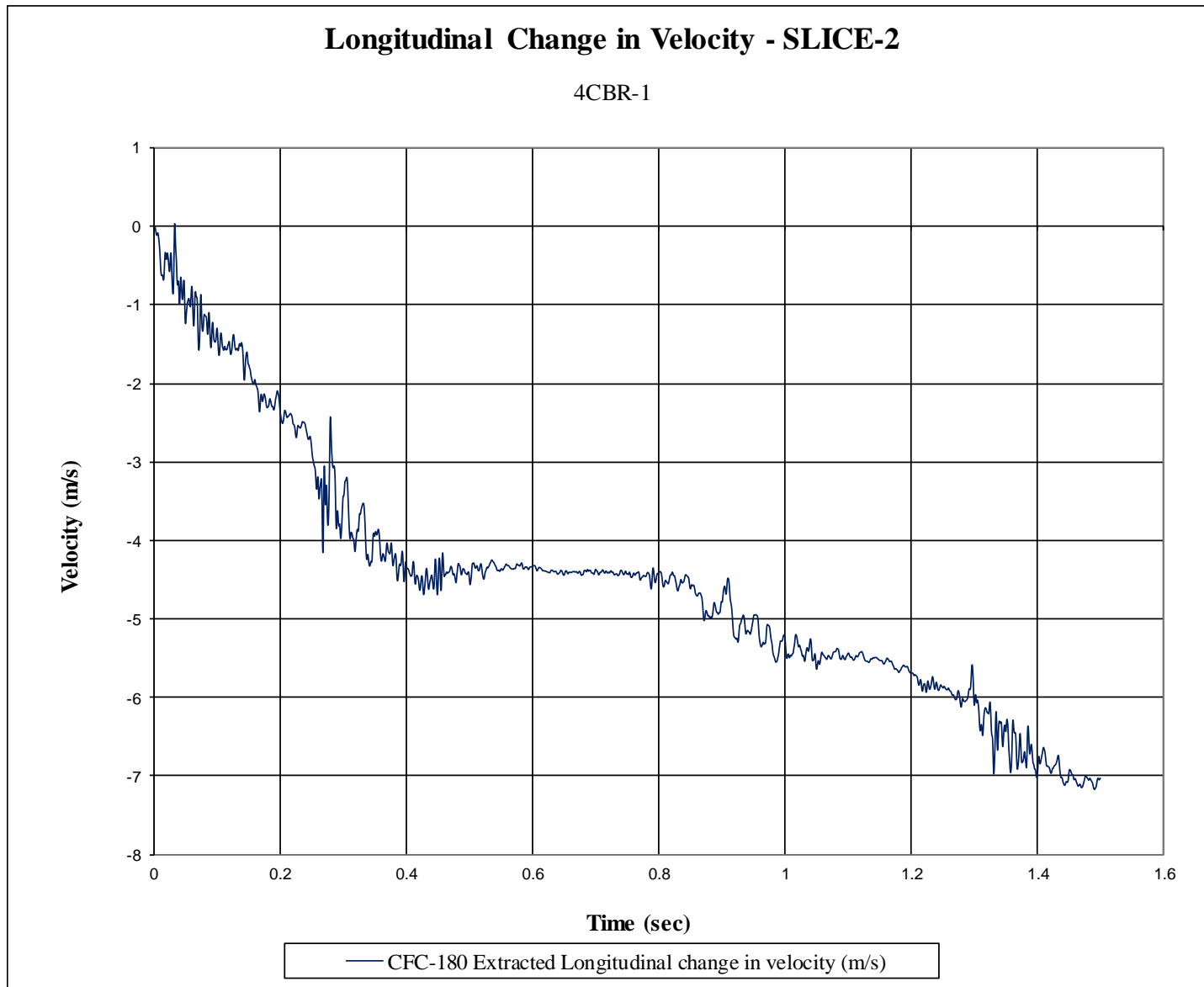


Figure D-10. Longitudinal Change in Velocity (SLICE-2, c.g.), Test No. 4CBR-1

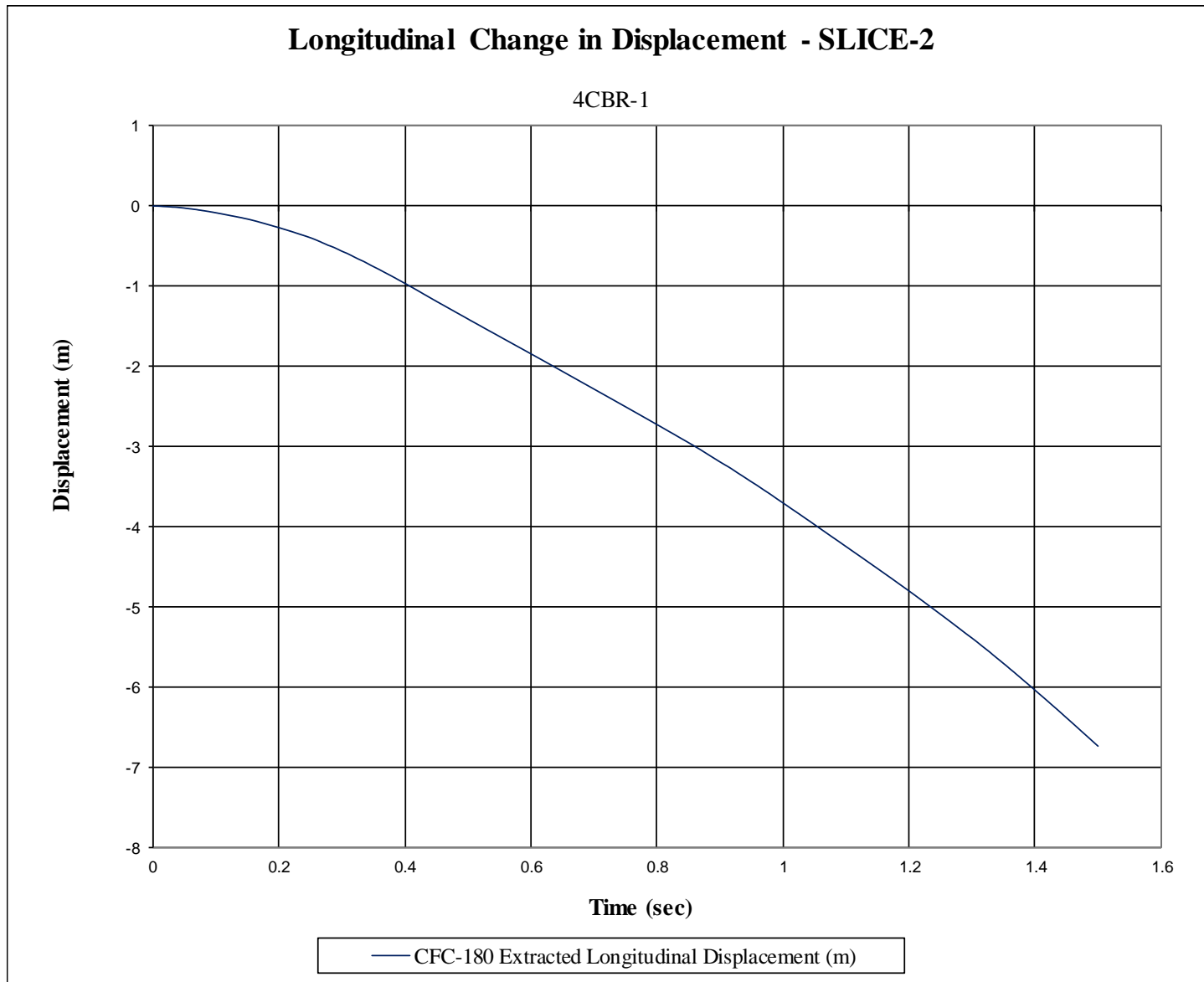


Figure D-11. Longitudinal Occupant Displacement (SLICE-2, c.g.), Test No. 4CBR-1

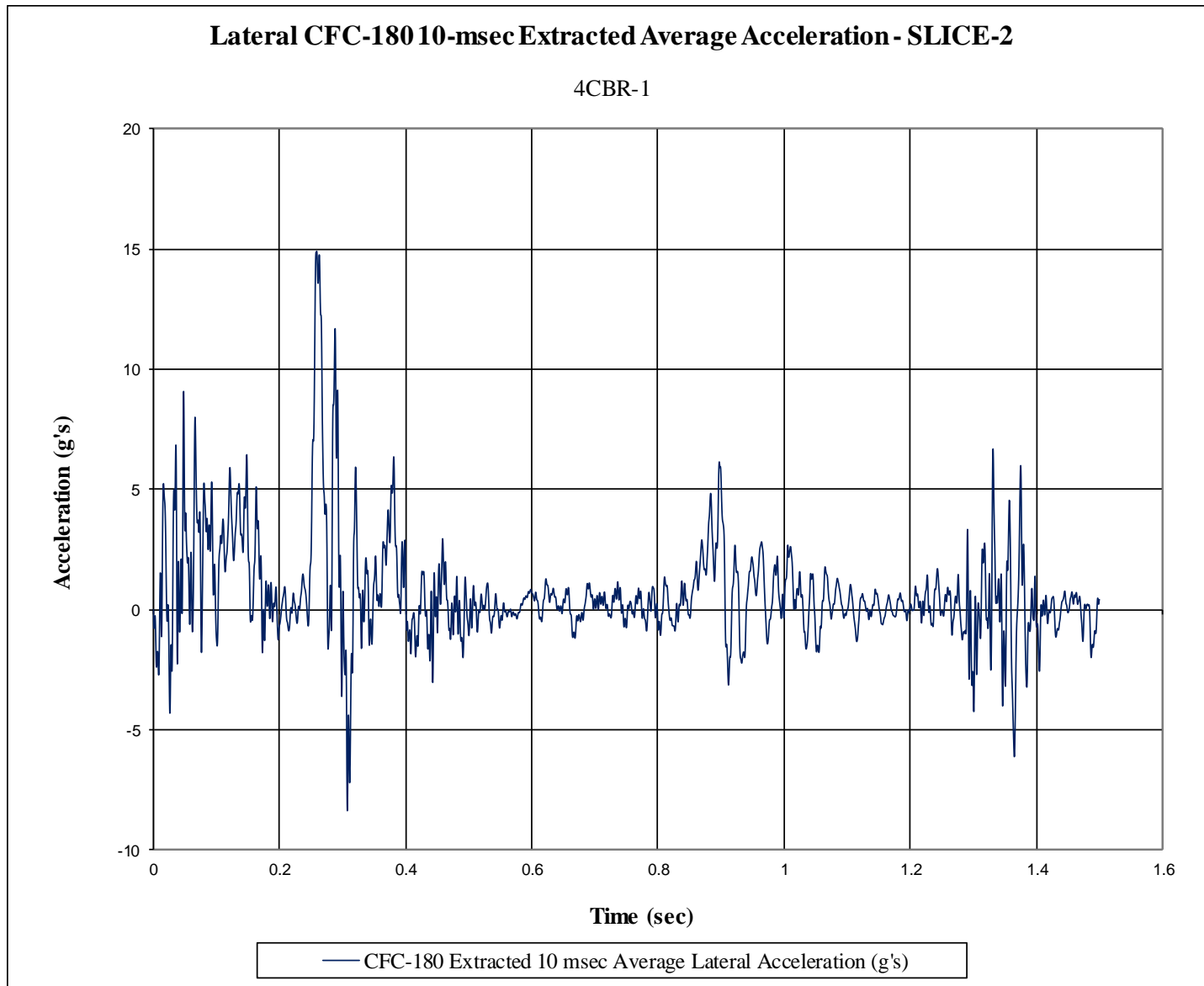


Figure D-12. 10-ms Average Lateral Acceleration (SLICE-2, c.g.), Test No. 4CBR-1

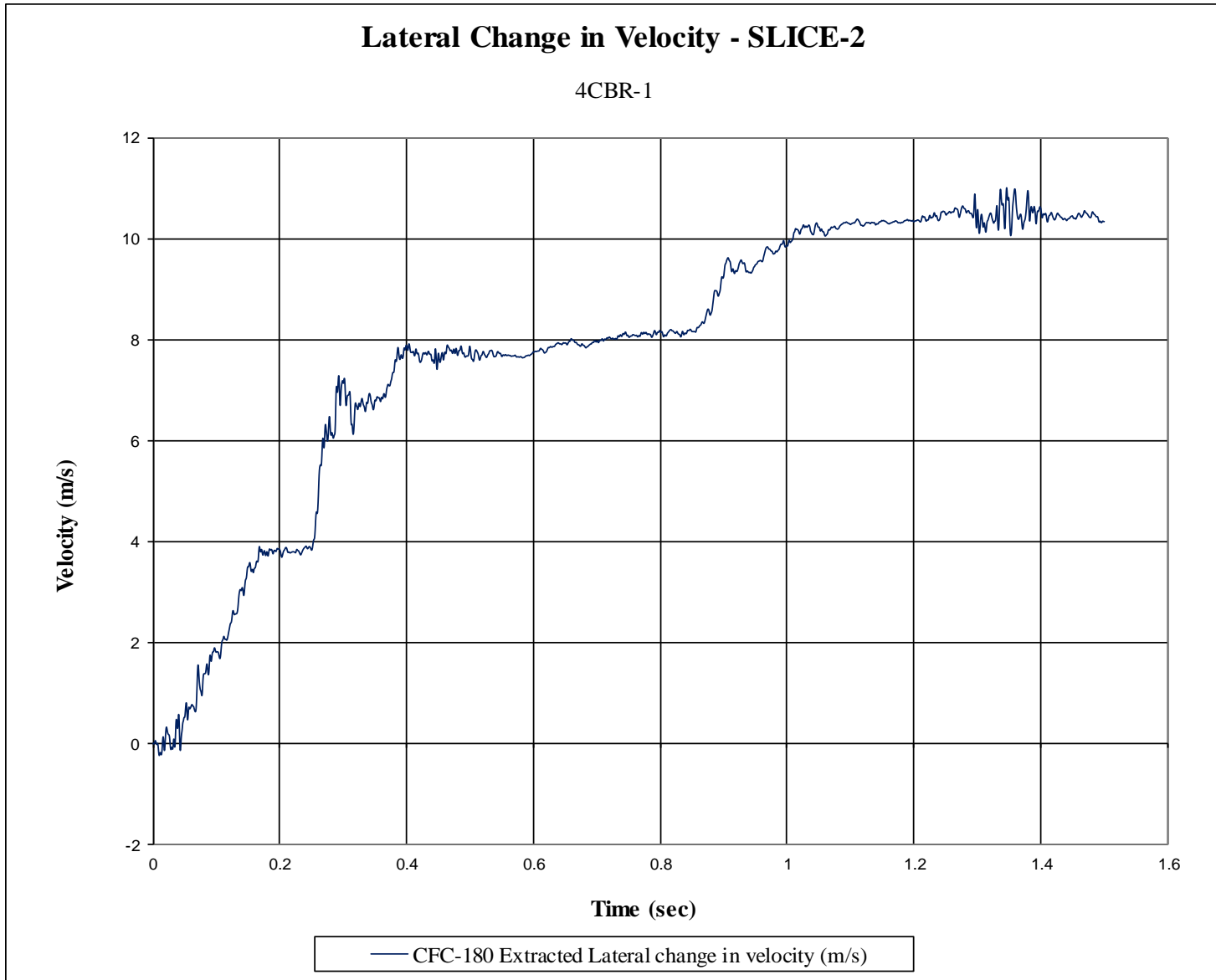


Figure D-13. Lateral Change in Velocity (SLICE-2, c.g.), Test No. 4CBR-1

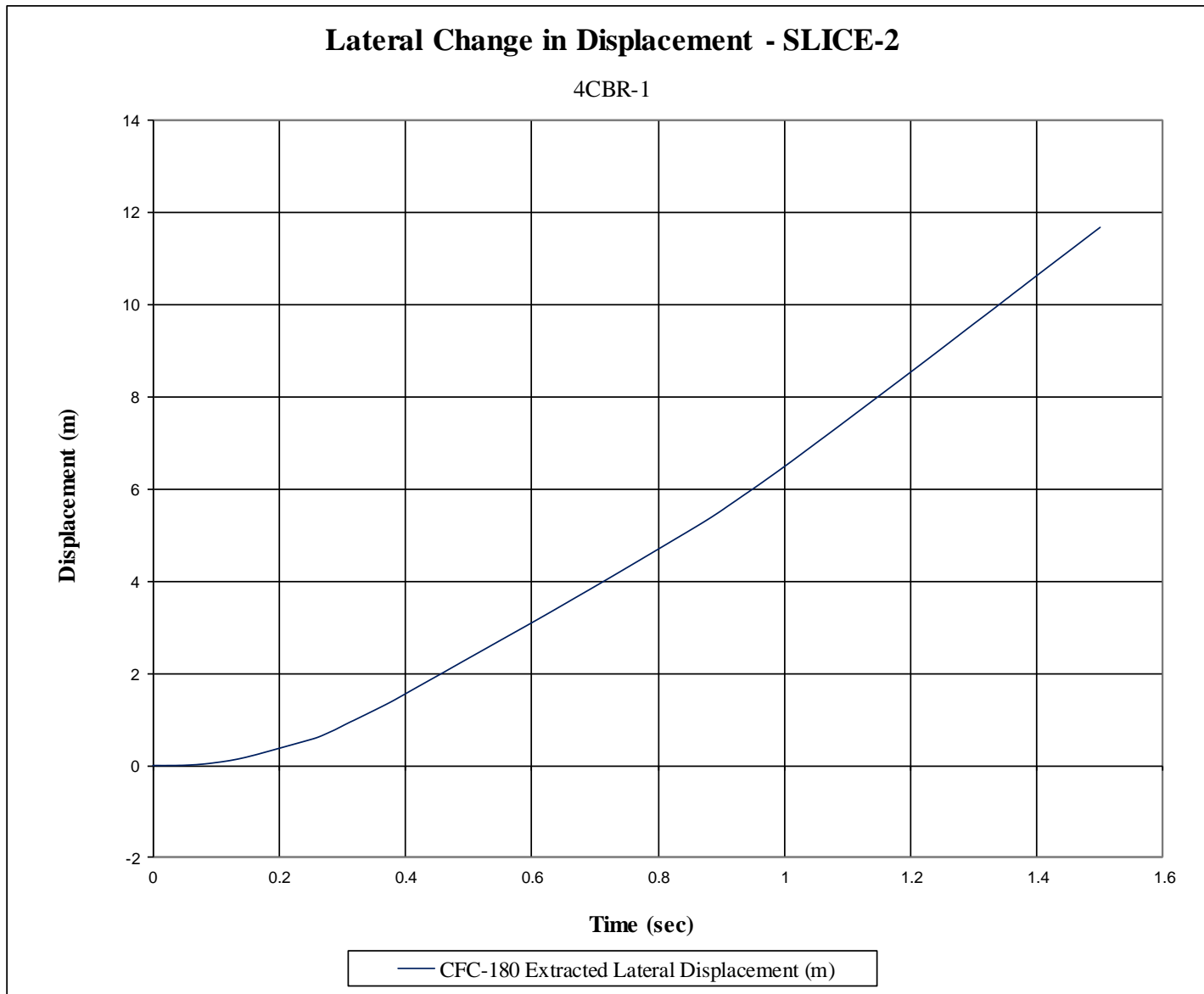


Figure D-14. Lateral Occupant Displacement (SLICE-2, c.g.), Test No. 4CBR-1

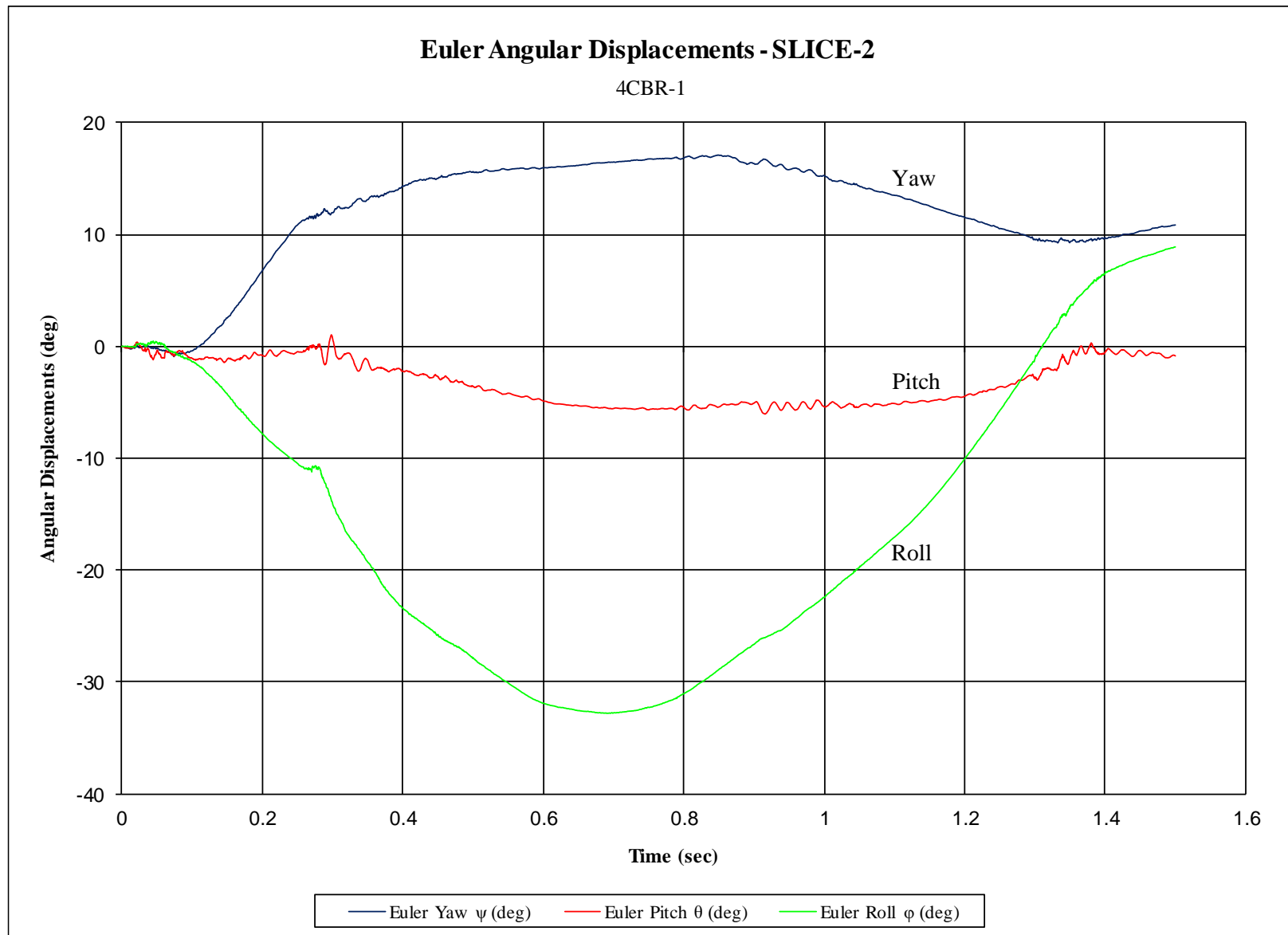


Figure D-15. Vehicle Angular Displacements (SLICE-2, c.g.), Test No. 4CBR-1

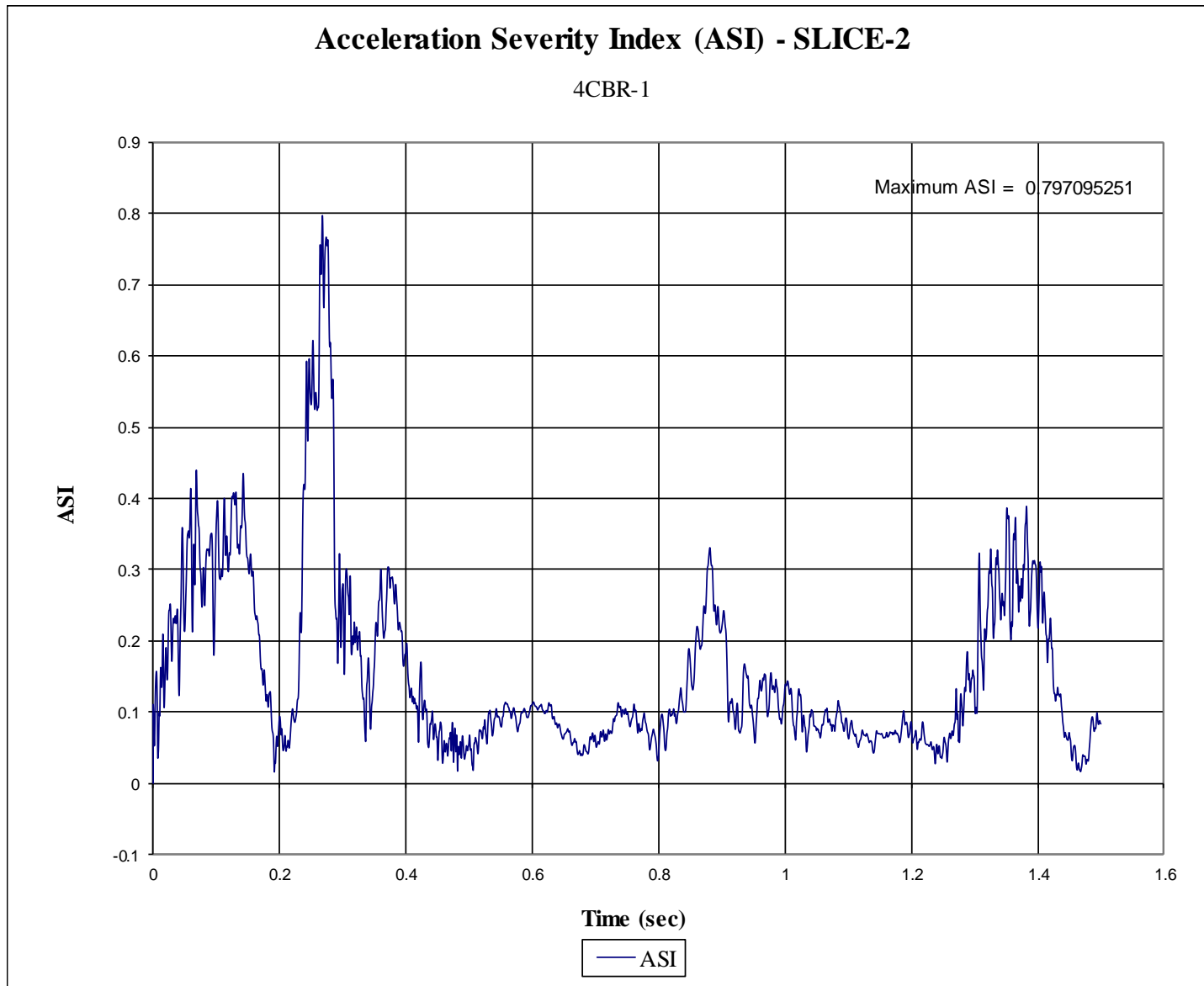


Figure D-16. Acceleration Severity Index (SLICE-2, c.g.), Test No. 4CBR-1

END OF DOCUMENT